PROCESS PARAMETER OPTIMISATION FOR DIMENSIONAL ACCURACY OF VACUUM-ASSISTED PRINTED SAMPLES USING RESPONSE SURFACE METHODOLOGY

MUHAMMAD HAZIM ISKANDAR BIN HAZMAN

UNIVERSITI TEKNIKAL MALAYSIA MELAKA
2024

PROCESS PARAMETER OPTIMISATION FOR DIMENSIONAL ACCURACY OF VACUUM-ASSISTED PRINTED SAMPLES USING RESPONSE SURFACE METHODOLOGY

This report is submitted in accordance with the requirement of the Universiti Teknikal Malaysia Melaka (UTeM) for a bachelor's degree in manufacturing engineering technology.

by

MUHAMMAD HAZIM ISKANDAR BIN HAZMAN

FACULTY OF INDUSTRIAL AND MANUFACTURING TECHNOLOGY AND ENGINEERING
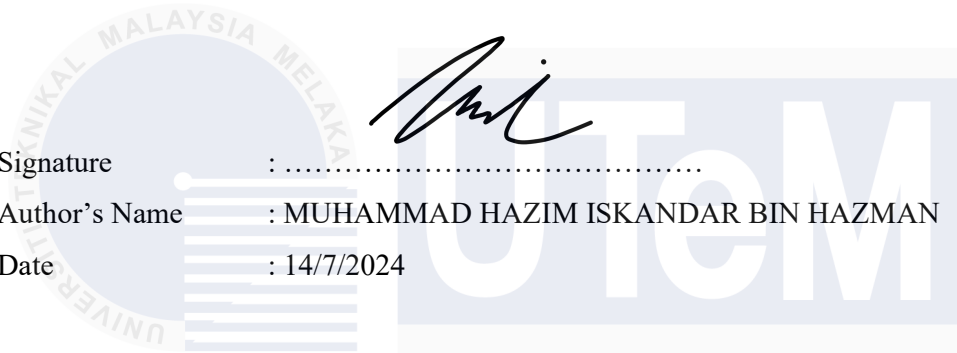
2024

DECLARATION

I hereby declare that this report entitled "PROCESS PARAMETER OPTIMISATION FOR DIMENSIONAL ACCURACY OF VACUUM-ASSISTED PRINTED SAMPLES USING RESPONSE SURFACE METHODOLOGY" is the result of my research except as cited in the references.

Signature   : ………………………………….
Author's Name : MUHAMMAD HAZIM ISKANDAR BIN HAZMAN
Date   : 14/7/2024

APPROVAL

This report is submitted to the Faculty of Manufacturing Engineering of Universiti Teknikal Malaysia Melaka as a partial fulfilment of the requirement for a Degree in Manufacturing Engineering. The members of the supervisory committee are as follows:

………………………...............................

(Associate Prof. Ir. Ts. Dr Shajahan Bin Maidin)
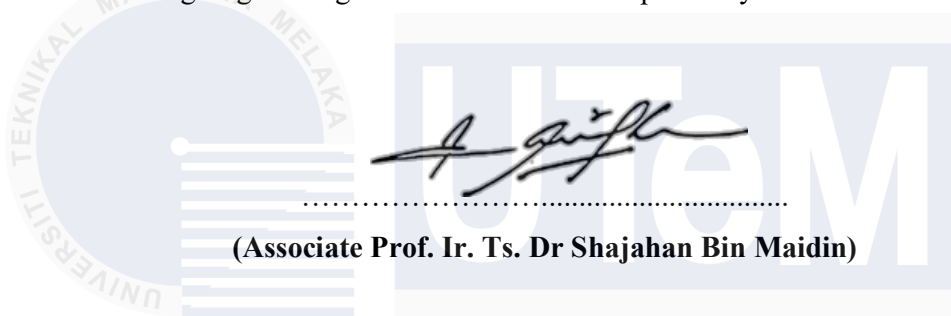
ABSTRAK

Fused Deposition Modelling (FDM) adalah teknik pembuatan tambahan (AM) yang banyak digunakan dan terkenal dengan kepelbagaian serta kos efektif dalam menghasilkan prototaip dan bahagian yang kompleks. Walaupun mempunyai kelebihan ini, FDM menghadapi cabaran seperti sifat mekanikal yang terhad, masalah kualiti permukaan, dan ketepatan dimensi yang rendah, yang menghalang penggunaannya secara meluas. Integrasi sistem vakum dapat meningkatkan ketepatan dimensi sampel yang dicetak dengan ketara. Matlamat kajian ini adalah untuk meningkatkan ketepatan dimensi sampel termoplastik FDM Acrylonitrile Butadiene Styrene (ABS) dan Polylactic Acid (PLA) dengan mengoptimumkan dua parameter proses: Ketumpatan Isi (20%, 55%, 80%) dan Tekanan Cetakan (101.3 kPa tekanan atmosfera dan 20 kPa tekanan vakum). Selepas proses pencetakan selesai, dimensi sampel dinilai dengan teliti menggunakan Mesin Ukur Koordinat (CMM), yang mengukur diameter lubang, diameter sudut, ketebalan, lebar, panjang, dan tegak lurus. Keputusan menunjukkan bahawa walaupun bahan tersebut belum mencapai 100% geometri yang diingini, sampel yang dicetak menggunakan vakum menunjukkan peningkatan ketepatan dimensi berbanding dengan yang dicetak pada tekanan atmosfera. Kaedah permukaan tindak balas (RSM) digunakan untuk mengaitkan parameter proses dengan ketepatan dimensi dan untuk menilai parameter proses yang optimum. Hasilnya menunjukkan bahawa parameter proses yang optimum untuk ABS adalah ketumpatan isi 55% dan tekanan vakum 20 kPa, manakala untuk PLA, ketumpatan isi 80% dan tekanan vakum 20 kPa untuk mencapai ketepatan dimensi yang baik.

ABSTRACT

Fused Deposition Modelling (FDM) is a widely used additive manufacturing (AM) technique renowned for its versatility and cost-effectiveness in producing complex prototypes and parts. Despite these advantages, FDM faces challenges such as limited mechanical properties, surface quality issues, and low dimensional accuracy, which hinder its broader adoption. Integrating a vacuum system can significantly improve the printed samples' dimensional accuracy. The goal of this paper is to enhance the dimensional accuracy of FDM thermoplastic Acrylonitrile Butadiene Styrene (ABS) and Polylactic Acid (PLA) samples by optimizing two process parameters: Infill Density (20%, 55%, 80%) and Printing Pressure (101.3 kPa atmospheric pressure and 20 kPa vacuum pressure). Upon completion of the printing process, the samples' dimensions were carefully assessed using a Coordinate Measuring Machine (CMM), measuring the hole diameter, corner diameter, thickness, width, length, and perpendicularity. The results indicated that while the material has yet to reach 100% of the desired geometry, the vacuum-printed samples for each material demonstrated improved dimensional accuracy compared to those printed at atmospheric pressure. The response surface methodology (RSM) was employed to relate the process parameters with dimensional accuracy and to evaluate the optimal process parameters. The results showed that the optimal process parameters for ABS are 55% infill density and 20 kPa vacuum pressure, while for PLA, they are 80% infill density and 20 kPa vacuum pressure to achieve good dimensional accuracy.

ii

DEDICATION

My Hero and beloved father, Hazman Hassan

My dearest mother, Zuzilawati Parni

My adored little sisters, Putri Amani Elysha, and Putri Hani Aleeya

My partner, Azwani Amira

My fellow friends

For giving me moral support, hope, cooperation, encouragement

and understanding

Thank you so much & love you all forever

ACKNOWLEDGEMENT

I want to thank Allah, the Almighty, for His mercy and blessings on me to complete my final project successfully.

I want to thank Associate Prof. Ir. Ts. Dr Shajahan Bin Maidin, my project supervisor, for allowing me to conduct the final year project and providing invaluable guidance. His wisdom, sincerity and professionalism have all made a huge impact on me. He assists me in doing research and presenting my results in a clear and straightforward manner. It is an honour to learn under his guidance. I am grateful for all he has done for me.

I want to thank my family and friends for their love, prayers, care, and sacrifices they have made for me throughout my whole life. All their efforts will never be forgotten, and I am endlessly grateful to have people like them.

Table of Contents

LIST OF ABBREVIATION

FDM - Fused Deposition Modelling

AM - Additive Manufacturing

CMM - Coordinate Measuring Machine

CAD - Computer Aided Design

ABS - Acrylonitrile Butadiene Styrene

PLA - Polylactic Acid

STL - Standard Triangle Language

RM - Rapid Manufacturing

SLB - Selective Laser Beam

PBF - Powder Bed Fusion

STL - Stereolithography

SLS - Selective Laser Sintering

DMLS - Direct Metal Laser Sintering

PC - Polycarbonate

DA – Dimensional Accuracy

ID – Infill Density

% - Percent

L – Length

W – Width

T – Thickness

CD – Corner Diameter

HD – Hole Diameter

P – Perpendicularity

VP – Vacuum Printed

PP – Printing Pressure

LIST OF TABLES

LIST OF FIGURES

CHAPTER 1
INTRODUCTION

This chapter provides an overview of the project, encompassing its background, problem statement, objectives, and scope.

1.1 Background of the project

Additive Manufacturing (AM) is a technology based on the principle of layer-by-layer manufacturing, enabling the production of intricate polymeric, metallic, and ceramic parts. This revolutionary method reduces both cycle time and the cost of product development (Herzberger et al., 2019). These techniques are comparable in adding and bonding materials in layers to create objects. These procedures are often known as tiered manufacturing procedures. In conventional methods, only 2D models are utilised. However, in the AM process, full 3D models are used. This 3D geometric data from the CAD is partitioned into layer data, and the layers are generated with the assistance of a computer. AM is a relatively new technology that is rapidly gaining market traction. This technology is being utilised in the agriculture, healthcare, automobile, and aviation industries for product customisation and the production of any form of complex design (Tura & Mamo, 2022). Early exposure to AM was limited, and it was challenging to change any sector due to pricey technology and cumbersome procedures. However, competition emerged when research and discoveries to produce new types of AM technology increased rapidly. As industrial businesses began to use AM technology, prices began to fall. AM differs from subtractive manufacturing techniques such as CNC (Computer Numerical Control) Machining, lathe, and milling, which remove a piece of material from a stock material to generate a desired shape.

Next, Fused Deposition Modelling (FDM) is an additive manufacturing process that creates 3D components using a continuous thermoplastic or composite material thread in filament form. An extruder feeds the plastic filament through an extruding nozzle, which is melted and then selectively deposited layer by layer onto the build platform in a

predetermined automated path (Novakova-Marcincinova et al., 2013). FDM is the most widely used 3D printing technique, with the most 3D printer users globally, and is typically the first 3D printing technology to which people are exposed. Due to its accessibility and affordability, polymer-based material is commonly employed in FDM.

ABS and PLA are two of the most used materials in 3D printing due to their versatility and mechanical properties (Syaefudin, 2023; Ujfalusi et al., 2020). PLA, a biodegradable thermoplastic, is extensively researched and utilized, making it promising for various applications, including medical purposes (Hodžić & Pandžić, 2019). On the other hand, ABS is known for its ease of extrusion and widespread availability, making it a popular choice in 3D printing (Arivalagan et al., 2023; Kim et al., 2020). Both materials have been extensively studied for their mechanical properties, tribological characteristics, and thermal behavior in the context of additive manufacturing (Hanon et al., 2019; Mourya, 2023; Ramadan et al., 2023). Understanding the properties and behaviours of ABS and PLA is crucial for optimizing 3D printing processes and ensuring the quality of printed objects.

Next, Response surface methodology (RSM) has been widely utilized in various fields, including additive manufacturing, to optimize process parameters and enhance product quality. In the context of additive manufacturing, RSM has proven effective in optimizing welding parameters for nickel-based alloys. (Moradi, Beygi, et al., 2023), comprehending the impact of additive manufacturing parameters on build quality. (Deng et al., 2020), optimizing selective laser melting process parameters for higher-quality parts. (Vilanova et al., 2020), and optimizing laser powder bed fusion parameters for superalloys (Adegoke et al., 2020). These studies collectively demonstrate the effectiveness of RSM in optimizing process parameters for additive manufacturing, leading to improved product quality and performance. Additionally, a review of laser powder bed fusion of gamma-prime-strengthened nickel-based superalloys highlights the significance of RSM in optimizing the laser powder bed fusion process for nickel-based superalloys, further emphasizing the widespread application of RSM in enhancing additive manufacturing processes.

This project will implement RSM to optimise the printing parameter to print the 3D-printed PLA and ABS parts with good dimensional accuracy in a vacuum-assisted FDM

printer. The test sample will be compared to atmospheric printed ABS and PLA samples to obtain the samples dimensional accuracy results. Finally, the best printing parameter for ABS and PLA discussed in detail.

1.2   Problem Statement

Dimensional accuracy in Fused Deposition Modelling (FDM) using ABS and PLA is a critical aspect that directly impacts the quality of printed parts. Several factors influence dimensional accuracy, including process parameters such as temperature, build orientation, layer height, filament colour, and infill density. Studies have shown that variations in these parameters can significantly affect the final dimensions of printed parts (Akbaş et al., 2019; Gao et al., 2019; Kholil, Asyaefudin, et al., 2022; Kholil, Syaefuddin, et al., 2022). For instance, the filament color has been identified as a key factor affecting dimensional accuracy in FDM-printed PLA parts (Frunzaverde, 2023). Additionally, the layer height parameter has been found to impact the impact strength and compression strength characteristics of ABS and PLA materials (Kholil, Asyaefudin, et al., 2022; Kholil, Syaefuddin, et al., 2022).

Moreover, the mechanical properties of the materials used, such as PLA and ABS, play a crucial role in determining dimensional accuracy. The viscosity of the polymer filaments can affect the ability to control the extruded material paths accurately, thus impacting dimensional accuracy (Gao et al., 2019). Furthermore, the presence of residual stresses due to uneven temperature distribution during FDM can lead to internal thermal stress and deformations, ultimately affecting the geometric accuracy of printed parts (Hou et al., 2023). Understanding the interplay between material properties, process parameters, and printing conditions is essential for achieving the desired dimensional accuracy in FDM-printed parts.

In conclusion, achieving precise dimensional accuracy in FDM using ABS and PLA requires a comprehensive understanding of the complex interactions between material properties and process parameters. Researchers have highlighted the significance of factors such as filament color, layer height, viscosity, and residual stresses in influencing dimensional accuracy. By optimizing these parameters and considering the mechanical properties of the materials, it is possible to enhance the dimensional accuracy of FDM-printed parts, ensuring high-quality and reliable outcomes in additive manufacturing processes.

1.3 Aim

The project aims to model the optimal process parameters using Response Surface Methodology (RSM) to achieve good dimensional accuracy in printed samples using ABS and PLA filaments. The AM system focused on in this project is fused deposition modelling (FDM), and the technique implemented in this project will be response surface methodology (RSM).

1.4 Objectives

The objectives are as follows:

(a) To select the process parameters to optimise the printing of ABS and PLA samples using RSM

(b) To measure the dimensional accuracy of the printed samples using a Coordinate Measuring Machine (CMM).

(c) To analyse the result to obtain the best process parameters settings for ABS and PLA with RSM.

(d) To compare the result of vacuum-assisted test samples with the atmospheric ABS and PLA samples.

1.5 Scopes

The extent of this project covers the use of a desktop FDM system assisted with a vacuum system. The materials employed in this project will be Acrylonitrile Butadiene Styrene (ABS) and Polylactic Acid (PLA). This project will implement Response Surface Methodology (RSM) to optimize the design process parameters to print good dimensional accuracy of the 3D printed PLA and ABS parts. A comparative study of the test samples with and without using a vacuum system will be carried out. To measure the dimensional accuracy of the printed samples, a Coordinate Measuring Machine (CMM) will be used for precise and accurate dimensional analysis.

1.6 Report Organisation

The organisation of this report is as follows. Chapter 1 begins with the project background, problem statement, objectives, and scope addressed in this report. Chapter 2, the literature review, comprises previous studies or research about the dimensional accuracy of FDM. Chapter 3 Methodology. Chapter 4, result and discussion. In Chapter 5, the conclusion and recommendation about this project are examined.

CHAPTER 2
LITERATURE REVIEW

This chapter mainly describes the theory and research defined and done by various researchers years ago. Related information from previous studies is extracted as references and discussion based on their research about Additive Manufacturing, dimensional accuracy of AM, Response Surface Methodology in AM, Vacuum technology, FDM materials and process parameters.

2.1 Definition of Additive Manufacturing

Additive manufacturing (AM) is a modern manufacturing process developed and applied since the second half of the 1980s (Godec et al., 2022). 3D printing or additive manufacturing is a digital manufacturing technique in which materials are added layer by layer to construct three-dimensional items directly from computer-aided design (CAD) models. Thus, AM fundamentally differs from traditional formative or subtractive manufacturing. It is the closest to 'bottom-up' manufacturing, where we can build a structure into its designed shape using a 'layer-by-layer' approach. This layer-by-layer manufacturing allows unprecedented freedom in manufacturing complex, composite, and hybrid systems with precision and control that cannot be achieved through traditional manufacturing routes (Hitzler et al., 2018; Tofail et al., 2018). Design freedom, low buy-to-fly ratio, short lead time, customised product manufacturing, little material wastage and requirement of a relatively minor amount of energy compared to traditional manufacturing are the key benefits of this technology (Vranić et al., 2017; Yap et al., 2020). Fortune Business Insights reported that the global AM market is projected to grow from USD 18.33 to 105.99 billion, exhibiting a Compound Annual Growth Rate (CAGR) of 24.9% during the forecast period (2022–2030). Industries, including aerospace, automobile and medicine, are increasingly using this technology (*3D Printing Market Size, Growth, Share | Global Report [2030]*, n.d.).

As a consequence of the emergency response to COVID-19, 3D printing (3DP) functioned as a mobile factory, aiding in the swift production of essential devices (Choong et al., 2020). The digital flexibility and rapid prototyping capabilities of 3D printing enable swift mobilization of the technology, facilitating a quick response to emergencies. Even amidst significant supply chain disruptions, essential components can be produced on demand by any decentralized 3D printing facility worldwide using designs shared online. Additionally, the additive process of 3D printing allows for product customization and the creation of complex designs (Choong et al., 2020). The broad spectrum of 3D-printing applications in the fight against COVID-19 includes personal protective equipment (PPE) (Bishop & Leigh, 2020; He et al., 2020; Kursat Celik et al., 2020) , medical (Armani et al., 2020; Iyengar et al., 2020) and testing devices (Callahan et al., 2020).

The availability of dependable, cost-effective, portable, easy-to-use, rapid, and precise 3D printers has grown the additive manufacturing technology (AMT) market to exceed trillions of dollars. The industry is advancing from a user interface focus to a large-scale production platform (Kleer & Piller, 2019).

2.2 Additive Manufacturing Process Flow

All additive manufacturing methods share similar processes for converting a virtual computer-aided design (CAD) model into a physical object. Typically, CAD software systems have the functionality to produce stereolithography (STL) files, which are then translated into machine instructions necessary for executing the additive manufacturing (AM) process. Figure 2.1 shows the additive manufacturing process flow.
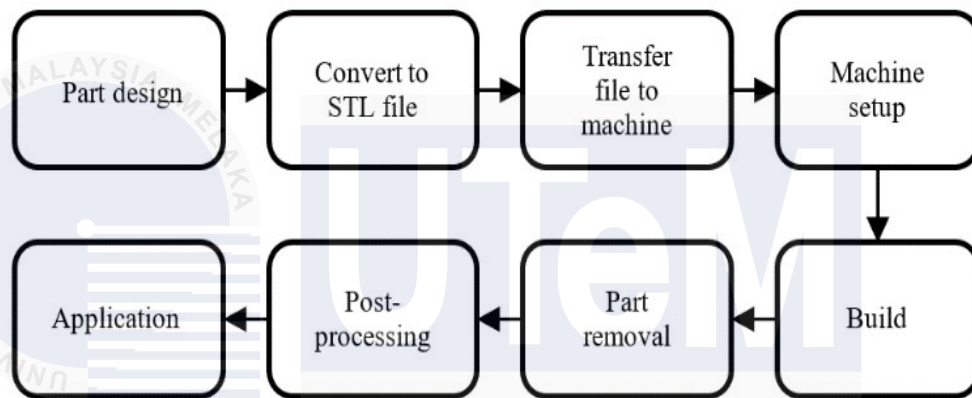
Figure 2.1: Additive Manufacturing Process, Source:(Leirmo & Martinsen, 2019)

Below is the detailed step of the Additive Manufacturing Process (Gibson et al., 2010).

i.   Part Design

All additive manufacturing (AM) parts must originate from a software model that comprehensively delineates the external geometry. This often involves utilizing professional CAD solid modeling software, provided that the output is a 3D solid or surface representation. Additionally, reverse engineering tools, such as laser scanning, can be employed to generate this representation.

9
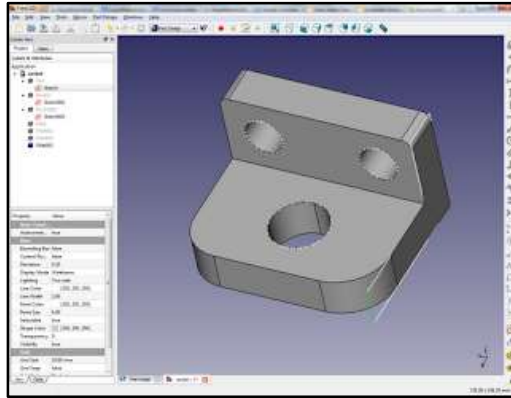
ii.   Convert to STL file.

Nearly all additive manufacturing (AM) machines accept the STL file format, which has become the de facto standard in the industry. Correspondingly, almost every CAD system is capable of exporting files in this format. The STL file represents the external closed surfaces of the original CAD model and serves as the foundation for calculating the slices necessary for the AM process.

iii.   Transfer to AM machine and STL file manipulation

The STL file that describes the part must be transferred to the additive manufacturing (AM) machine. At this stage, the file may undergo general manipulation to ensure it is correctly sized, positioned, and oriented for the building process.

iv.   Machine Setup

Before initiating the build process, the additive manufacturing (AM) machine must be properly configured. This setup involves adjusting build parameters, including material constraints, energy source, layer thickness, and timing, among others.

v.   Build

The part is mainly automated, and the machine can carry on without supervision. Only superficial monitoring of the machine is needed to ensure no errors have occurred, like running out of material, power or software glitches, etc.

Figure 2.2: Example of 3D printing process (*7 Amazing Real-World Examples Of 3D Printing | Bernard Marr*, n.d.)

vi.   Part Removal

Upon the completion of the build by the additive manufacturing (AM) machine, the parts must be extracted. This process might necessitate interaction with the machine, which could be equipped with safety interlocks. These interlocks are designed to ensure that operating temperatures are adequately reduced or that no parts are inactive motion.

Figure 2.3: Example of Part Removal (*3D Print Stuck to Bed: What to Do?*, n.d.)

vii.   Post-processing

After removal from the machine, parts often necessitate further cleaning before they are ready for use. At this stage, parts may be fragile or have supporting structures that need to be eliminated. Consequently, this process frequently demands considerable time and meticulous, skilled manual handling.

Figure 2.4: Example of the post processing being done to the printed part

viii.   Application

The parts might now be ready for use, though additional treatment may still be necessary to meet quality standards. For instance, they might need priming and painting to achieve an acceptable surface texture and finish. If the finishing requirements are highly demanding, these treatments can be labour-intensive and time-consuming. Additionally, the parts may need to be assembled with other mechanical or electronic components to create the final model or product.

2.3 Seven Categories of Additive Manufacturing Systems

In additive manufacturing, there are seven categories, which are material extrusion (MEX), vat photopolymerisation (VPP), powder be fusion (PBF), sheet lamination (SL), binder jetting (BJ), directed energy deposition (DED) and material jetting. They are different in using materials and technology (Jasiuk et al., 2018). Figure 2.3 shows the categories of AM.
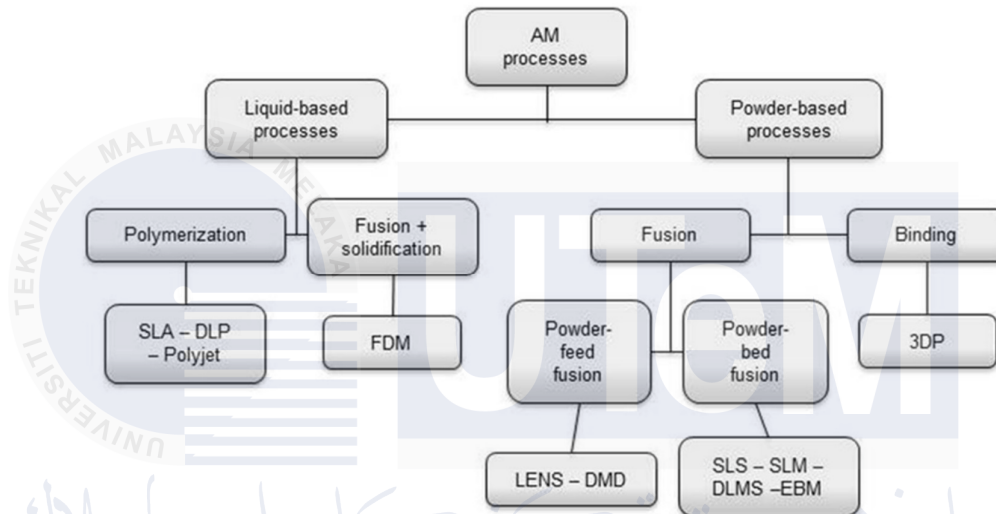
Figure 2.5: The Categories of Additive Manufacturing, Source: (Bahnini et al., 2018)

2.3.1 Material Extrusion

Material extrusion is an additive manufacturing process where material is extruded through a nozzle under constant pressure. The extruded material is deposited at a consistent speed and fully solidifies on the substrate after exiting the nozzle. Furthermore, the material must adhere to the previously deposited layers to form a solid part that maintains its structure throughout the process (Lee et al., 2017). Material extrusion refers to the process of selectively dispensing material through a nozzle or orifice. This group is based on Stratasys's first technology, Fused Deposition Modeling (FDM) (Boschetto & Bottini, 2015). Examples of machines utilizing the ME process include Stratasys's Fortus Production Series (380 mc, 450 mc, and 900 mc). Thermoplastic materials used in fused deposition modeling (FDM) encompass (1) acrylonitrile butadiene styrene (ABS); (2) acrylonitrile styrene acrylate (ASA); (3) nylon 12; (4) polycarbonate (PC); (5) polyphenyl sulfone (PPSF/PPSU); (6) polyetherimide (PEI or ULTEM); (7) polylactic acid (PLA); and (8) thermoplastic polyurethane (TPU). These FDM materials offer properties such as UV resistance, biocompatibility, translucence, and toughness, as detailed in Table 2.1. These properties of the material make it perfect for harsh environments in automotive, aerospace, medical and other industries (Lee et al., 2017). The Fused Deposition Modeling (FDM) technique is a 3D printing method that creates three-dimensional parts by extruding a filament layer by layer to achieve the desired geometry (Yap et al., 2020).

Table 2.1: Material Properties of FDM thermoplastics and their application in various industries.

Material properties of FDM thermoplastic and their application in various industries.

Material	Properties	Applications/industries
ABS	Tough and strong	Automotive, aerospace, medical-device
ASA	Mechanical Strength and UV stability	Functional prototyping from brackets and electrical housings to automotive prototypes and practical production parts for outdoor use under the sun
Nylon 12	Good chemical resistance, high fatigue resistance and high impact strength	Ideal material for applications that demand impact-protective components and high fatigue endurance, including antenna covers, custom production tooling, friction-fit inserts and snap fits in automotive and aerospace industries
PC	High tensile and flexural strength	Functional prototypes, tooling and fixtures, blow-molding master in automotive and aerospace industries
PPSF/PPSU	Excellent chemical and heat resistance and mechanical strength	PPSF/PPSU can withstand various sterilization methods including ethylene oxide, autoclaving, and radiation. Sterilizable medical devices, automotive prototypes, and tooling for demanding applications in a variety of industries
PEI or ULTEM	Biocompatible, excellent mechanical, chemical and thermal stability	Due to its high strength-to-weight ratio and existing certification, ULTEM is ideal for rapid prototyping and advanced tooling applications in aerospace, automotive, medical and food-production industries
PLA	Good tensile strength and surface quality	Ideal for model and prototypes that require aesthetic detail and environmentally-friendly for both home and office
TPU	Excellent tear and wear resistance, high impact strength and hardness	Exceptional flexibility (i.e. elongation at break) and corrosion resistance to many common industrial chemicals and oils. Highly versatile material with the both rubber and plastics properties for a variety of industrial application

FDM encompasses multiple processes, starting from the virtual model and culminating in the production of the final pieces. The initial stage involves creating a three-dimensional model, usually using computer-aided design software or reverse engineering methods. The next step is converting the file to the interchange format. The Standard Triangulation Language (STL) file format is used to encompass tessellated surfaces and has become the widely accepted standard for Additive Manufacturing (AM). During the third phase, the file is transmitted to the prototyping system, and process parameters are selected inside a Computer-Aided Manufacturing (CAM) setting. Subsequently, the geometry is divided into distinct layers, and the resulting curves are thoroughly examined for accuracy. The fifth step pertains to the establishment of support. Subsequently, the toolpaths for the model, support, and transition motions are generated and stored. The system is prepared for the automated production of the tangible component. The final phase is the post-processing procedure, which encompasses the separation of the component from the table and the elimination of any supporting structures (Boschetto & Bottini, 2015). Due to the process's simplicity, reliability, and affordability, the FDM has been widely recognised and adopted by industry, academia, and consumers.
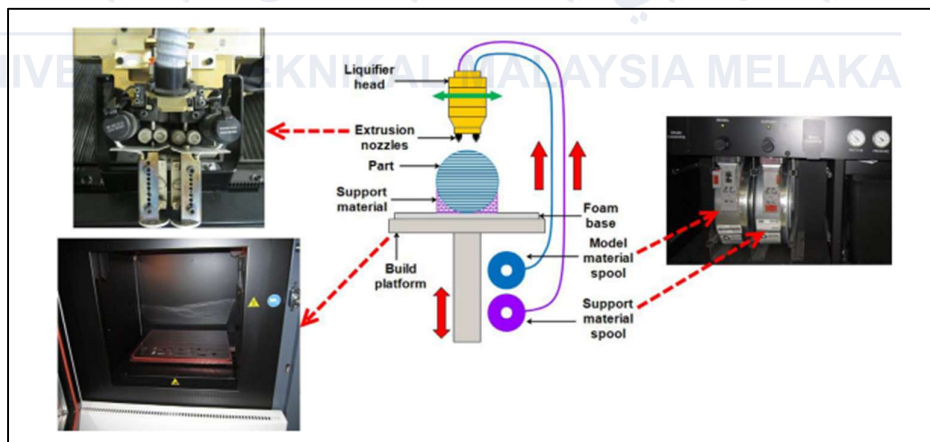
Figure 2.6: Schematic representation of FDM process

2.3.2 Fused Deposition Modeling

Fused Deposition Modeling (FDM) is a widely used additive manufacturing technology that enables the creation of three-dimensional objects by depositing melted thermoplastic polymer filaments layer by layer (Yang et al., 2023). Several studies have focused on investigating the impact of FDM process parameters on dimensional accuracy. et al. explored the effects of process parameters on dimensional accuracy using ABS polymer parts and demonstrated that FDM can achieve accuracies of 0.1 mm for linear dimensions and 0.4° for angles (Singh, 2024). highlighted that the dimensional accuracy of FDM parts is influenced by their shape, with cylindrical shapes exhibiting high dimensional deviation (Dey & Yodo, 2019). Furthermore, studied the impact of process parameters like temperature and build orientation on dimensional accuracy and hardness of materials produced by FDM 3D printing (Pratama & Adib, 2022). Moreover, the dimensional accuracy of FDM parts can be influenced by the type of filament used. PLA filaments have been shown to offer higher dimensional accuracy compared to ABS filaments due to less warp behavior (Baran & Yildirim Erbil, 2019). Additionally, the use of composites in FDM, such as graphene nanoplatelet reinforcement, can affect the mechanical properties and dimensional accuracy of the printed parts (Caminero et al., 2019; Zhang et al., 2022). The choice of materials and their properties play a crucial role in achieving the desired dimensional accuracy in FDM-printed parts. While FDM is known for its ease of use in producing complex geometries and three-dimensional models (Mishra & Das, 2021), other additive manufacturing technologies like Multi-Jet Fusion (MJP) have been reported to provide better dimensional accuracy and surface properties compared to FDM (Chand et al., 2023). However, FDM remains popular due to its affordability, adaptability, and relevance in various fields, including biotechnology (Abdullah et al., 2022). In conclusion, FDM is a versatile additive manufacturing technology that offers the capability to achieve high dimensional accuracy in printed parts. Understanding the influence of process parameters, material properties, and filament types is essential for optimizing dimensional accuracy in FDM-printed objects.

2.4   Advantages and Disadvantages of Additive Manufacturing

Advantages of AM

Additive manufacturing, also known as 3D printing, offers numerous advantages across various fields. One of the key advantages is the ability to produce complex geometries without significantly increasing the cost of manufacturing, which is a limitation in traditional manufacturing methods (Impey et al., 2021; Zakharov et al., 2022). This capability allows for the creation of intricate designs and structures that were previously unattainable using conventional manufacturing processes. Additionally, additive manufacturing enables the customization of products, minimal material wastage, rapid prototyping, and fast manufacturing, all of which contribute to cost-effectiveness and efficiency (Adil & Lazoglu, 2023a; Bikas et al., 2019). The technology also facilitates the direct manufacturing of complicated 3D objects without the need for molds, tooling, or assembly, thereby streamlining the production process (Li et al., 2020; Velu et al., 2019). Furthermore, it offers the advantage of high manufacturing accuracy and large manufacturing size, particularly in the case of large-scale ceramic additive manufacturing (Liu et al., 2023).

In the biomedical field, additive manufacturing has revolutionized the production of medical implants and tools, allowing for the customization of dental implants and other medical devices based on computer-aided design (CAD) data (Demiralp et al., 2021; Javaid & Haleem, 2019). Moreover, it has been instrumental in the development of biomedical applications, such as the production of polyhydroxyalkanoates, overcoming limitations of traditional approaches (Giubilini et al., 2021). Additive manufacturing also plays a crucial role in the fabrication of bio-nanomaterials for medical implants, demonstrating its feasibility and potential in the medical sector (Velu et al., 2019).

The technology's impact extends to the production of advanced materials, such as carbon fiber-reinforced polymers and WC-Co hardmetals, offering the advantage of high specific strength and the ability to produce complex geometries with features like U-shaped or helical cooling channels (Adil & Lazoglu, 2023b; Y. Yang et al., 2020). Furthermore, in the construction industry, additive manufacturing with 3D printing presents benefits in terms of constructability and sustainability, showcasing its potential for innovative applications in civil engineering (El-Sayegh et al., 2020; Guimarães et al., 2021).

In the pharmaceutical field, additive manufacturing enables personalized medicine through the production of drug dosage forms tailored to individual patients' needs, showcasing its potential for enhancing healthcare delivery (Gal-Or et al., 2019; Goh et al., 2022). Additionally, the technology has been explored to produce 3D-printed foods, with studies indicating its potential to reduce the cost of food production and improve consumer acceptability (Manstan & McSweeney, 2020; Tesikova et al., 2022).

In conclusion, additive manufacturing offers a wide range of advantages, including the ability to produce complex geometries, customization, cost-effectiveness, and efficiency, with applications spanning various industries, from biomedical and materials science to construction and pharmaceuticals.

Disadvantages of AM

AM, also known as 3D printing, has gained significant attention and application across various industries due to its potential for improved functionality, productivity, and competitiveness (Vafadar et al., 2021). However, despite its advantages, AM is not without limitations and challenges. One of the primary disadvantages of AM is the presence of metallurgical defects resulting from multiple heating-cooling cycles, which can lower the formability of additively manufactured sheets (Pragana et al., 2021). Additionally, the low throughput and limited build envelope of additive manufacturing techniques pose challenges, particularly in the production of mission-critical structural components (Dolev et al., 2021). Furthermore, the technology suffers from low precision, large distortion, and limitations in compatible materials, especially in large-scale additive manufacturing machines (Yi & Saitou, 2021).

In the context of metal additive manufacturing, the technology presents challenges related to high melting points, oxygen susceptibility, and low-temperature brittleness, particularly for intermetallic structural materials (Rittinghaus et al., 2021). Moreover, the emergence of defects during the manufacturing process can lead to a low fatigue limit in additively manufactured metals, impacting their mechanical properties and performance (Tsuchiya & Takahashi, 2021). Another significant challenge is the limited availability of filaments for fused deposition modeling (FDM) manufacturing, hindering the additive

manufacturing of certain materials such as pure polycaprolactone or filled PCL composites (Chen et al., 2020).

Furthermore, the application of additive manufacturing in the construction sector, particularly in 3D concrete printing, presents challenges related to material properties, bespoke designs, and the need for effective 3D concrete printing technologies (Kareem, 2022). These challenges highlight the need for further research and development to address the limitations of additive manufacturing and enhance its capabilities across various industries.

2.5   Application of Additive Manufacturing

2.5.1   Aerospace Application

3D printing technology provides unparalleled freedom in component and industrial design. 3D printing technology in the aerospace business offers the capacity to manufacture lightweight parts with precise and intricate shapes, reducing energy and resource requirements (Praveena et al., 2022). Additive manufacturing machines are increasingly utilized in aerospace and missile applications for both military and civilian purposes. They are employed in layered manufacturing and the construction of facilities for both sectors, as well as in the production of guided missiles and civil aircraft. This technology enables rapid prototyping, streamlines testing and design processes, and promises to reduce delivery times. With these capabilities, additive manufacturing is poised to significantly impact both military and civilian manufacturing sectors (Kalender et al., 2019).

Numerous companies in the aviation industry have initiated production trials for various aircraft components using 3D printing technology. For instance, Boeing has successfully fabricated prototype thermoplastic parts using commercially available laser sintering techniques for its commercial aircraft models, including the 737, 747, 777, and 787 (*Boeing Turns to 3D-Printed Parts to Save Millions on 787 Dreamliner - TechCentral.Ie*, n.d.).

The inaugural 3D printer developed by NASA as part of the Made in Space programme, specifically designed to operate in the space environment, has been dispatched to the International Space Station. The 3D printer, specifically tailored for astronauts, is

distinct from the printers commonly used in our daily lives, since it is designed to fulfil their basic requirements. To endure the impact of fire during deployment, the long-utilized 3D printer was included among the damaged food and supplies provided to the astronauts for their usage in space (Kalender et al., 2019).

In advanced stages, layered manufacturing can also be employed in the production of energy components, such as explosives and solid rocket propellants, which are crucial for missile energy. This ensures that these materials are used in the most efficient and reliable manner. In July 2017, NASA tested the world's first three-dimensional rocket engine igniter, which was manufactured using copper alloy and Inconel (a chrome and steel alloy). This approach resulted in significant cost and time savings in the production of the igniter (*Explosiv3Design | Discover Los Alamos National Laboratory}*, n.d.).

Figure 2.7: Polymer-based 3D printed aerospace components, Source:(*Hexcel Launches Conductive New HexPEKK Polymer for 3D Printing "Flight Ready" Aerospace Parts - 3D Printing Industry*, n.d.)
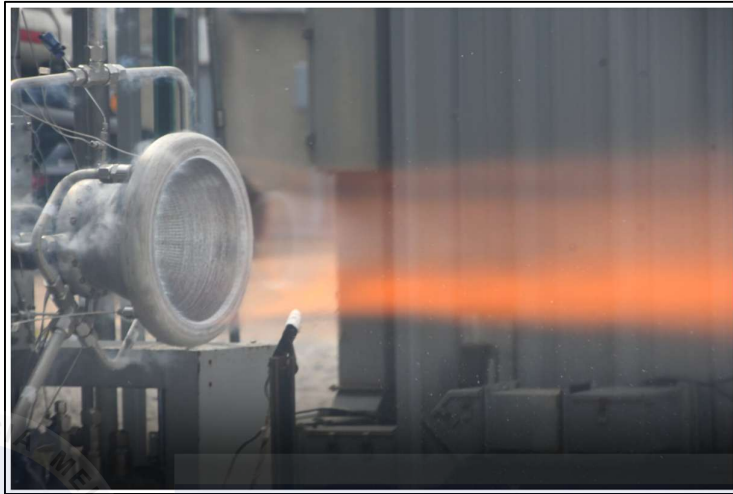
Figure 2.8: Hot Fire testing of the 3D printed RAMFIRE nozzle. Courtesy of NASA
(*NASA 3D Prints Aluminum RAMFIRE Rocket Engine Nozzles to Enable Deep Space Exploration - 3D Printing Industry*, n.d.)

Figure 2.9: Airbus A350 cabin bracket connector made by AM, Source: (Blakey-Milner et al., 2021)

2.5.2 Automotive Application

According to Mohanavel et al., (2021), The utilisation of 3D printing is increasingly prevalent in all facets of vehicle production. Besides its application in rapid prototyping, the technology is also utilised for the production of tools and, in certain instances, final components. Automobile designers can utilise 3D printing to efficiently produce physical prototypes of various components, such as interior elements, dashboards, or even full car models. Companies employ rapid prototyping to convert ideas into convincing proofs of concept. The reduction in cycle time across all future stages of the production process is substantial due to the time saved during the prototyping phase. This provides significant benefits to the company in terms of cost savings and improved flexibility. 3D printing in automotive design decreases consumption and waste, in contrast to traditional car design methods. Reducing time and energy consumption at various production stages decreases the overall production cost. Reducing costs across all tiers enables firms to transfer a greater portion of the cost savings to their customers.

When discussing additive manufacturing, there is no universally applicable solution. Various additive manufacturing technologies have been created specifically to meet the component, area, and production requirements of the automotive industry. Furthermore, it is evident that there are appropriate additive manufacturing technologies and procedures available depending on the specific component that requires printing. The technology, techniques, and components currently being manufactured are detailed in Table 2.2.

Table 2.2: Additive Manufacturing Technologies and component mapping

AM Technology	Process	Target Components
Fused Deposition Modelling (FDM)	The FDM process uses thermoplastics such as Acrylonitrile Butadiene Styrene (ABS) for the designing and rapid prototyping of automotive components. This particular process deposits the material in ultra-fine beads along the extrusion path, after heating the material to a semi-liquid state for printing 3D objects and working prototypes.	• Component/Vehicle design prototyping • Emission filter and filter housing caps and housing units • Physical model of fuel doors, dashboard, and cluster • Gauge pod, fork tube covers, headlight bezel, floorboard mounts, floorboard undercover, and wheel spacer cover • Working prototype and low-volume components
Stereolithography (SLA)	SLA process uses materials such as composite photopolymers, resins, photopolymers, and thermoplastics for manufacturing automotive components. The technology uses an ultraviolet laser to produce the design of the component layer-by-layer using a liquid material. The material quickly hardens when it comes in contact with the laser light.	• Gear shift knobs • Prototypes of pneumatic and hydraulic systems • Transparent prototypes for engine components and tooling devices • Headlamp, tail lamp, and lenses prototype • Body kits and bumpers for a vehicle manifold and engine covers
Selective Laser Sintering (SLS)	The SLS process uses metal alloys, polymers, ceramic, and carbon fiber materials. It uses a power source to selectively melt and fuse powdered materials layer-by-layer to create a 3D printed object. The process involves a counter-rotating roller that spreads the material powder in precise amounts, as the laser fuses the powder to build the desired component or object.	• Gearbox prototypes • Grills and fenders • Fuel tanks • Small engine components • Hydraulic actuator systems • Heat exchangers • Rapid prototyping of low volume parts • Tubes and nodes
Electron Beam Melting (EBM)	The EMB technique uses an electron beam in high vacuum as its power source, which selectively melts the metal powder bed to print the design of the object layer-by-layer. This novel technology is compatible with metal materials, such as aluminum and its alloys, superalloys, titanium and its alloys, cobalt chrome, and so on. Material is layered according to the data obtained from a 3D Computer-aided Design (CAD) model.	• Pump impeller • Wheel rims • Small compressor components • Frame construction • Variable density system • Turbine blades

Figure 2.10: Bugatti Brake Calliper made by AM (Blakey-Milner et al., 2021)

Figure 2.11: Alternator bracket printed using SLS nylon (Blakey-Milner et al., 2021)

Figure 2.12: Sample metal 3D printed water connectors for the Audi W12 engine.

2.5.3 Medical Application

Additive manufacturing, particularly 3D printing, has significantly transformed medical applications by enhancing medical education, surgical training, and medical device development (Olatunji, 2023). This technology has also influenced pharmaceuticals, being utilized in drug development processes from research to frontline medical treatment (Huanbutta et al., 2023)(Huanbutta et al., 2023). Its impact is evident in the creation of patient-specific models for anatomy education, surgical guides, and customized implants (Pugalendhi et al., 2021)(Pugalendhi et al., 2021).

Moreover, 3D printing has found increased utilization across various medical fields, including otolaryngology, cardiovascular disease, and the management of hepatocellular carcinoma (Christou & Tsoulfas, 2022; Hong et al., 2019; Sun, 2020). The versatility of 3D printing in healthcare is highlighted by its ability to customize medical products, guide surgical procedures, and produce custom prosthetics (Baig, 2023). As the technology continues to advance, its applications in healthcare are expected to expand further, offering innovative solutions to various medical challenges.

Additionally, the growing availability of medical computer-aided design (CAD) software and low-cost 3D printers is enabling more hospitals to establish 3D printing laboratories (Javaid et al., 2022). This democratization of technology is poised to further revolutionize the healthcare sector, providing accessible and personalized medical care

Figure 2.13: Knee Tec source:(Gaillard et al., 2016)

Figure 2.14: 3D printed for skull implant. Source: (https://3dwithus.com/3d-printing-in-medicine)

2.6 Respond Surface Methodology (RSM)

The statistical modelling employed in this project entails the application of statistical approaches to model and comprehend the behaviour of the 3D printing process parameters that impact dimensional accuracy. Statistical modelling is used to describe the connections between process parameters, material qualities, and the quality of the printed parts. It facilitates the discovery of crucial aspects that impact the process and aids in optimising the process settings to attain desired results. Conversely, mathematical optimisation is employed to specifically target the identification of the optimal solution within a predefined set of limitations. The process entails creating an objective function and determining the best values of the choice variables that either maximise or minimise the objective function. Mathematical optimisation is employed in 3D printing to identify the most effective combination of process parameters for achieving specific objectives outlined in the optimisation section. (Moradi, Karamimoghadam, et al., 2023).

A response variable and many predictor variables are modelled and analysed using the statistical design of experiments approach known as RSM (Abdellatief et al., 2023; Panwar et al., 2020). The goal of RSM is to identify the optimal combination of predictor variables that produces the highest (or lowest) response value (Mohammed & Adamu, 2018; Myers et al., 2004).

Response Surface Methodology (RSM) comprises a collection of mathematical and computational techniques used to construct empirical models. It is particularly effective for studying scenarios where multiple variables impact a response or output variable, with the goal of optimizing this response function. RSM provides enhanced understanding with minimal experimental data (Panwar et al., 2020).

The development of a Response Surface Methodology (RSM) model involves three essential steps (Adamu et al., 2022):

 i) Collecting experimental data concerning the response variable of interest.

 ii) Constructing the RSM model and verifying its accuracy through validation.

 iii) Optimizing the parameters to achieve the desired response variables

28

2.7 Dimensional Accuracy

Dimensional accuracy stands out as a crucial quality indicator in Additive Manufacturing (AM) production (Lemeš et al., 2022). It plays a pivotal role in determining the quality and functionality of the final parts in the additive manufacturing process. Eisenbarth et al. highlight the significance of the process sequence in achieving dimensional accuracy, as noted by (Soffel et al., in 2021). Additionally, (Alkentar & Mankovits, 2022) underscore the importance of additive manufacturing in achieving high shape and dimensional accuracy for fabricated parts. Furthermore, the influence of processing parameters on the dimensional accuracy of 3D printed objects is stressed, irrespective of the additive manufacturing method, according to (Momenzadeh et al., in 2020). In summary, these references collectively emphasize the crucial role of the process sequence, additive manufacturing, and processing parameters in ensuring dimensional accuracy in the additive manufacturing process.

2.7.1 Measurement of Dimensional Accuracy

According to Maurya et al., (2019), dimensional accuracy refers to the degree of precision with which physical models are generated by a 3D printer. The author emphasized that for precise measurement of dimensions, the measuring instrument must exhibit high precision. Therefore, a coordinates measuring machine (CMM) was selected for measuring both linear and radial dimensions. The author further noted two primary reasons for dimensional errors in parts fabricated by the FDM process: first, errors due to slicing and layer alignment, and second, errors arising from layer shrinkage during cooling. Equations (1) and (2) were employed to calculate the deviation in linear and radial dimensions.

$$\Delta L = |Lexp - Lcad| \tag{1}$$

$$\Delta R = |Rexp - Lcad| \tag{2}$$

2.7.2 Statistical analysis of measured data

Continuation from the same author (Maurya et al., 2019), statistical analysis of the measured data was performed using Minitab-14 software. The effect of process parameters was evaluated based on the Signal-to-Noise (S/N) ratio. The S/N ratio values for the deviation of linear and radial dimensions were calculated using Equations (3) and (4).

$$\eta = -\log(MSD) \tag{3}$$

$$MSD = \sigma^2 - (Yave - Y_{\circ})^2 \tag{4}$$

Yave is the average value of (n) data points, M.S.D. is the Mean-Square Deviation, σ^2 is the variance, and Y_{o} is the desired value for (0 in this design). Minitab14 software was used to conduct the experiment analysis. S/N ratios for every experiment were calculated and shown in Table 2.1. The main effect plot for the S/N ratio was employed to choose the best factor level. ANOVA Eqs. (5)-(8) determined how the various process parameters affected each other (Kumar Maurya et al., 2020).

$$ST = (\eta - \tilde{\eta}) \tag{5}$$

Where (ST) stands for the total sum of squares, n for the number of experiments, and for the average (S/N) ratio.

$$SSj = \sum (\eta ji - \tilde{\eta})^2 \, i \, i{=}1 \tag{6}$$

Sum of square deviation of jth factor (SSj), where l is jth factor level.

$$Vj = SSj / fj \tag{7}$$

The variance and degree of freedom of the jth parameter are Vj and fj.

$$Fj = Vj / Ve \tag{8}$$

Fj is F-ratio of jth factor and Ve is variance of error.

$$i = 0.45 \sqrt{D} \, 3 + 0.001D \tag{9}$$

$$n = (\,\lvert Dn - Dm / i \rvert\,) \tag{10}$$

The essential tolerance "i" served as the basis for evaluating the tolerance unit. Equations (9) and (10) were used, respectively, to derive the tolerance unit and essential tolerance (Aslani et al., 2020).

This research investigates the influence of process variables on both linear and radial dimensional accuracy. The study successfully explores the fabrication of PLA components through FDM. As shown in Table 2.3, the cutting and squaring of edges are demonstrated to result in increased dimensional inaccuracy in the radial dimension compared to the linear dimension, as reported by Kumar et al. (2020).

Table 2.3: Measured value of linear and radial dimension.

Experime ntNo	Average Linear dimension (mm)	Average Radial dimensio n(mm)	ΔL	S/N ratio for linear deviation	ΔR	S/N ratio for radial deviatio n
1	114.57	13.2	0.43	7.33	0.78	2.16
2	114.36	13.3	0.64	3.88	0.74	2.62
3	114.21	13.1	0.79	2.05	0.86	1.31
4	114.34	13.2	0.66	3.61	0.85	1.41
5	114.22	12.8	0.78	2.16	1.18	-1.44
6	114.4	13.4	0.6	4.44	0.63	4.01
7	114.25	12.9	0.75	2.50	1.12	-0.98
8	114.41	13.4	0.59	4.58	0.61	4.29
9	114.2	13.3	0.8	1.94	0.74	2.62

2.7.3 Optimising Dimensional accuracy using RSM

According to the research done by Garg et al., (2022), RSM is used to optimise the process parameters to improve the dimensional accuracy of 3D printing thermoplastic polyurethane (TPU). Three significant process parameters were selected to optimise i.e. Layer Thickness, Infill Density, and Printing Speed with five different levels to fabricate the samples as shown in Table 2.4.

Table 2.4: Different level of selected process parameter

S.No.	Process Parameters	Levels				
		1	2	3	4	5
1	Layer Thickness, LT (mm)	0.1	0.15	0.2	0.25	0.3
2	Infill Density, ID (%)	40	55	70	85	100
3	Printing Speed, PS (mm/s)	10	20	30	40	50

The Central Composite Design (CCD) of Response Surface Methodology (RSM) was employed in the experimental design to minimize the number of samples needed for optimizing process parameters. A total of 20 experimental runs were conducted, consisting of 14 axial points and 6 central points, as outlined in Table 3. These settings were utilized to investigate the dimensional accuracy of TPU material, with cylindrical pins fabricated to dimensions of 12 mm in diameter and 20 mm in length, based on the specified process parameter settings.

Table 2.5: Different process parameter settings and responses

Experimenation Order	Process Parameter			Responses	
	LT (mm)	ID (%)	PS (mm/s)	Length (L) (mm)	Diameter (D) (mm)
1	0.25	85	40	20.29	11.85
2	0.25	55	40	20.17	11.88
3	0.2	100	30	20.25	11.84
4	0.2	70	30	20.15	11.92
5	0.25	85	20	20.23	11.91
6	0.2	70	30	20.17	11.94
7	0.2	40	30	20.26	11.85
8	0.15	55	20	20.22	11.88
9	0.3	70	30	20.24	11.86
10	0.2	70	30	20.16	11.94
11	0.15	55	40	20.24	11.87
12	0.2	70	30	20.16	11.95
13	0.2	70	10	20.16	11.99
14	0.25	55	20	20.15	11.87
15	0.1	70	30	20.28	11.86
16	0.2	70	30	20.18	11.93
17	0.2	70	30	20.18	11.95
18	0.15	85	20	20.18	11.89
19	0.15	85	40	20.25	11.85
20	0.2	70	50	20.17	11.85

The relationship between the three selected FDM process parameters and the two resulting responses was analysed using Response Surface Methodology (RSM). Second-order regression models were developed and analysed using the Minitab software (Version 18). This analysis enabled the identification of optimal process parameter settings.

The research identified that the optimal process parameter to print good dimensional accuracy of TPU material are layer thickness 0.2010 mm, infill density 77.5758%, and printing speed 10 mm/s for obtaining minimum length 20.143 mm and maximum diameter 11.9664 mm with 91.78 % desirability. Also mentioned by Garg et al., (2022), the most important component in getting good dimensional accuracy is LT, followed by PS and ID.

2.8 FDM Material
2.8.1 PLA

Polylactic acid (PLA) is currently the most widely used material in 3D printing, based on current statistics. Its popularity stems from its ease of use due to its low melting point, which simplifies printing processes and reduces the likelihood of warping, thus eliminating the need for heated build plates. PLA is derived from starch-containing products rather than petroleum, unlike ABS, making it a more environmentally friendly option. It is also considered safer for health. However, PLA's main drawback is its lower strength compared to ABS, and it has poor resistance to high temperatures compared to ABS (Kalender et al., 2019). The mechanical and chemical properties of the PLA material are shown in the diagram in Figure 2.15 (*What's the Ideal Filament for FDM 3D Printing? 3D Printing Materials Compared | Hubs*, n.d.). According to Vardhan et al., (2019), PLA material can melt at temperatures between 130 and 180 degrees Celsius, whereas glass transition temperatures fall between 60 and 65 degrees Celsius. PLA is utilised in the production of mould material, screws, plates, microwaveable trays, and dental equipment, bottles, and plastic cups, among other biomedical uses.
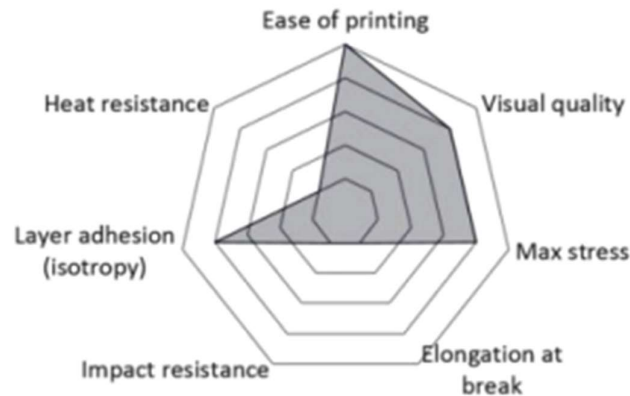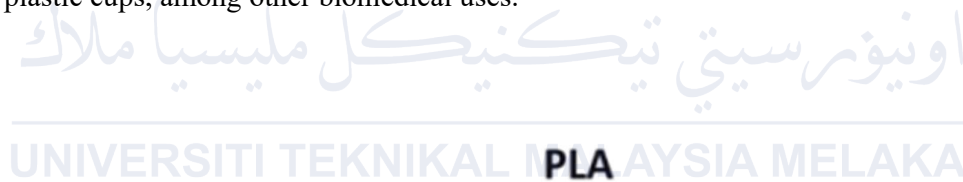
Figure 2.15: Chart of the mechanical and chemical properties of PLA material.

2.8.2 ABS

ABS plastic (Acrylonitrile Butadiene Styrene) is a rigid thermoplastic polymer derived from petroleum. It can be dissolved using acetone. Products printed with ABS are suitable for use within a temperature range of 20 to 80°C. However, its initial melting temperature is 105°C, so exposure to temperatures above 80°C can cause softening and deformation. ABS is also susceptible to degradation from intense UV radiation. Despite these drawbacks, ABS is favored in 3D printing for its high durability and impact resistance. Unlike PLA, ABS requires higher printing temperatures, making calibration more complex. Achieving high-quality prints with ABS can be challenging due to the risk of warping and distortion, particularly with larger parts (Kalender et al., 2019). The mechanical and chemical properties of the ABS material are shown in the diagram in Fig. 5 (*What's the Ideal Filament for FDM 3D Printing? 3D Printing Materials Compared | Hubs*, n.d.)
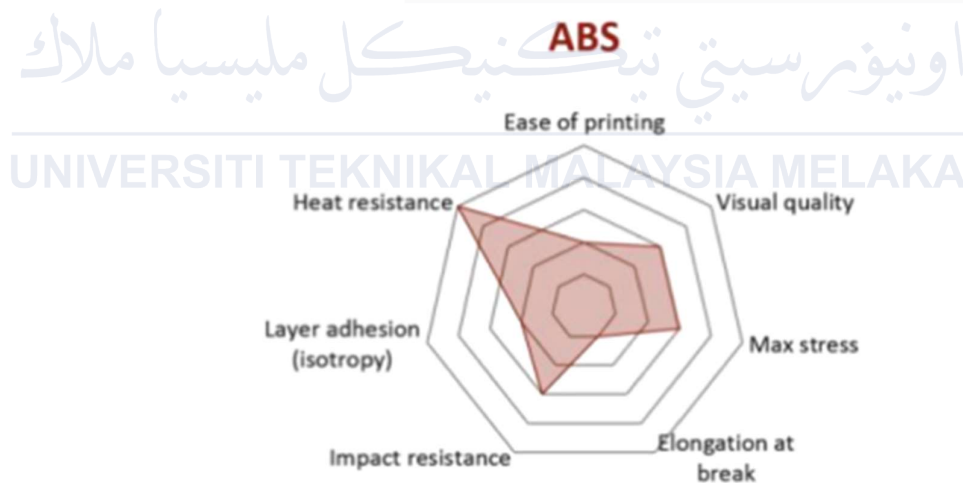
Figure 2.16: Chart of the mechanical and chemical properties of ABS material.

2.9 Vacuum Technology

A vacuum is defined as a space devoid of matter where particles do not exist. Achieving a perfect vacuum in laboratory conditions is unattainable. Therefore, the term "vacuum" typically refers to a region or space with a gaseous pressure lower than atmospheric pressure. For example, at 30 inches of mercury (inHg), atmospheric pressure consists of air molecules constantly colliding with each other.

Vacuum technology finds widespread use across various applications, industries, and research endeavours. The ability to create a vacuum by removing air and fluids enables diverse applications such as drying, food processing, die casting, and resin infusion moulding (Colligon, 2022). One unique property of vacuum is its reduction of air molecules, which diminishes convection by inhibiting the transfer of heat from one molecule to another. Depending on the level of vacuum achieved, heat retention can be prolonged significantly. By decreasing the number of air molecules inside a chamber, vacuum effectively restricts thermal energy transfer via convection (Maidin & Wong, et al., 2018). Therefore, depending on the strength of the vacuum used, heat loss can be minimized and sustained for an extended period (Maidin et al., 2018).

As per the findings presented by (Maidin, Md, et al., 2022), the study underscores the influence of vacuum pressure on the strength of 3D-printed samples, highlighting reductions in stress concentration and mitigation of rapid cooling and heating effects. Results show a notable enhancement in the compressive strength of ABS samples under vacuum pressure. Additionally, comparisons between ABS and PLA samples reveal distinct impacts of vacuum versus atmospheric pressure. Vacuum systems create a space devoid of air molecules, and as pressure increases, the molecule count decreases. Consequently, fluctuations in air pressure significantly affect the thermal behaviour of the samples.

2.9.1 Gases in Vacuum System

The main responsibility of the vacuum engineer, as indicated in Figure 2.17, is to decrease the gas density within a container to a level suitable for its intended use. This is accomplished by attaching a pump to the container, which can either safely release the withdrawn gas into the atmosphere or store it in a condensed form.
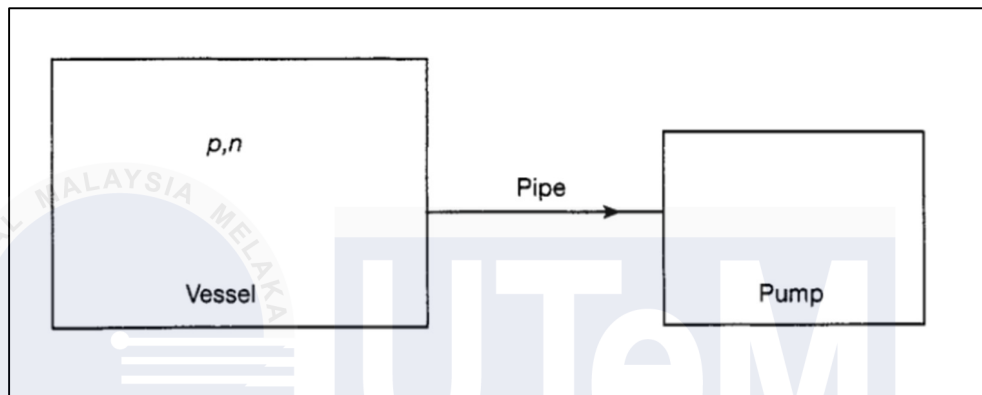
Figure 2.17: Schematic representation of a vacuum system (Steckelmacher, 1991, p38)

Figure 2.17 portrays a schematic representation of a vacuum system, as described by Steckelmacher in 1991 on pages 38 to 42. Irrespective of its intended application, the suitability of the vacuum is determined by the number density (n) of molecules within the vessel. In many cases, the gas pressure (p) itself lacks direct physical significance. Instead, it serves as a convenient measure of vacuum quality through the relationship $p = nkT$ (Steckelmacher, 1991, p38-p42).

Therefore, a vacuum is measured by the total pressure of residual gases in the container. It can be expressed in a variety of units related by the following statement:

1 atmosphere = 760 torr = 1013 millibar = 1.013 x 105pascal

The table should present data on number density (n), mean free path (λ), and impingement rate (J) for various pressure values at a representative scale. Table 2.6 showcase information for nitrogen gas (N_2) at 22 °C (295 K), which is the main component of air.

Table 2.6: n, λ, and J at various p for N_2 at 295 K.

p (mbar)	n (m^{-3})	λ	J ($cm^{-2} \, s^{-1}$)
10^3 = 1 atm	2.5×10^{25}	6.6×10^{-6} cm	2.9×10^{23}
1	2.5×10^{22}	6.6×10^{-3} cm	2.9×10^{20}
10^{-3}	2.5×10^{19}	<u>6.6 cm</u>	2.9×10^{17}
10^{-6} , HV	2.5×10^{16}	66 m	<u>2.9×10^{14}</u>
10^{-10} , UHV	2.5×10^{12}	660 km	2.9×10^{10}

The number density, represented by 'n,' undergoes significant fluctuations across a vast range. In a conventional high vacuum at 10^{-6} mbar, which is one billionth of atmospheric pressure, the value of 'n' is remarkably reduced. However, even in ultra-high vacuum (UHV) conditions at 10^{-6} mbar, the number density remains notably high at 2.5 x 10^{12} per m³ or equivalently, 2.5 x 10^6 per cm³.

As the pressure decreases, the mean free path ('λ') increases. For instance, at a pressure of 10^{-4} mbar, where 'λ' equals 66 cm, the dimensions are comparable to those of ordinary containers. The impingement rate ('J') is substantial regardless of the applied force. Notably, at 10^{-6} mbar, the impingement rate is 2.9 x 10^{-14} $cm^{-2}s^{-1}$, and its significance lies in the fact that, according to the preceding table, a surface would be entirely coated with adsorbed gas in approximately three seconds at this pressure. This implies that the formation time for a monolayer at millibar pressures is on the order of seconds.

Analysing the values in Table 2.6, one can infer that in a cubic vessel with a side length of 0.5 m (a typical size, though not shape), the rates would be comparable at 10^{-3} mbar. However, at 10^{-6} and 10^{-10} mbar, surface collisions would dominate by factors on the order of one thousand and ten million, respectively. Consequently, surfaces play a crucial role in influencing the condition of the gas within at these vacuum levels. Inside the gas molecule body, molecule-to-molecule collisions are infrequent and generally inconsequential.

2.9.2 Application of vacuum Technology in AM

Vacuum-assisted printing has been demonstrated to significantly enhance dimensional accuracy and production quality in various additive manufacturing processes. The integration of vacuum technology in additive manufacturing, also known as 3D printing, has garnered significant attention due to its potential to revolutionize various industrial sectors, including aerospace, automotive, semiconductor, and biomedical applications (Bastin & Huang, 2022; Caminero et al., 2019).

Research has shown that the use of vacuum systems can improve dimensional accuracy in different materials and printing techniques. For example, studies on acrylonitrile butadiene styrene (ABS) and polylactic acid (PLA) samples printed in a vacuum-assisted material extrusion system revealed notable enhancements in dimensional accuracy (Shahrum, 2024). Vacuum-assisted fused deposition modeling (FDM) has been recognized as a method to enhance printing quality by improving bonding between layers, thus contributing to better dimensional accuracy (Syrlybayev et al., 2021). Additionally, vacuum-assisted microcontact printing has been employed for aligned patterning of nano and biochemical materials, demonstrating the effectiveness of vacuum assistance in achieving precise and uniform pressure control for improved accuracy (Kang et al., 2013).

The incorporation of vacuum technology into additive manufacturing processes has also enhanced the production of components with complex geometries and improved the quality of manufactured products (Carneiro et al., 2019; Rana et al., 2021). For instance, the combination of additive manufacturing and investment casting with vacuum assistance has been explored to produce thin-rib and high aspect-ratio scaffolds (Carneiro et al., 2019). Additionally, vacuum use has been shown to reduce void content in manufactured laminates, thereby improving the structural performance of composites (Rana et al., 2021).

Moreover, the extension of vacuum-assisted multipoint molding (VAMM) technology to a broader field of geometries has led to the development of enhanced vacuum-assisted multipoint molding with additive attachments (EMMA) technology (Herzog et al., 2022). This advancement demonstrates continuous innovation and integration of vacuum technology in additive manufacturing processes to expand its capabilities.

Furthermore, the vacuum-assisted resin transfer molding (VARTM) process, which utilizes vacuum to assist in the manufacturing of lightweight, large complex composite

components, has been identified as a cost-effective technique (Ouezgan et al., 2022). This highlights the potential of vacuum technology to optimize the manufacturing process and reduce production costs in additive manufacturing.

For example, a study on 3D printed liquid crystal polymer (LCP) thermosiphons highlighted the potential of LCPs for creating vacuum-tight components with intricate geometries, underscoring the role of vacuum in achieving functional design possibilities (Seshadri et al., 2023). Additionally, vacuum-assisted printing techniques have been investigated in the fabrication of perovskite films for photovoltaic applications, showing improved device performance and reproducibility, especially in high humidity environments (Parvazian et al., 2019).

In summary, the use of vacuum assistance in printing processes has proven to be a valuable technique for enhancing dimensional accuracy and production quality across various materials and applications. By establishing a controlled environment with reduced pressure, vacuum-assisted printing methods contribute to improved bonding, precise patterning, and overall better quality in additive manufacturing processes. The integration of vacuum technology continues to drive innovation and expand the capabilities of additive manufacturing, promising significant advancements in various industrial sectors.

2.10 Process Parameter of FDM

Several parameters exert a dominant influence on the characteristics of built parts and their production efficiencies in additive manufacturing. Key factors include the thickness of the layer, raster angle, build orientation, density of infill, printing speed, infill pattern, extrusion temperature, raster width, nozzle diameter, contour width, contour-to-contour airgap, and the number of contours. These parameters collectively impact various aspects such as the quality, strength, dimensional accuracy, and overall performance of 3D-printed parts. Optimal adjustment of these factors is critical for achieving desired outcomes and maximizing the effectiveness of additive manufacturing processes (Dey & Yodo, 2019).

2.10.1 Layer Thickness & Layer Height

Layer height refers to the amount of material deposited along the vertical axis of an FDM machine in a single pass, always less than the nozzle diameter of the extruder and entirely dependent on the extruder tip diameter. In their experimental studies, (Elena Verdejo de Toro et al. (2020) demonstrated that layer height significantly influences the bending and impact properties of fabricated components. They found that a minimum layer thickness enhances bending properties, while an increased layer thickness improves impact properties. Additionally, Barrios & Romero (2019) utilized an orthogonal experimental design to determine optimal values for various printing parameters, including layer height. Their study aimed to reduce the angle of slide and surface roughness in FDM printed components, with layer height being one of the key factors. The graphical illustration of these parameters, including layer height, is shown in Figure 2.18: Parameter involve in FDM source: (Barrios & Romero, 2019)
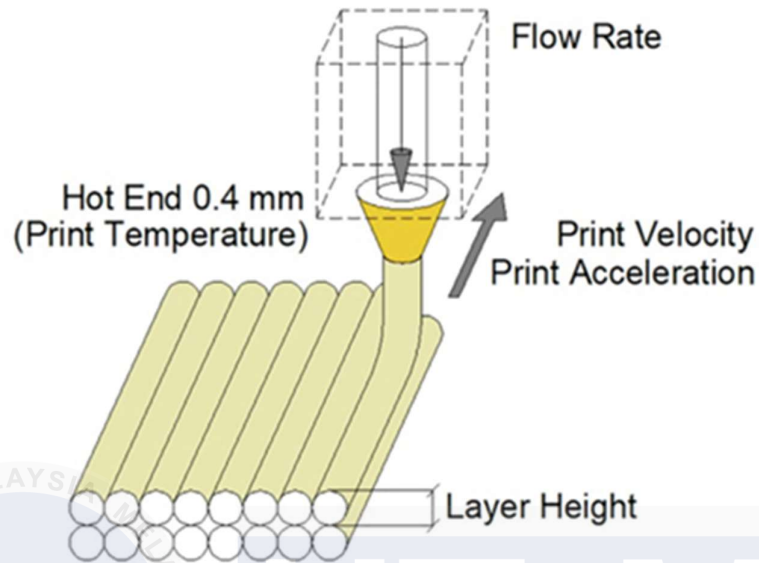
Figure 2.18: Parameter involve in FDM source: (Barrios & Romero, 2019)

2.10.2 Raster Angle

The raster angle denotes the direction of material deposition along the build area's x-axis in the employed FDM machine. Typically, raster angles can range from 0 to 90 degrees (Rayegani & Onwubolu, 2014). (Wu et al., 2015) conducted an experimental study to investigate the influence of raster angle (45°, 30°, and 0°) and layer thickness (400 μm, 300 μm, and 200 μm) on the properties of 3D printed parts using a high-performance material, polyether-ether-ketone (PEEK). The schematic depiction of the raster angles utilized in this investigation is illustrated in Figure 2.19.
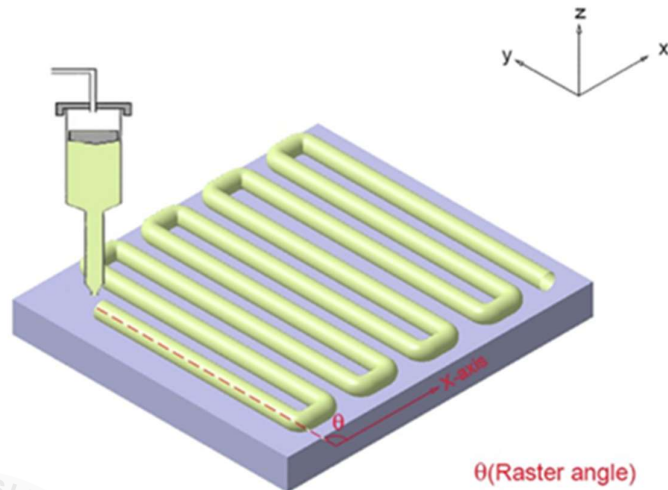
Figure 2.19: Graphical illustration of the raster angle Source: (Wu et al., 2015)

2.10.3 Printing speed

According to Solomon et al., (2020), the printing speed can be defined as the rate at which the build nozzle traverses and deposits material on the build platform along the XY plane. The time taken to print a component directly correlates with the printing speed. Higher printing speeds are known to induce greater deformation in the build component due to increased residual stress from faster material deposition. However, the influence of printing speed is less pronounced when printing thinner layers.

2.10.4 Print temperature

According to Maidin et al., (2022), the printing temperature regulates the temperature of the extruding nozzle. Further research investigated the effects of temperature on ABS printed parts. Non-uniform temperature gradients can lead to stress accumulation, resulting in dimensional inaccuracies and internal cracking due to rapid heat dissipation. Temperature differences affect conduction and convection, hastening material solidification. This thermal dynamic can cause melting of previous layers when new layers are added, leading to inconsistent temperature fluctuations and increased stress.

2.10.5 Infill Density

Infill density is a critical factor in determining the mechanical properties and dimensional accuracy of 3D printed parts. Rath & Pandey, (2020) recommend an infill density of over 20% for ensuring good durability of 3D printed parts. Pandžić et al., (2019) emphasize that infill type and density are key parameters affecting the mechanical properties of 3D printed materials. Ganeshkumar et al., (2022) point out that infill helps in reducing material usage, printing time, and maintaining the aesthetics of the products.

Optimizing infill density is crucial for achieving desired mechanical properties. Studies by Jung (2023) and Latiff (2024) demonstrate the impact of infill density on the mechanical properties of 3D printed parts. Latiff (2024) identifies 20% as an optimized infill density for specific 3D printed structures, while Jung (2023) explores different infill densities (20%, 50%, and 80%) and patterns (zigzag, triangle, honeycomb) to understand their effects on the printed cubes.

Moreover, the literature suggests that infill density influences various properties of 3D printed materials. Şirin et al. (2022) highlight the importance of infill density and build orientation on the mechanical properties of 3D printed specimens. Mayandi (2024) found that increasing fiber content and infill density enhances the flexural strength and modulus of 3D printed polymer composites. Additionally, Öztürk (2024) notes that Fused Filament Fabrication (FFF) allows for a wide range of infill densities and geometric variations in 3D printed polymers.

In conclusion, infill density significantly impacts the mechanical properties and dimensional accuracy of 3D printed parts. While a general recommendation of over 20% infill density exists for durability, the optimal infill density may vary based on the specific application and material used. Researchers continue to explore the effects of different infill densities on mechanical properties to guide the optimization of 3D printing parameters for desired outcomes.

2.11 Summary

Chapter 2 of this report provides an extensive literature review on Additive Manufacturing (AM), focusing particularly on the critical aspect of dimensional accuracy in Fused Deposition Modelling (FDM). The chapter begins by defining AM and outlining its evolution since the 1980s. It emphasizes AM's unique layer-by-layer manufacturing process, which allows for unprecedented design freedom, complex geometries, and efficient material use compared to traditional subtractive methods. The chapter discusses the various categories of AM technologies, highlighting material extrusion as the most relevant to this study. FDM, a prevalent form of material extrusion, is examined in detail, underscoring the importance of process parameters such as layer thickness, print speed, and infill density in achieving high-dimensional accuracy. These parameters significantly affect the mechanical properties and precision of the printed parts.

Several previous studies are reviewed to understand the factors influencing dimensional accuracy in FDM. Key findings from these studies include material properties and process parameters. PLA and ABS are the primary materials discussed. PLA, being biodegradable and easier to print with due to lower melting points, offers higher dimensional accuracy but is less durable than ABS. ABS, though more challenging to print due to higher melting points and warping issues, provides better strength and durability. The chapter highlights the critical role of process parameters such as temperature, build orientation, layer height, and infill density. For instance, studies indicate that lower layer heights generally improve dimensional accuracy but may increase print time. Optimal print temperatures are crucial to minimize warping and ensure consistent layer adhesion.

The measurement and optimization techniques are also discussed in depth. The use of Coordinate Measuring Machines (CMM) for precise measurement of printed parts' dimensions is emphasized. The Response Surface Methodology (RSM) is identified as an effective statistical tool for optimizing process parameters to achieve the best dimensional accuracy. Previous studies using RSM have demonstrated significant improvements in dimensional accuracy by systematically varying and optimizing process parameters. Additionally, the integration of vacuum technology in FDM is explored. The literature suggests that vacuum-assisted printing can enhance dimensional accuracy by reducing air

entrapment and improving layer adhesion. Studies comparing vacuum-assisted and atmospheric pressure printing have shown that vacuum conditions generally yield better dimensional accuracy.

This literature review sets a solid foundation for the subsequent research, which aims to optimise these parameters to improve the dimensional accuracy on the printed samples. This comprehensive review of previous studies not only highlights the challenges and advancements in achieving high-dimensional accuracy in FDM but also underscores the importance of continued research and optimisation in this field.

CHAPTER 3
METHODOLOGY

3.1 Introduction and Overview

This chapter describes the methodology applied to the research and the proposed framework for this study. Then, the collection of ideas, planning process, simulation, and data testing proposal will be presented after close attention to the specification and the previous study. Finally, the primary technique suggests practical methods, tools, and processes for this investigation.

3.2 Flow Chart

3.2.1 Flow Chart Project

This project was carried out in the experiment of projects one and two, as illustrated in Figure 3.1 below. The PSM 1 project flow focused on objective one for the experiment: the study of the title selection, objective identifying, determining problem statement, research, literature review, and lastly, designing the methodology. In addition, the project of PSM 2 expressed objectives two and objective 3, which are printing the sample, testing and examination, and optimizing the data. The data gathered from the testing will go through the analysis to achieve objective 3. Finally, the value of the analysis will go through the result and discussion session, and if all project aims are achieved, the experiment result will conclude and end.
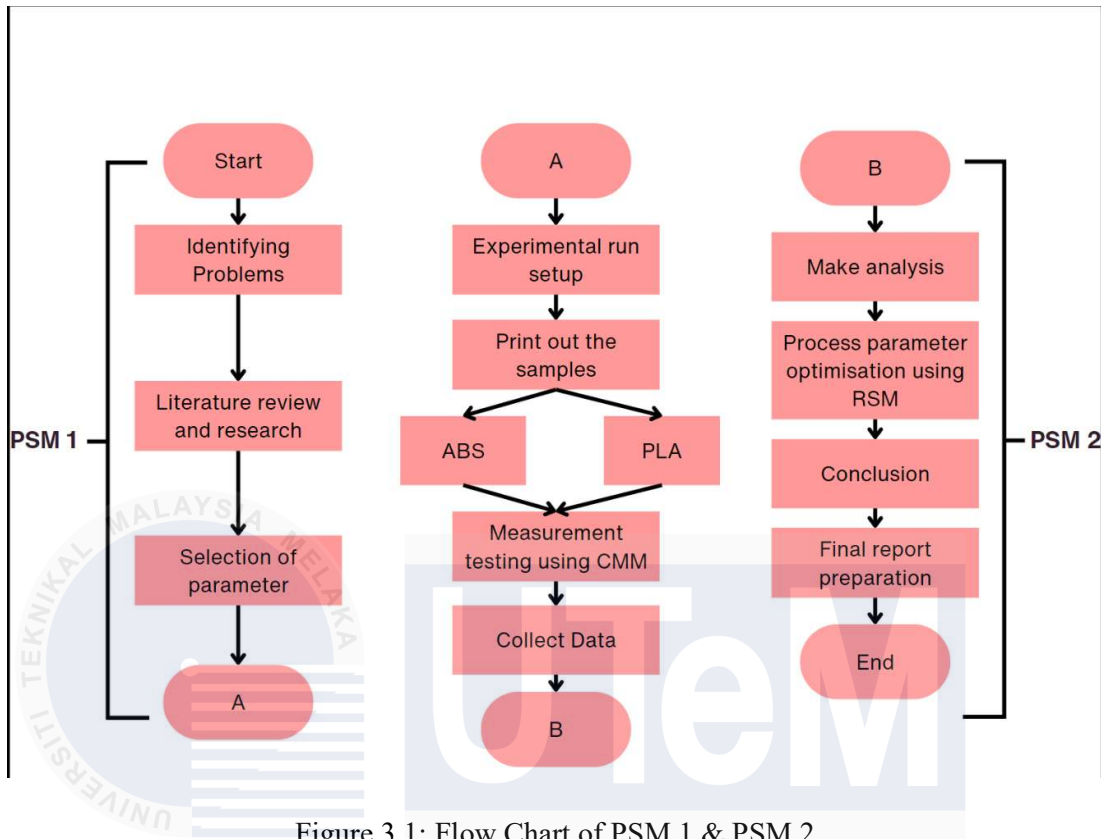
Figure 3.1: Flow Chart of PSM 1 & PSM 2

3.3 Experimental Equipment

3.3.1 Ultimaker S3 3D Machine

The Ultimaker S3 stands at the forefront of 3D printing technology, epitomizing the synthesis of cutting-edge innovation and user-friendly design. As part of the esteemed Ultimaker brand, founded in the Netherlands in 2011, it embodies a commitment to delivering high-quality, accessible 3D printing solutions. Renowned for its precision and versatility, the Ultimaker S3 caters to both professionals and enthusiasts with its robust build volume, dual extrusion capabilities, and advanced features like active bed leveling. Beyond its technical prowess, Ultimaker fosters a global community of users, embracing an open-source philosophy that encourages collaboration and knowledge sharing. The brand's dedication to empowering creative minds has solidified its status as a global leader, making Ultimaker and its flagship S3 model the go-to choice for those seeking reliable, high-performance 3D printing solutions.

Figure 3.2: Ultimaker S3

Table 3.1: Ultimaker S3 Specifications

Brand: Ultimaker S3	
Material to be Printed	PLA ABS
Weight	20.6 kg
Printer Dimension	394 x 489 x 637 mm
Build Volume	230 x 190 x 200 mm
Print Technology	Fused Filament Fabrication (FFF)
Software	Ultimaker Cura

The SOP of the Ultimaker S3:

1. Power on the Ultimaker S3 3D printer by connecting it to a stable power source and turning on the power switch.
2. Load the desired filament into the Ultimaker S3 following the filament loading procedures outlined in the user manual.
3. Calibrate the print bed using the active bed levelling system on the Ultimaker S3, referring to the detailed instructions in the user manual.
4. Calibrate the print cores (nozzles) to ensure accurate printing by following the procedures outlined in the user manual.
5. Design or import a 3D model using compatible 3D modeling software, ensuring the model is in a supported file format.
6. Choose appropriate print settings in Ultimaker Cura, including layer height, print speed, and temperature, adjusting settings based on the filament type.
7. Transfer the prepared 3D model to the Ultimaker S3 using Ultimaker Cura or a connected device.
8. Select the 3D model and adjust print settings as necessary using the Ultimaker S3 interface or touchscreen.

9. Initiate the 3D printing process through the Ultimaker S3 interface or touchscreen, monitoring initial layers for proper adhesion.

10. Monitor the print progress through the Ultimaker S3 interface or touchscreen, addressing any issues promptly.

11. Allow the print to cool on the Ultimaker S3 build plate, and if necessary, perform post-processing such as removing support structures.

12. Turn off the Ultimaker S3 3D printer once the print is complete.

13. Clean the print bed and nozzles as needed following guidelines in the user manual and perform routine maintenance tasks.

14. If changing filament, follow the manufacturer's instructions to safely unload the filament.

15. Record relevant information, such as print settings and any encountered issues, and refer to the troubleshooting section in the Ultimaker S3 user manual if needed.
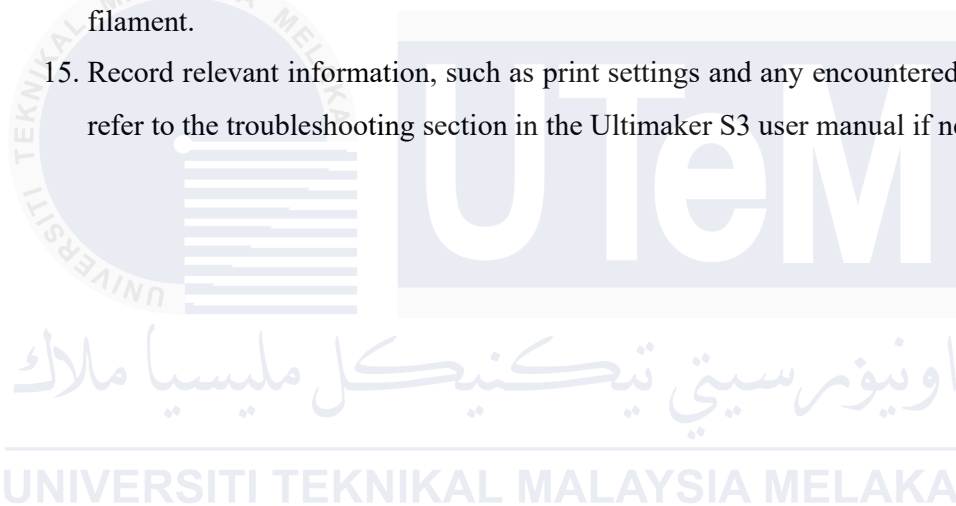
3.3.2 Coordinate Measuring Machine (CMM)

A coordinate measuring machine (CMM) is a device used to measure the geometry of physical objects by sensing discrete points on the object's surface. It typically consists of a rigid structure, a measurement probe, and a computer system. The probe can be moved manually or computer-controlled along the x, y, and z-axes to gather points, forming a "point cloud" that represents the object's shape. CMMs are used for quality control in manufacturing to ensure that components meet tolerance specifications. There are various types of CMMs, including bridge, gantry, cantilever, portable measuring arm, and optical CMMs, each with its own advantages and applications (*What Is CMM | Coordinate Measuring Machine Types*, n.d.).

The three axes of the CMM's machine coordinate system trace map coordinates like our fingertips. The CMM employ a probe rather than a finger to measure point on a workpiece. Each point on the workpiece is distinct in the machine's coordinate system. In a three-dimensional Cartesian coordinate system, the conventional 3D "bridge" CMM permits probe movement over three orthogonal axes, X, Y, and Z. Figure 3.3 shown the example of CMM.

Figure 3.3: Coordinate Measuring Machine

The SOP of CMM is stated as below:

1. Check the measuring device's environment, machine, and component temperatures.
2. In addition to checking the air pressure, cleaning the worktable's surface and the guide rail of the measurement machine, and draining the oil and water from the filter,
3. Run for a while to ensure the host, control system, and software are all functional.
4. Look at the component designs, understand the measurement standards and methods, develop an inspection plan, or describe the inspection technique.
5. Adhere to the crane's safety operating regulations to prevent damage to the measurement apparatus and its components. The Abbe error is diminished and ultimately rectified, and the parts are placed in a testing-friendly location.
6. Install the probe and its attachments following the measurement plan, press the emergency stop button before beginning, and handle and release the probe with sufficient force. Verify that the probe protection feature is functioning correctly after replacing the probe.
7. After ensuring that the programming is accurate, proceed with the measurement at the average speed.
8. Press emergencies stop right away to stop any anomalous scenario, protect everyone's safety, and alert the maintenance team so they can make repairs.
9. Archive the measurement programme, programme operation settings, and probe configuration, and disassemble (replace) the parts once the test is over.
10. Return to the starting position, remove the components, deactivate the measurement device and any associated power sources, and tidy up the workspace.

3.3.3 Chamber and Vacuum Pump

A vacuum chamber and vacuum pump are required to regulate the pressure for some of the samples produced under vacuum. The utilised had an internal size of 350x390x400 mm and the thickness of 12 mm and it was made of acrylic. The oil- flooded vacuum pump was then used to remove air atoms from the vacuum chamber until the pressure was maintained at 20 kPa. The vacuum chamber and pump utilised for this project are shown in Figure 3.4
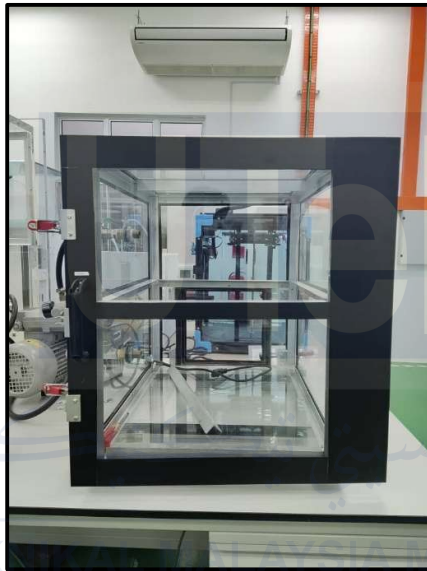
Figure 3.4: Vacuum Chamber and Vacuum pump

3.3.4 Setting Parameter

A lot of Process parameters, such as nozzle and build temperature, printing speed, and layer thickness, are adjustable in the most FDM machine. The most of process parameters have been defined during the finding in the literature review. Depending on the material like ABS and PLA used in this project, the process parameters is adjusted accordingly. The process parameters for FDM printing with PLA and ABS materials are as follows:

- ❖ Temperature: The ideal extruder temperature for PLA is generally between 185-220ºC, whereas for ABS, it is between 220-260ºC (Maurya et al., 2019; Vardhan et al., 2019).
- ❖ Bed Temperature: The best bed temperature for PLA is around 50-60ºC.while the optimal bed temperature for ABS is around 90-110ºC.
- ❖ Printing Speed: Depending on the layer thickness and other conditions, the optimum print speed from 30 to 60mm/s (Beniak et al., 2019).
- ❖ Layer Thickness: A layer thickness of 0.1-0.2 mm for FDM printing with PLA and ABS is generally considered optimum (Dey & Yodo, 2019; Kam et al., 2023).

To reduce the variable parameters needed to be optimised, the fixed process parameters for ABS and PLA are indicated in the table below.

Table 3.2: Fixed process parameters

Parameter	values
Printing Temperature (ºC)	245 for ABS and 200 for PLA
Bed Temperature (ºC)	95 for ABS and 60 for PLA
Material	ABS and PLA
Raster angle (º)	0
Layer Thickness (mm)	0.15

Process parameters that are vital in the dimensional accuracy of part were selected to optimise the process parameters. The selected process parameter is varied at three levels each that shown below in table.

Table 3.3: Levels of selected process parameters

No	Process Parameters	Level		
		-1	0	1
1	Infill Density, ID (%)	20	55	80
3	Printing Speed, PS (mm/s)	30	45	60
		1	2	
4	Printing Pressure, (Kpa)	101.3 (1 atm)	20	

The selected process parameter to be optimise were obtained from the journal and previous studies have shown that infill densities ranging from 20% to 80% can be effective for achieving good dimensional accuracy in ABS and PLA parts. For example, an infill density of 80% has been identified as optimal for enhancing tensile properties in PLA specimens (Heidari-Rarani et al., 2020). Additionally, an infill density of 75% has been recommended for improving tensile strength in bi-layered printed PLA-ABS parts (Rasheed, 2023). However, limited studies have been done to study the effect of infill density to the dimensional accuracy which will be conducted in this project. Moreover, printing speed within the range of 30-60 mm/s could be suitable for printing ABS and PLA materials (Mourya, 2023; Naveed, 2024; Unger et al., 2018). Finally, this project also investigates the comparison of dimensional accuracy between printed samples printed at atmospheric pressure and 20 kPa vacuum pressure.

3.4 Design of Experiment (DOE)
3.4.1 Response Surface Methodology (RSM)

Response Surface Methodology (RSM) is a valuable experimental technique employed to analyse and resolve problems by investigating relationships between predictors and responses, aiming to identify influential variables on product quality and properties and optimise process parameters within a specified region of interest (Mohamed et al., 2016). In this study, the impact of processing parameters on Length, Width, Thickness, Corner Diameter, Hole Diameter, and Perpendicularity was explored through a RSM model, encompassing 3 factors at varying levels with a total of 26 runs for each material. Statistical data collected during experimentation were analysed using Design Expert software to develop the experimental plan and generate mathematical models, ensuring precision in parameter prediction and estimation. The emphasis on accurate planning and meticulous execution of the experimental study underscores the commitment to reliable outcomes for optimising the processing parameters.

3.5 Experimental Preparation and Procedure
3.5.1 Experiment Set Up

The samples, which measures 5 cm x 2.5 cm x 0.3 cm, was manufactured using ABS and PLA material on a Ultimaker S3 3D printer. The printing process's parameters will be set up to achieve the highest level of dimensional accuracy. The CMM then examined the printed samples. Geometrical analysis was performed on corner diameter, length, thickness, perpendicularity, width, and hole diameter. The gathered data were combined, and the target dimension of the product's CAD design was examined. Figure 3.5 and Figure 3.6 depicts the printing process in its entirely.
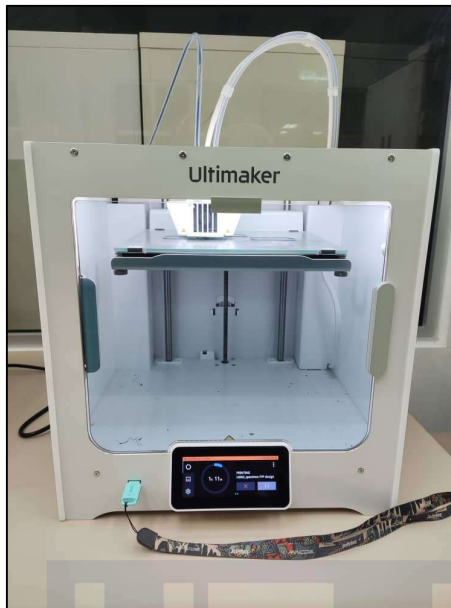
Figure 3.5: Sample printing set up for atmospheric
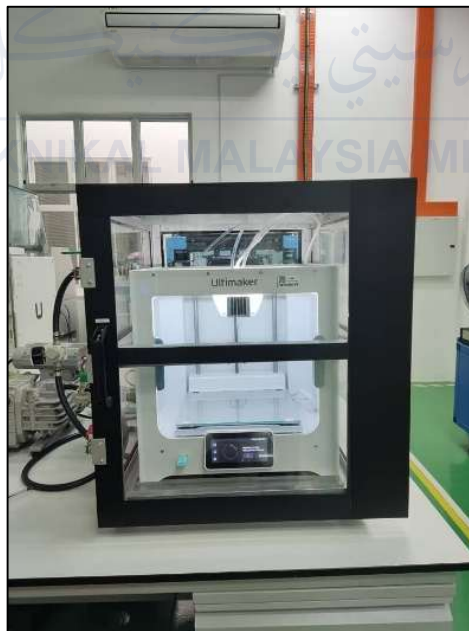
Figure 3.6: Sample printing set up for printing in vacuum pressure

3.5.2 Dimensions Measured
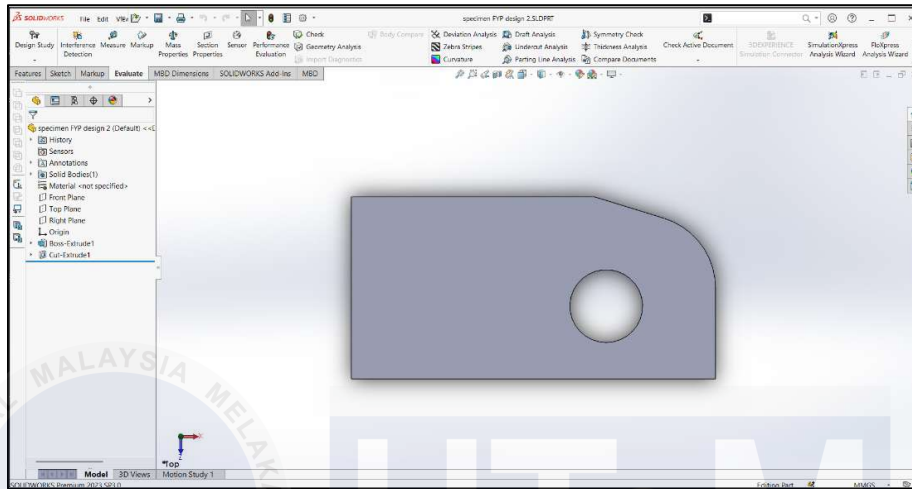
Figure 3.8: 2D Drawing of the sample.
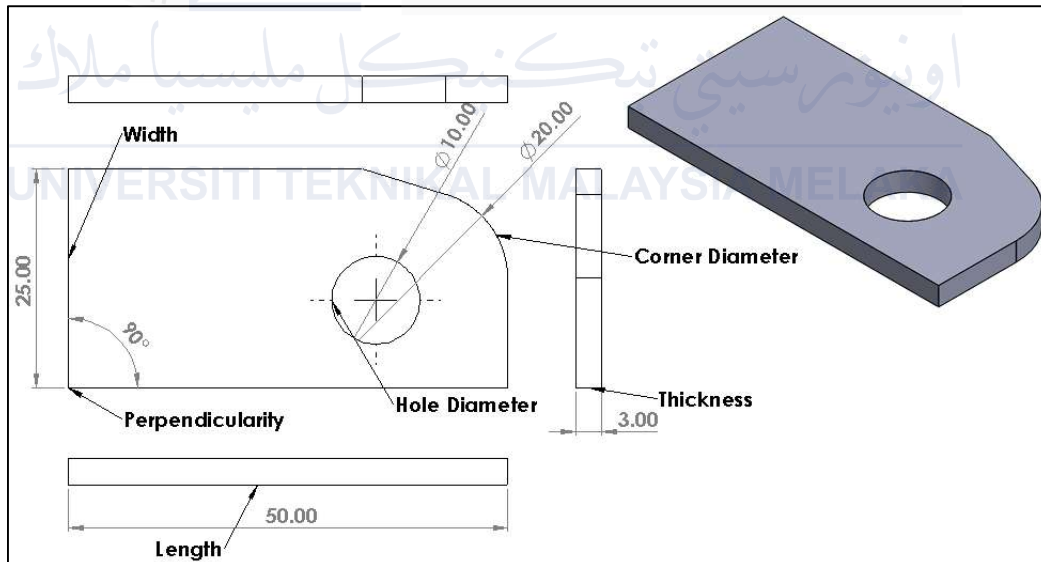
Figure 3.7: Drafting of the design.

58

Figure 3.8 shows the design drawing, whereas Figure 3.7 shows the drawing drafting. All the printed sample will be measured using the CMM. The list of geometries dimensions of the sample is shown in the Table 3.4 below as follows:

Table 3.4: Geometry dimensions of 3D model samples to be measured.

Geometry	Dimension
Length, mm (L)	50
Width, mm (W)	25
Thickness, mm (T)	3
Corner Diameter (CD)	20
Hole Diameter, mm (HD)	10
Perpendicularity, degree (P)	90

Table 3.5: Plan experimental run per material.

Experimentation Order	ID (%)	PS (mm/s)	PP (Kpa)	L (mm)	W (mm)	T (mm)	HD (mm)	CD (mm)	P (Degree)
1	55	66.2132	101.3						
2	55	45.0000	20						
3	80	45.0000	101.3						
4	20	60.0000	101.3						
5	55	66.2132	20						
6	55	45.0000	101.3						
7	80	45.0000	20						
8	20	45.0000	20						
9	55	45.0000	101.3						
10	20	60.0000	20						
11	55	45.0000	101.3						
12	80	30.0000	20						
13	80	60.0000	20						
14	80	30.0000	101.3						
15	55	45.0000	20						
16	80	60.0000	101.3						
17	55	23.7868	20						
18	20	30.0000	20						
19	55	23.7868	101.3						
20	55	45.0000	20						
21	55	45.0000	20						
22	20	45.0000	101.3						
23	20	30.0000	101.3						
24	55	45.0000	101.3						
25	55	45.0000	20						
26	55	45.0000	101.3						

Central composite design (CCD) of response surface methodology (RSM) based experiment design effectively reduces the number of samples needed for process parameter optimization. This approach utilizes a total of 26 experimental designs per material, with the parameter settings detailed in Table 3.5

3.6   Summary

The methodology of the project is intricately designed, guided by a comprehensive flow chart that delineates the sequential steps of the entire process. This visual representation aids in maintaining a structured approach throughout the project. The experimental setup comprises essential equipment such as the Ultimaker S3 for 3D printing, a Coordinate Measuring Machine (CMM) for precision measurements, and auxiliary components like a chamber and vacuum pump. These elements collectively contribute to the controlled environment necessary for the experiment.

In adherence to meticulous procedures, the Ultimaker S3 and CMM have designated Standard Operating Procedures (SOPs) for optimal utilization. The Ultimaker S3 serves as a pivotal tool for additive manufacturing, while the CMM ensures accurate measurements crucial for the experiment's success. The chamber and vacuum pump are integral to creating and maintaining the desired experimental conditions.

Parameter settings play a crucial role in the experiment, and a strategic division is made between fixed process parameters and those earmarked for optimisation using Response Surface Methodology (RSM). This approach allows for the systematic enhancement of variables to achieve the desired outcomes. The dimensional measurements, critical to the experiment, are conducted using the CMM, with specific dimensions outlined alongside drawings and 3D models. This ensures precision and consistency in the measurement process, contributing to the reliability of the experimental results.

CHAPTER 4
RESULT AND DISCUSSION

This chapter primarily focuses on presenting the data collected after completing the sample fabrication and testing experiment. It will include hypotheses and discussions supported by previous research, particularly concerning the effects of infill density and vacuum pressure.

4.1 Introduction

Due to the time constraint to conduct the planned experiment run for both materials, the number of process parameters to be optimised were reduced into two. Hence, the number of samples required for the experimental run will also reduce into six from 26 samples for both materials. The printing speed that initially included in the experimental plan will be fixed at 45 mm/s at the middle of the suitable range for printing ABS and PLA. The sample result obtained from the measurement testing via CMM and inserted to the Design Expert software for the process parameters optimisation. Table 4.1 and Table 4.2 shows the result of the experimental run for ABS and PLA samples.

Table 4.1: Experimental run for ABS printed samples

Run	A: Infill Density	B: Printing Pressure	Length	Width	Thickness	Corner Diameter	Hole Diameter	Perpendicularity
	%	Kpa	mm	mm	mm	mm	mm	Degree
1	80	101.3	49.6386	24.7893	3.06475	20.9837	9.7864	89.9775
2	55	101.3	49.692	24.7735	3.073	19.6177	9.79433	89.9573
3	20	20	49.8098	24.8306	2.8668	19.9104	9.8708	89.8347
4	55	20	49.9191	24.9195	3.024	20.0497	9.97983	89.986
5	80	20	50.1531	25.1145	3.0858	19.9684	9.8423	89.9865
6	20	101.3	49.6709	24.795	2.9226	19.204	9.7931	89.994

Table 4.2: Experimental run for PLA printed samples

Run	A: Infill Density	B: Printing Pressure	Length	Width	Thickness	Corner Diameter	Hole Diameter	Perpendicularity
	%	Kpa	mm	mm	mm	mm	mm	Degree
1	80	101.3	49.9356	25.0703	3.0064	22.5225	9.7271	89.963
2	55	101.3	50.0098	25.1412	3.0174	19.1414	9.8518	89.9737
3	20	20	49.9666	25.2031	3.0403	20.0145	9.6913	89.987
4	55	20	49.8811	25.014	3.08343	20.1437	9.84617	89.8223
5	80	20	49.9931	25.0377	3.0012	19.9892	9.9675	89.988
6	20	101.3	50.0203	25.1977	3.0504	21.2546	9.8677	89.963

4.2 ABS Printed sample Result.

Table 4.3 below shows the result of the measurements of ABS sample tested using CMM. The table shows the nominal accuracy and the actual result obtained. On the other hand, Table 4.4 shows the percentage of accuracy of the actual value relative to the nominal value. These two tables will help to identify the degree of accuracy that can be used as a reference for printing.

Table 4.3: Nominal Accuracy vs Actual Value

Geometry	Nominal Value	Actual Value		
		20% ID	55% ID	80% ID
Length, mm	50	49.6709	49.692	49.6386
Width, mm	25	24.7942	24.7735	24.7893
Thickness, mm	3	3.0314	3.073	3.0648
Corner Diameter, mm	20	19.8245	19.6177	20.9837
Hole Diameter, mm	10	9.8931	9.7943	9.7864
Perpendicularity, Degree	90	89.994	89.9573	89.9775

Table 4.4: Percentage of Accuracy of ABS Samples

Geometry	Percentage Accuracy, %		
	20% ID	55% ID	80% ID
Length, mm	99.34	99.38	99.28
Width, mm	99.18	99.49	99.16
Thickness, mm	97.42	97.62	97.89
Corner Diameter, mm	96.02	98.09	95.31
Hole Diameter, mm	97.93	97.94	97.86
Perpendicularity, Degree	99.99	99.95	99.98
Average percentage accuracy	98.31	98.75	98.25

Nominal value vs Actual value of Atmospheric ABS sample

	Length, mm	Width, mm	Thickness, mm	Corner Diameter, mm	Hole Diameter, mm	Perpendicularity, Degree
Nominal Value	50	25	3	20	10	90
Actual Value 20% ID	49.6709	24.795	2.9226	19.204	9.7931	89.994
Actual Value 55% ID	49.692	24.7735	3.073	19.6177	9.7943	89.9573
Actual Value 80% ID	49.6386	24.7893	3.0648	20.9837	9.7864	89.9775

Figure 4.1: Nominal Accuracy vs Actual value of ABS sample

Percentage Accuracy of Atmospheric ABS printed samples

	Length, mm	Width, mm	Thickness, mm	Corner Diameter, mm	Hole Diameter, mm	Perpendicularity, Degree
Percentage Accuracy, % 20% ID	99.34	99.18	97.42	96.02	97.93	99.99
Percentage Accuracy, % 55% ID	99.38	99.49	97.62	98.09	97.94	99.95
Percentage Accuracy, % 80% ID	99.28	99.16	97.89	95.31	97.86	99.98

Figure 4.2: Percentage Accuracy of Atmospheric ABS printed samples

The Table 4.3 shows the comparison between nominal and actual values of ABS samples printed at different infill densities (20%, 55%, and 80%) in atmospheric pressure reveals noteworthy insights into dimensional accuracy. For length, with a nominal value of 50 mm, the deviations are minimal, with actual values of 49.6709 mm, 49.692 mm, and 49.6386 mm for 20%, 55%, and 80% ID respectively, showing the closest approximation at 55% ID. Width, with a nominal value of 25 mm, also shows minimal deviations with actual values of 24.7942 mm, 24.7735 mm, and 24.7893 mm, again demonstrating the highest accuracy at 55% ID. Thickness values, with a nominal value of 3 mm, tend to be slightly higher, especially at 55% ID, with actual values of 3.0314 mm, 3.073 mm, and 3.0648 mm, indicating a marginal over-deposition of material. The corner diameter, nominally 20 mm, shows significant deviations, particularly at 80% ID, with actual values of 19.8245 mm, 19.6177 mm, and 20.9837 mm, suggesting over-extrusion at higher densities. Hole diameters, nominally 10 mm, are consistently smaller, with actual values of 9.8931 mm, 9.7943 mm, and 9.7864 mm, with the most considerable under sizing at 80% ID, potentially due to shrinkage. Perpendicularity, with a nominal value of 90 degrees, is maintained with minimal deviation, showing actual values of 89.994 degrees, 89.9573 degrees, and 89.9775 degrees, reflecting excellent angular accuracy essential for structural integrity.

Overall, on the Table 4.4 , the average percentage accuracy is highest at 55% ID, with 98.75%, compared to 98.31% at 20% ID and 98.25% at 80% ID, demonstrating that mid-range infill density offers the best balance between material deposition and structural precision. These findings highlight the importance of selecting appropriate infill densities to optimize the dimensional accuracy and functionality of 3D printed ABS components.

4.3   PLA Printed Sample Result

Table 4.5 presents the measurement results obtained from the CMM testing of the samples, with the expected measurement data listed on the right side and the corresponding actual data recorded using CMM on the left side. This table is a valuable resource for assessing the dimensional accuracy of the printed samples. Furthermore, Table 4.6 specifically focuses on PLA samples printed using FDM technology and showcases the percentage of accuracy achieved concerning the actual accuracy. This table provides crucial insights into the level of precision that can be expected when printing PLA using FDM. Both tables play a significant role in establishing reference points for evaluating the dimensional accuracy of the printed PLA samples.

Table 4.5: Nominal Accuracy vs Actual Value

Geometry	Nominal Value	Actual Value		
		20% ID	55% ID	80% ID
Length, mm	50	50.0203	50.0098	49.9356
Width, mm	25	25.1977	25.1212	25.0703
Thickness, mm	3	3.0504	3.0174	3.0064
Corner Diameter, mm	20	21.2546	19.1414	22.5225
Hole Diameter, mm	10	9.8677	9.8518	9.7271
Perpendicularity, Degree	90	89.963	89.9737	89.963

Table 4.6: Percentage of Accuracy of PLA sample

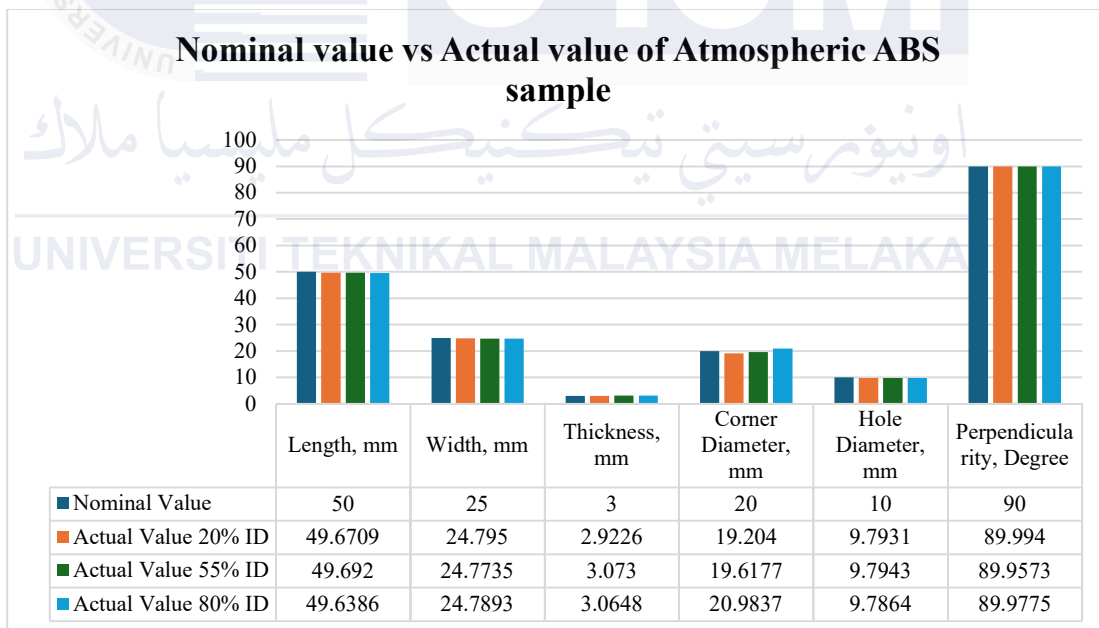| Geometry	Percentage Accuracy, %		
	20% ID	55% ID	80% ID
Length, mm	99.9595	99.98	99.87
Width, mm	99.22	99.52	99.72
Thickness, mm	98.35	99.42	99.79
Corner Diameter, mm	94.1	95.71	88.8
Hole Diameter, mm	98.68	98.518	97.73
Perpendicularity, Degree	99.95	99.97	99.96
Average Percentage accuracy	98.37478	98.853	97. 645

Nominal value vs Actual value of Atmospheric PLA sample	Length, mm	Width, mm	Thickness, mm	Corner Diameter, mm	Hole Diameter, mm	Perpendicularity, Degree
Nominal Value	50	25	3	20	10	90
Actual Value 20% ID	50.0203	25.1977	3.0504	21.2546	9.8677	89.963
Actual Value 55% ID	50.0098	25.1212	3.0174	19.1414	9.8518	89.9737
Actual Value 80% ID	49.9356	25.0703	3.0064	22.5225	9.7271	89.963

Figure 4.3: Nominal Accuracy vs Actual value of PLA sample

Percentage Accuracy of Atmospheric PLA printed samples

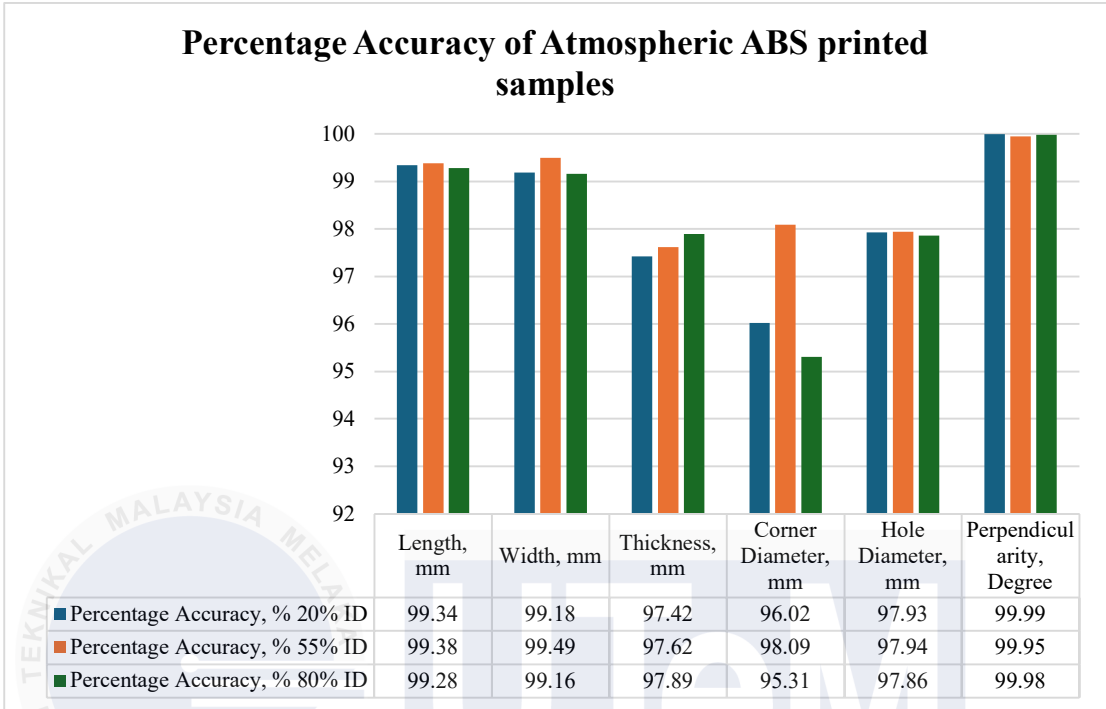|	Length, mm	Width, mm	Thickness, mm	Corner Diameter, mm	Hole Diameter, mm	Perpendicularity, Degree
■ Percentage Accuracy, % 20% ID	99.9595	99.2092	98.35	94.1	98.68	99.95
■ Percentage Accuracy, % 55% ID	99.98	99.52	99.42	95.71	98.518	99.97
■ Percentage Accuracy, % 80% ID	99.87	99.72	99.79	88.8	97.73	99.96

Figure 4.4: Percentage Accuracy of Atmospheric PLA printed samples

The comparison between the nominal values and actual values of PLA samples printed at different infill densities (20%, 55%, and 80%) in atmospheric pressure reveals insightful details about dimensional accuracy. For length, with a nominal value of 50 mm, the actual values recorded are 50.0203 mm, 50.0098 mm, and 49.9356 mm for 20%, 55%, and 80% ID, respectively. The percentage accuracy for length is impressively high across all densities, ranging from 99.87% to 99.99%. Similarly, for width with a nominal value of 25 mm, the actual values are 25.1977 mm, 25.1212 mm, and 25.0703 mm, corresponding to percentage accuracies of 99.22%, 99.52%, and 99.72%. Thickness, with a nominal value of 3 mm, shows actual values of 3.0504 mm, 3.0174 mm, and 3.0064 mm, and the percentage accuracy ranges from 98.35% to 99.79%, indicating slight over-deposition.

The corner diameter, nominally 20 mm, presents more significant deviations, with actual values of 21.2546 mm, 19.1414 mm, and 22.5225 mm, reflecting percentage accuracies of 94.10%, 95.71%, and 88.8%, respectively. This suggests that higher infill densities might lead to over-extrusion affecting corner precision. The hole diameter, with a nominal value of 10 mm, records actual values of 9.8677 mm, 9.8518 mm, and 9.7271 mm, translating to percentage accuracies of 98.68%, 98.52%, and 97.73%, showing consistent

69

undersizing across all densities. Perpendicularity, nominally 90 degrees, maintains high accuracy with actual values of 89.963 degrees, 89.9737 degrees, and 89.963 degrees, yielding percentage accuracies of 99.95%, 99.97%, and 99.96%.

Overall, the average percentage accuracy is highest at 55% ID (98.85%), followed by 20% ID (98.38%), and lowest at 80% ID (97.645%). This indicates that mid-range infill density offers the best balance between material deposition and structural precision. The findings highlight the critical role of selecting appropriate infill densities to optimize dimensional accuracy and functionality in 3D printed PLA components.

4.4 ABS printed in vacuum sample result

Table 4.7 presents the measurement results obtained from CMM testing of the samples. The expected measurements are listed on the right side of the table, while the actual measurements recorded using the CMM are shown on the left side. This table offers a direct comparison between the expected and actual data, enabling assessment of the accuracy of the printed parts. In addition, Table 4.8 focuses specifically on ABS samples printed in a vacuum environment and displays the percentage of accuracy achieved relative to the actual accuracy. This table provides valuable information on the level of accuracy that can be expected when printing ABS in a vacuum-assisted setting. Both tables serve as important references for evaluating and benchmarking the dimensional accuracy of the printed samples.

Table 4.7: Nominal Accuracy vs actual result of Vacuum ABS samples

Geometry	Nominal Value	Actual Value		
		20% ID VP	55% ID VP	80% ID VP
Length, mm	50	49.8098	49.9191	50.1531
Width, mm	25	24.8306	24.9195	25.1145
Thickness, mm	3	2.8668	3.024	3.0858
Corner Diameter, mm	20	19.9104	20.0497	19.9684
Hole Diameter, mm	10	9.8708	9.97983	9.8423
Perpendicularity, Degree	90	89.8347	89.986	89.9865

Table 4.8: Percentage of Accuracy Vacuum ABS samples

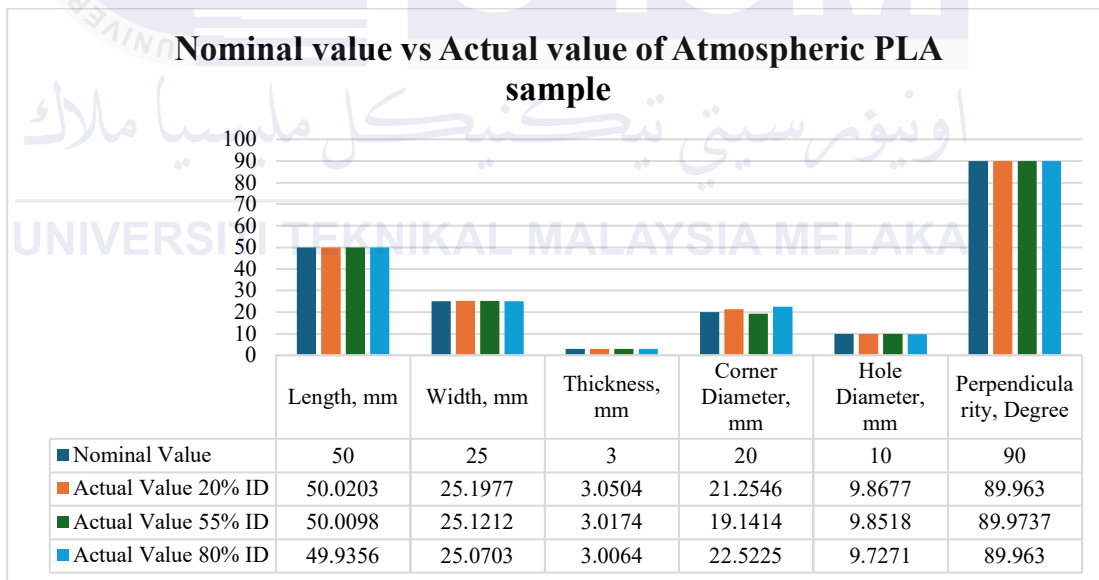| Geometry	Percentage Accuracy, %		
	20% ID VP	55% ID VP	80% ID VP
Length, mm	99.62	99.84	99.69
Width, mm	99.32	99.68	99.54
Thickness, mm	95.56	99.21	97.22
Corner Diameter, mm	99.55	99.75	99.84
Hole Diameter, mm	98.71	99.8	98.42
Perpendicularity, Degree	99.82	99.98	99.99
Average Percentage accuracy	98.76	99.71	99.12

Nominal value vs Actual value of Vacuum ABS sample

	Length, mm	Width, mm	Thickness, mm	Corner Diameter, mm	Hole Diameter, mm	Perpendicularity, Degree
Nominal Value	50	25	3	20	10	90
Actual Value 20% ID VP	49.8098	24.8306	2.8668	19.9104	9.8708	89.8347
Actual Value 55% ID VP	49.9191	24.9195	3.024	20.0497	9.97983	89.986
Actual Value 80% ID VP	50.1531	25.1145	3.0858	19.9684	9.8423	89.9865

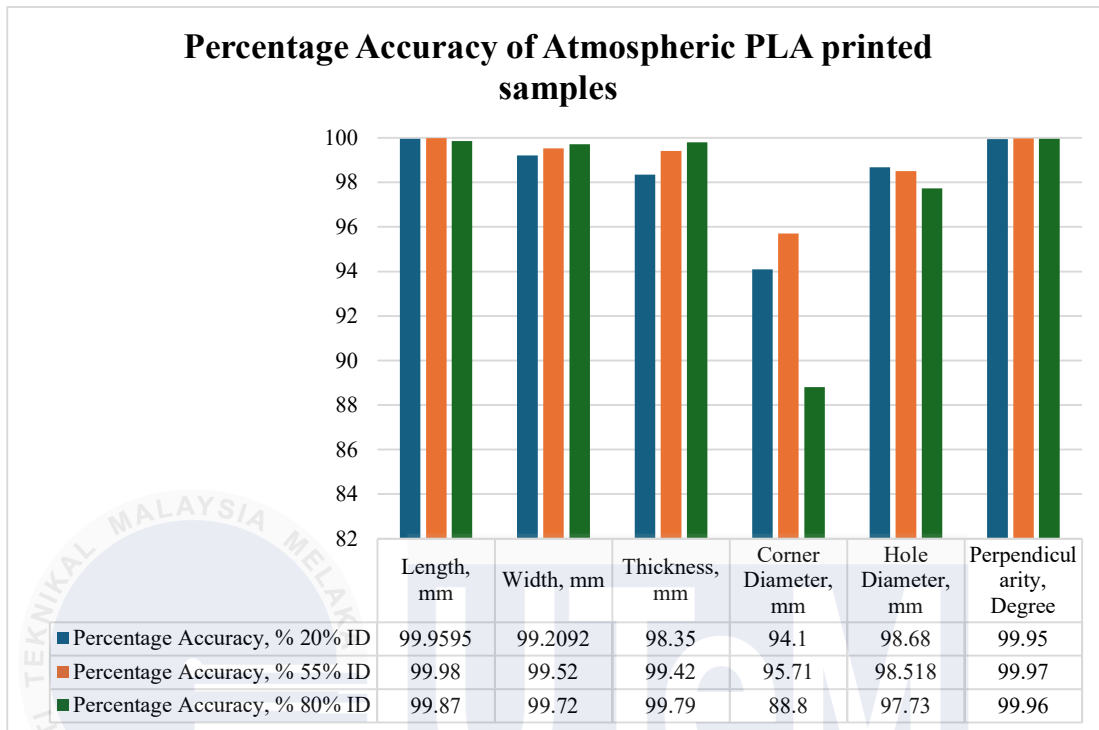Figure 4.5: ABS in vacuum sample Nominal value vs Actual Value

72
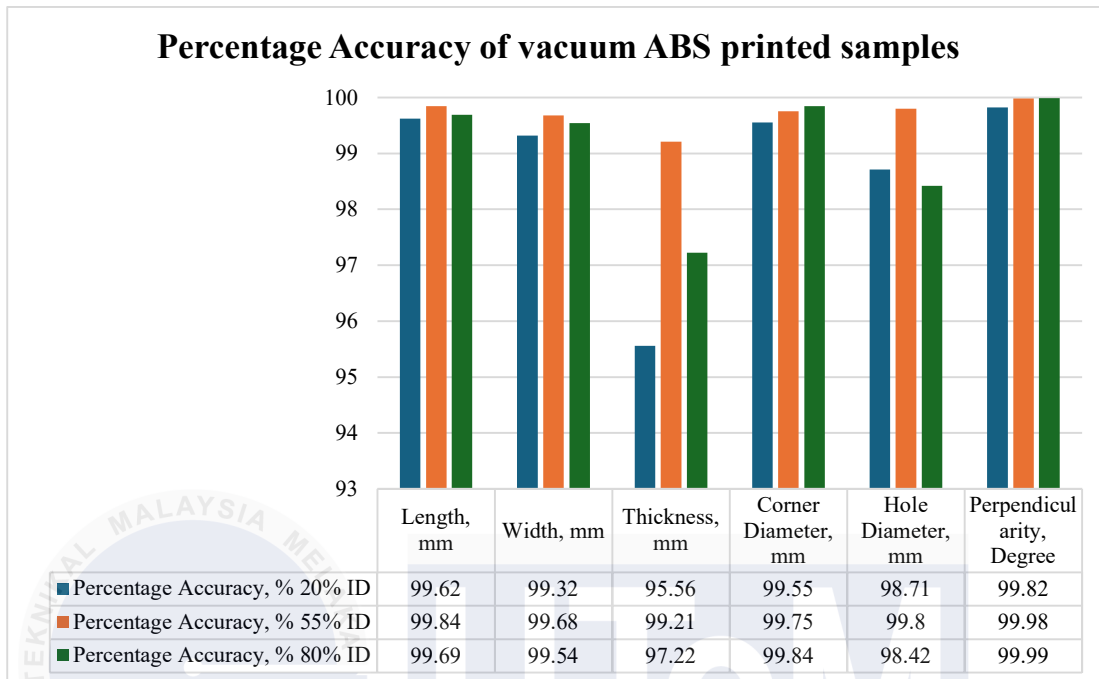
Figure 4.6: Percentage Accuracy of vacuum ABS printed samples

The comparison between the nominal values and actual values of ABS samples printed under vacuum conditions at different infill densities (20%, 55%, and 80%) reveals crucial insights into dimensional accuracy (see Table 4.8 and Figure 4.5). For length, with a nominal value of 50 mm, the actual values recorded are 49.8098 mm, 49.9191 mm, and 50.1531 mm for 20%, 55%, and 80% ID VP (Vacuum Printed), respectively. The percentage accuracy for length is high across all densities, ranging from 99.62% to 99.84% (Table 4.8). Similarly, for width with a nominal value of 25 mm, the actual values are 24.8306 mm, 24.9195 mm, and 25.1145 mm, corresponding to percentage accuracies of 99.32%, 99.68%, and 99.54%. Thickness, with a nominal value of 3 mm, shows actual values of 2.8668 mm, 3.024 mm, and 3.0858 mm, and the percentage accuracy ranges from 95.56% to 99.21%, indicating slight under-deposition and over-deposition depending on the infill density.

The corner diameter, nominally 20 mm, presents minor deviations, with actual values of 19.9104 mm, 20.0497 mm, and 19.9684 mm, reflecting percentage accuracies of 99.55%, 99.75%, and 99.84%, respectively, suggesting high precision in corner features across all densities. The hole diameter, with a nominal value of 10 mm, records actual values of 9.8708 mm, 9.9798 mm, and 9.8423 mm, translating to percentage accuracies of 98.71%, 99.8%,

and 98.42%, showing consistent accuracy with slight under sizing across all densities. Perpendicularity, nominally 90 degrees, maintains high accuracy with actual values of 89.8347 degrees, 89.986 degrees, and 89.9865 degrees, yielding percentage accuracies of 99.82%, 99.98%, and 99.99%.

Overall, the average percentage accuracy is highest at 55% ID VP (99.71%), followed by 80% ID VP (99.12%), and lowest at 20% ID VP (98.76%), indicating that mid-range infill density offers the best balance between material deposition and structural precision under vacuum printing conditions. These findings highlight the critical role of selecting appropriate infill densities to optimize the dimensional accuracy and functionality of vacuum printed ABS components.
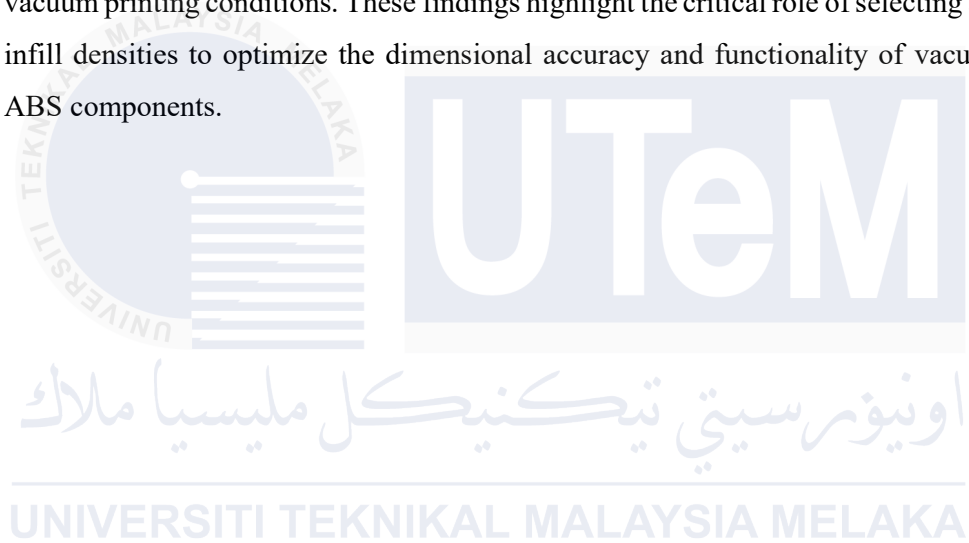
4.5 PLA printed in vacuum sample result

Table 4.9 Table 4.9 displays the measurement outcomes from CMM testing of the samples. The expected measurement data is presented on the right side, while the corresponding actual data recorded using CMM is shown on the left side. This table is a valuable resource for evaluating the dimensional accuracy of the printed samples. Additionally, Table 4.10 focuses on PLA samples printed using FDM technology in a vacuum environment. It illustrates the percentage of accuracy achieved relative to the actual accuracy. This table provides essential insights into the level of precision that can be expected when printing PLA in a vacuum using FDM. Both tables play a crucial role in establishing reference points for assessing the dimensional accuracy of the printed PLA samples.

Table 4.9: Nominal Accuracy vs Actual Result

Geometry	Nominal Value	Actual Value		
		20% ID VP	55% ID VP	80% ID VP
Length, mm	50	49.9666	49.8811	49.9931
Width, mm	25	25.2031	25.014	25.0377
Thickness, mm	3	3.0403	3.08343	3.0012
Corner Diameter, mm	20	20.0145	20.1437	19.9892
Hole Diameter, mm	10	9.6913	9.84617	9.9675
Perpendicularity, Degree	90	89.987	89.8223	89.988

Table 4.10: Percentage of Accuracy vacuum PLA samples

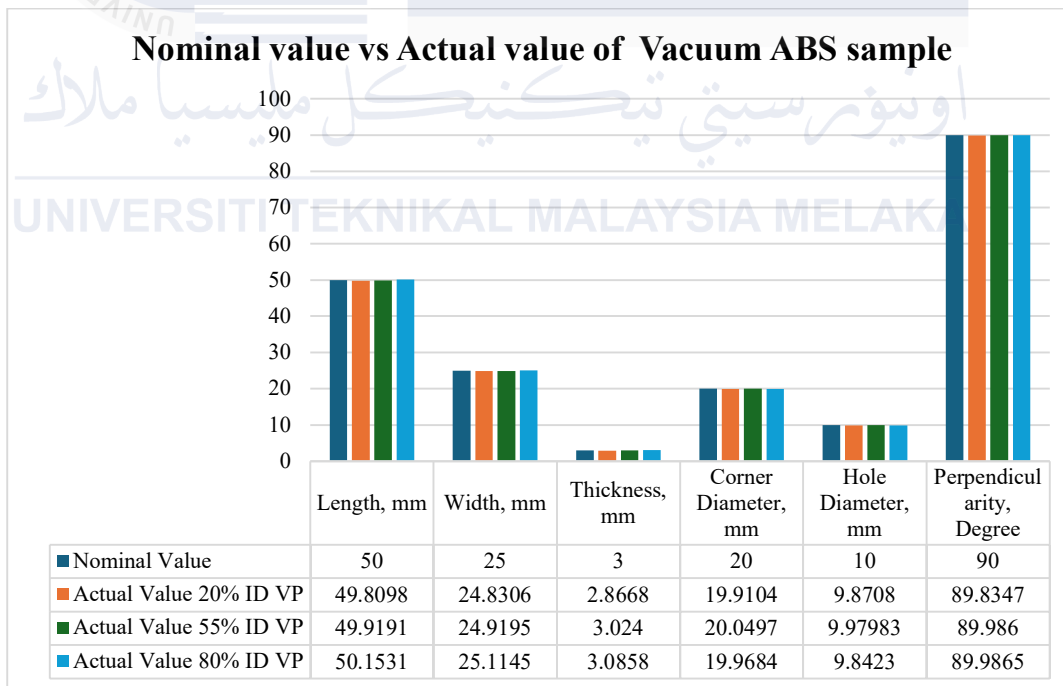| Geometry	Percentage Accuracy, %		
	20% ID VP	55% ID VP	80% ID VP
Length, mm	99.93	99.76	99.99
Width, mm	99.19	99.94	99.85
Thickness, mm	98.67	97.29	99.96
Corner Diameter, mm	99.93	99.29	99.95
Hole Diameter, mm	96.91	98.46	99.68
Perpendicularity, Degree	99.99	98.8	99.99
Average Percentage accuracy	99.1	98.92	99.89

Nominal value vs Actual value of vacuum PLA sample

	Length, mm	Width, mm	Thickness, mm	Corner Diameter, mm	Hole Diameter, mm	Perpendicularity, Degree
Nominal Value	50	25	3	20	10	90
Actual Value 20% ID VP	49.9666	25.2031	3.0403	20.0145	9.6913	89.987
Actual Value 55% ID VP	49.8811	25.014	3.08343	20.1437	9.84617	89.8223
Actual Value 80% ID VP	49.9931	25.0377	3.0012	19.9892	9.9675	89.988
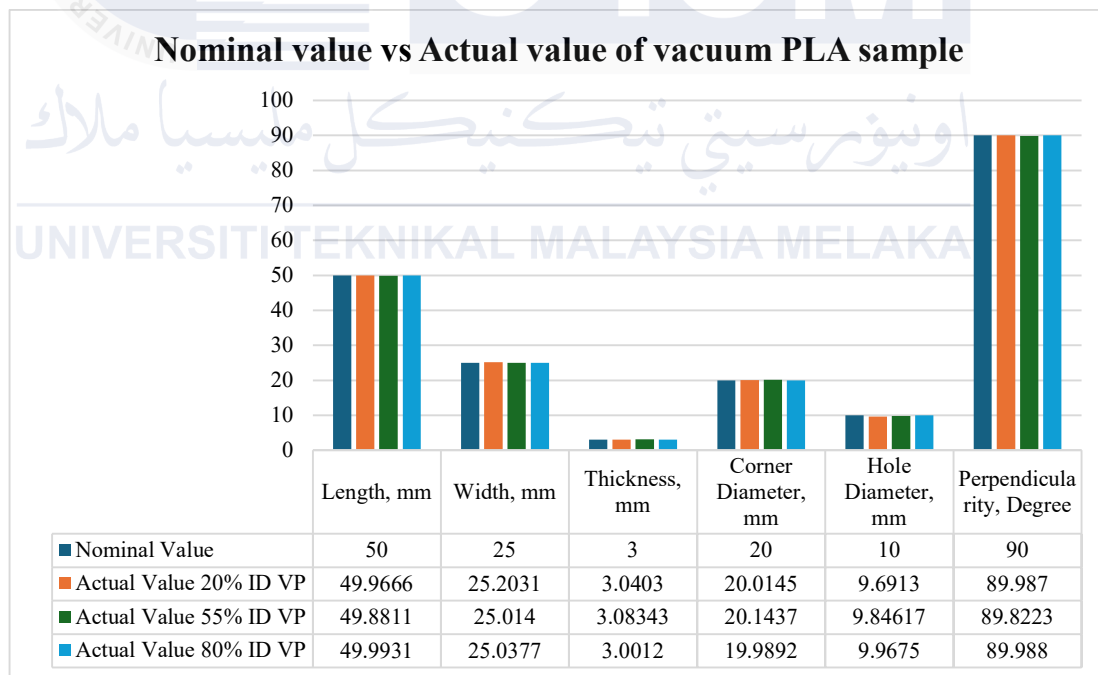
Figure 4.7: PLA in vacuum sample Nominal Accuracy vs Actual Result

Percentage Accuracy of vacuum PLA printed samples

	Length, mm	Width, mm	Thickness, mm	Corner Diameter, mm	Hole Diameter, mm	Perpendicularity, Degree
Percentage Accuracy, % 20% ID	99.93	99.19	98.67	99.93	96.91	99.99
Percentage Accuracy, % 55% ID	99.76	99.94	97.29	99.29	98.46	98.8
Percentage Accuracy, % 80% ID	99.99	99.85	99.96	99.95	99.68	99.99
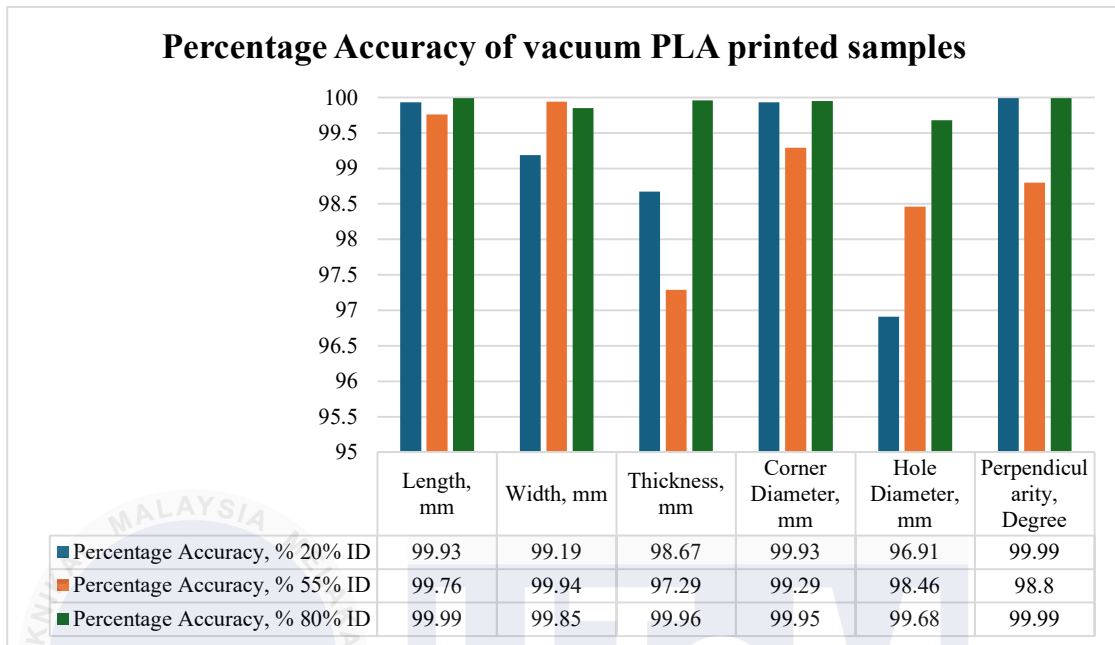
Figure 4.8: Percentage Accuracy of vacuum PLA printed samples

The comparison between the nominal values and actual values of PLA samples printed under vacuum conditions at different infill densities (20%, 55%, and 80%) reveals crucial insights into dimensional accuracy (see Table 4.10 and Figure 4.7). For length, with a nominal value of 50 mm, the actual values recorded are 49.9666 mm, 49.8811 mm, and 49.9931 mm for 20%, 55%, and 80% ID VP (Vacuum Printed), respectively. The percentage accuracy for length is impressively high across all densities, ranging from 99.76% to 99.99% (Table 4.10). Similarly, for width with a nominal value of 25 mm, the actual values are 25.2031 mm, 25.014 mm, and 25.0377 mm, corresponding to percentage accuracies of 99.19%, 99.94%, and 99.85%. Thickness, with a nominal value of 3 mm, shows actual values of 3.0403 mm, 3.0834 mm, and 3.0012 mm, and the percentage accuracy ranges from 97.29% to 99.96%, indicating slight under-deposition and over-deposition depending on the infill density (Figure 4.8).

The corner diameter, nominally 20 mm, presents minor deviations, with actual values of 20.0145 mm, 20.1437 mm, and 19.9892 mm, reflecting percentage accuracies of 99.93%, 99.29%, and 99.95%, respectively, suggesting high precision in corner features across all densities. The hole diameter, with a nominal value of 10 mm, records actual values of 9.6913 mm, 9.8467 mm, and 9.9675 mm, translating to percentage accuracies of 96.91%, 98.46%, and 99.68%, showing consistent accuracy with slight under sizing across all densities (Table

4.10). Perpendicularity, nominally 90 degrees, maintains high accuracy with actual values of 89.897 degrees, 89.8223 degrees, and 89.988 degrees, yielding percentage accuracies of 99.99%, 98.8%, and 99.99%.

Overall, the average percentage accuracy is highest at 20% ID VP (99.1%), followed by 80% ID VP (99.89%), and lowest at 55% ID VP (98.92%), indicating that lower and higher infill densities offer excellent balance between material deposition and structural precision under vacuum printing conditions. These findings highlight the critical role of selecting appropriate infill densities to optimize the dimensional accuracy and functionality of vacuum printed PLA components.

4.6 Comparison of Percentage Accuracy between ABS and PLA

The results comparing ABS and PLA samples with and without vacuum assistance demonstrate a substantial improvement in dimensional accuracy when vacuum technology is utilized. Initially, ABS and PLA samples printed without vacuum assistance showed lower accuracy percentages compared to expected and actual values. However, a clear enhancement in dimensional accuracy was observed when printing ABS and PLA samples in a vacuum environment.
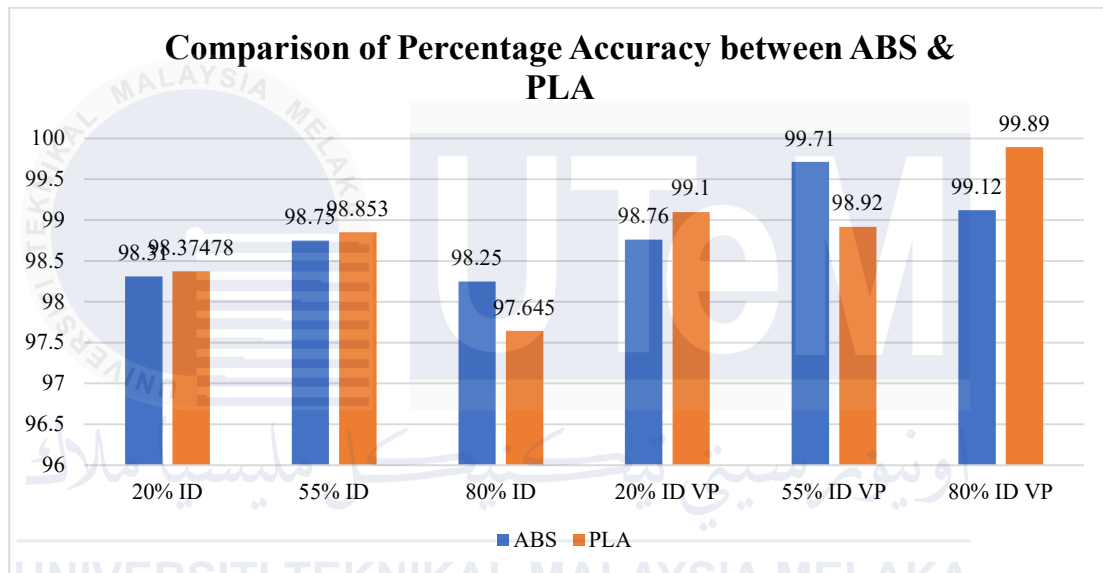
Figure 4.9: Percentage accuracy comparison between ABS and PLA samples

The comparison of percentage accuracy between ABS and PLA samples shown in Figure 4.9 presents data across six different conditions: 20% infill density (ID), 55% ID, 80% ID, 20% ID with vacuum pressure (VP), 55% ID VP, and 80% ID VP. The first three conditions involve printing at atmospheric pressure, while the latter three involve printing under vacuum pressure. Each condition reveals how the two materials perform in terms of accuracy, measured in percentage.

At 20% infill density, PLA sample shows a slight edge over ABS with an accuracy of 98.37% compared to ABS's 98.31%. The difference is minimal, indicating that both materials perform almost equally well at this lower infill density in atmospheric pressure. As the infill density increases to 55%, PLA marginally surpasses ABS, achieving 98.85%

79

accuracy while ABS maintains an accuracy of 98.75%. This shift suggests that PLA may handle increased density slightly better than ABS, though the difference remains under 0.1%. This can be attributed to the less warp behaviour of PLA compared to ABS, which allows PLA to achieve high accuracy for dimensional parts, as mentioned by Baran & Yildirim Erbil, (2019). Additionally, PLA samples have higher dimensional accuracy compared to ABS due to their higher tensile strength. This difference in mechanical properties can affect the stability and precision of the printed parts, ultimately influencing their accuracy (Syaefudin et al., 2023).

At 80% infill density, ABS manage to outperform PLA with 98.25% accuracy compared to PLA's 97.65%. This indicates that ABS might be more reliable than PLA at higher infill densities in atmospheric pressure, as the accuracy of PLA declines more significantly.

Introducing vacuum pressure (VP) at 20% infill density shows a significant improvement for both materials. PLA reaches 99.1% accuracy, while ABS stands at 98.76%. Here, vacuum pressure boosts PLA's accuracy considerably more than ABS, highlighting PLA's enhanced performance when combined with this printing technique. The reduction of porosity or voids in the printed parts when produced in a vacuum can lead to better layer adhesion, ultimately improving dimensional accuracy and mechanical performance (Thumsorn et al., 2022). At 55% infill density with vacuum pressure, both materials show a marked increase in accuracy, with ABS achieving 99.71% and PLA at 98.92%. This substantial improvement, particularly for ABS, suggests that the combination of higher infill density and vacuum pressure greatly benefits ABS's accuracy. Finally, at 80% infill density with vacuum pressure, PLA reaches its peak accuracy of 99.89%, whereas ABS achieves 99.12%. This scenario demonstrates the superior performance of PLA under the most demanding conditions of high infill density and vacuum pressure, making it the more accurate material in this setting.

The comparative analysis of ABS and PLA across different conditions reveals that while both materials exhibit high accuracy, PLA generally performs better, especially when combined with vacuum pressure. ABS maintains consistent accuracy across varying densities but does not benefit as significantly from vacuum pressure as PLA. Therefore, for

applications requiring utmost precision, particularly with higher infill densities and vacuum pressure, PLA appears to be the preferable choice. The less warp behaviour of PLA and its higher tensile strength compared to ABS contribute to its superior performance, ensuring greater stability and precision in printed parts. Additionally, the benefits of vacuum pressure in reducing porosity, improving layer adhesion, and mitigating warpage further enhance PLA's accuracy and mechanical performance.

4.7 Optimisation of process parameters for ABS and PLA

The Figure 4.10 and Figure 4.11 illustrate the results of an optimization process for determining the optimal settings for two key parameters in the 3D printing of two materials: ABS (Acrylonitrile Butadiene Styrene) and PLA (Polylactic Acid). The parameters considered were infill density and printing pressure. Infill density was categorized into three levels: 20%, 55%, and 80%, while printing pressure had two levels: atmospheric pressure (101.3 kPa) and vacuum pressure (20 kPa). The optimization aimed to enhance various output characteristics, including width, thickness, length, corner diameter, hole diameter, and perpendicularity, all measured in millimeters (mm).

For ABS material, the optimal settings were an infill density of 55% and a printing pressure of 20 kPa (vacuum pressure). These settings resulted in the following optimized output characteristics: a width of 24.9195 mm, a thickness of 3.024 mm, a length of 49.9191 mm, a corner diameter of 20.0497 mm, a hole diameter of 9.97983 mm, and a perpendicularity of 89.986 degrees. The optimization achieved a desirability score of 0.829, indicating a balanced compromise between the different output characteristics. This solution ensures high-quality printed parts with the specified dimensional and geometrical properties.

For PLA material, the optimal settings were an infill density of 80% and a printing pressure of 20 kPa (vacuum pressure). These settings resulted in the following optimized output characteristics: a width of 25.0377 mm, a thickness of 3.0012 mm, a length of 49.9931 mm, a corner diameter of 19.9892 mm, a hole diameter of 9.9675 mm, and a perpendicularity of 89.988 degrees. The optimization achieved a higher desirability score of 0.966, indicating a more favorable outcome in balancing the different output characteristics compared to the ABS material. This solution provides an effective optimization strategy for the 3D printing of PLA material, ensuring the production of high-quality parts with the desired dimensional and geometrical properties.

In conclusion, the optimization process for both ABS and PLA materials shows the effectiveness of using specific infill density and printing pressure settings to achieve high-quality printed parts. While the optimal infill density differed between the two materials (55% for ABS and 80% for PLA), the optimal printing pressure remained consistent at 20 kPa. The higher desirability score for PLA indicates a slightly better overall performance in terms of meeting the desired output characteristics.
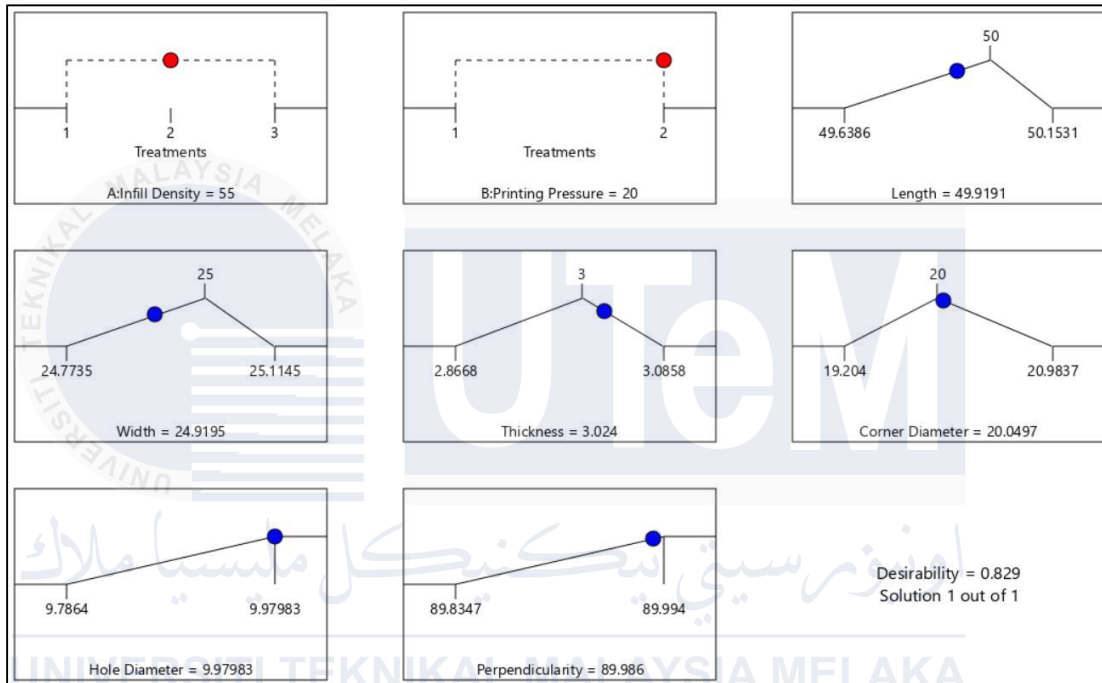
Figure 4.10: Optimal Process parameters for printing ABS
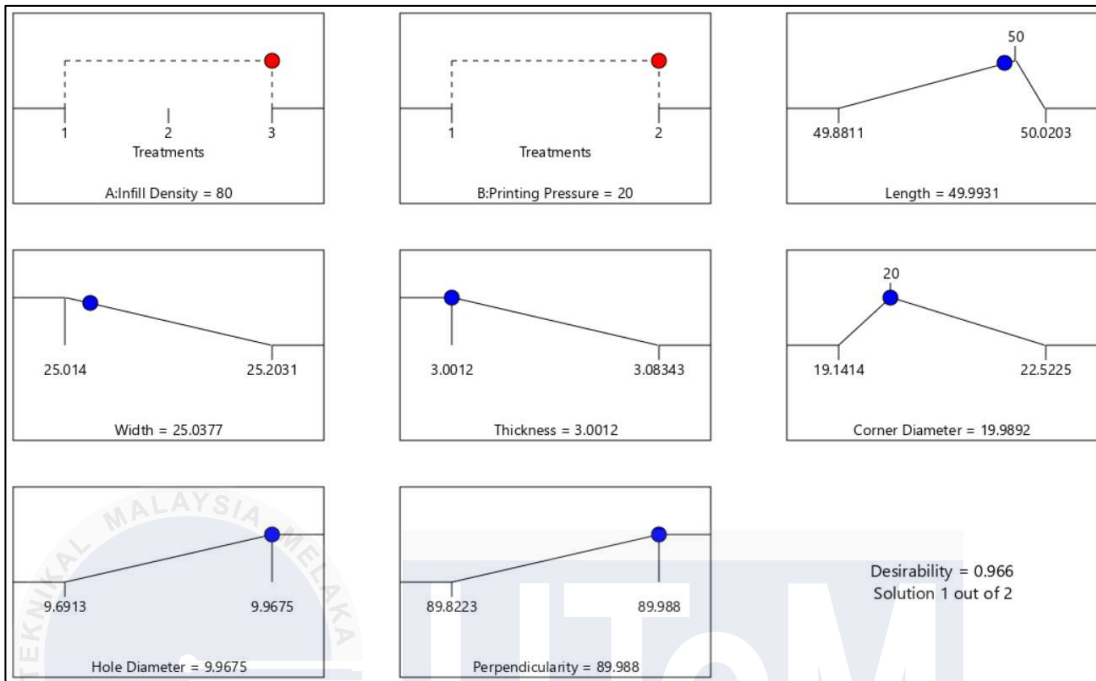
Figure 4.11: Optimal process parameters for printing PLA

4.8 Limitation of printing

Printing with FDM, both with and without vacuum assistance, has certain limitations that can affect the dimensional accuracy of the printed parts. These limitations become more apparent when considering the geometry criteria such as curves and holes. Additionally, the complexity of these parts makes it challenging to measure them accurately using CMM. The improvements may be relatively small, even with a high-end machine like the Ultimaker S3.

In the context of vacuum assistance, increasing the vacuum pressure can positively affect the printing process. In this research, a vacuum pressure of 20 kPa was utilized. However, based on the results obtained, it may be beneficial to increase the vacuum pressure further. Higher vacuum pressures can help eliminate air bubbles or voids within the printed material, improving material flow and better layer adhesion. By increasing the vacuum pressure, the dimensional accuracy of the printed parts can be further enhanced.

When dealing with complex parts, such as those with curves and holes, accurately measuring them using CMM machines can be challenging. The intricate geometry of these features makes it difficult for the CMM probe to access and accurately measure certain areas. As a result, the measured values may deviate from the true dimensions of the part. This limitation emphasizes optimizing the printing process to achieve the desired dimensional accuracy rather than relying solely on post-print measurements

4.9   Summary

In summary, finding optimal process parameter can enhance the dimensional accuracy of ABS and PLA-printed samples. Addition to that, using vacuum assistance in 3D printing can proved to be enhance the dimensional accuracy of ABS and PLA-printed parts although some of the results obtained have shown no improvement compared to the samples printed in atmospheric. Although neither ABS nor PLA achieves 100% accuracy, the infill density of 55% with vacuum pressure 20 kPa are the most optimal process parameters for ABS obtaining length 49.9191mm, width 24.9195 mm, thickness 3.024 mm, corner diameter 20.0097 mm, hole diameter 9.97983 mm and perpendicularity 89.986º meanwhile the infill density of 80% with vacuum pressure 20 kPa obtaining length 49.9931mm, width 25.0377 mm, thickness 3.0012 mm, corner diameter 19.7892 mm, hole diameter 9.8675 mm and perpendicularity 89.988º are the most optimal process parameters for PLA. However, measuring complex features, such as curves and holes, proves challenging, particularly with the limitations of a CMM machine. To achieve better accuracy in future print, optimising parameters such as layer thickness and printing speed is crucial as they are also one of the critical factors affecting the dimensional accuracy of printed parts. In conclusion, the variation of infill density thus affected the dimensional accuracy and the most optimal infill density for the printed samples were discovered. Other than that, vacuum assistance improves the dimensional accuracy of ABS and PLA prints. However, achieving 100% accuracy remains challenging. By considering the material properties, part design, process parameters, and measurement limitations, it is possible to establish practical expectations for achieving precise dimensional accuracy in 3D printing applications.

CHAPTER 5
CONCLUSION AND RECOMMENDATIONS

5.1 Conclusions

The project's predetermined parameters and justifications were derived from an extensive review of previous journals and relevant studies, as well as the recommended parameters provided by the filament manufacturer. Fixed parameters for the project, including layer thickness, printing speed, and orientation, were selected based on a comprehensive understanding of the literature. At the project's inception, four primary objectives were established to guide the research and development process:

a) Modeling Process Parameters Using RSM:

The first objective aimed to model the process parameters using Response Surface Methodology (RSM) to print ABS and PLA samples. The key parameters selected for optimization were Infill Density (ID) and Printing Pressure (PP). These variables were chosen to identify the optimal settings for achieving high dimensional accuracy in ABS and PLA samples and to observe the effects of these parameters on dimensional accuracy. RSM suggested six experimental runs for each material, involving varying the process parameters. Infill Density was categorized into three levels: 20%, 55%, and 80%, while Printing Pressure was categorized into two levels: atmospheric pressure (101.3 kPa) and vacuum pressure (20 kPa). The samples were designed using CAD software SolidWorks, based on common geometries used in 3D printing.

b) Measuring Dimensional Accuracy Using CMM:

The second objective was to measure the dimensional accuracy of the printed samples using a Coordinate Measuring Machine (CMM). Upon completion of the printing process, each sample was meticulously tested using the CMM, measuring parameters such as length, width, thickness, corner diameter, hole diameter, and perpendicularity. The collected data was then analyzed to perform result analysis and optimization.

c) Comparing Vacuum Assisted and Atmospheric Samples:

The third objective involved comparing the dimensional accuracy of vacuum-assisted test samples with those printed under atmospheric conditions for both ABS and PLA materials. The results indicated that vacuum-assisted samples achieved higher dimensional accuracy. Notably, PLA samples demonstrated more significant benefits from vacuum assistance compared to ABS.

d) Optimizing Process Parameters Using RSM:

The final objective was to optimize the process parameters using RSM to determine the best settings for ABS and PLA. According to RSM analysis, the optimal parameters for ABS were identified as 55% ID and 20 kPa vacuum pressure, achieving an average accuracy of 99.71%. For PLA, the optimal parameters were 80% ID and 20 kPa vacuum pressure, resulting in an average accuracy of 99.98%.

In summary, this project systematically explored and optimized the process parameters for 3D printing ABS and PLA materials, providing valuable insights into achieving high dimensional accuracy through methodical experimentation and analysis. The findings underscore the importance of vacuum assistance, particularly for PLA, and demonstrate the efficacy of RSM in optimizing 3D printing parameters.

5.2 Recommendations

Based on this study, even though all the goals have been completed, there is still opportunity for further improvement that may be incorporated in further research. These are the recommendations that have been made:

a) More study should be undertaken to study the optimal setting for layer height to improve the accuracy of the printed part.

b) Increasing the vacuum pressure during printing has a positive effect on dimensional accuracy. Higher pressure helps eliminate trapped air and moisture, improving material flow and reducing warping or shrinkage.

c) Installing pressure gauge and temperature meter inside the vacuum chamber during printing process could potentially observe the temperature differential to identify the relation of temperature differential and warpage.

5.3   Sustainable design and development

Sustainability in design and development is a crucial consideration in modern engineering practices. It involves creating products and processes that are not only efficient and effective but also minimize environmental impact and promote resource conservation. This project focuses on optimizing the process parameters for the dimensional accuracy of thermoplastic polymers, specifically ABS (Acrylonitrile Butadiene Styrene) and PLA (Polylactic Acid), using a vacuum-assisted material extrusion system. Both materials have distinct sustainability profiles, which will be discussed in the context of this project.

ABS (Acrylonitrile Butadiene Styrene) is a common thermoplastic polymer known for its toughness, impact resistance, and ease of machining. It is widely used in various applications, including automotive parts, consumer electronics, and LEGO bricks. However, ABS is derived from petroleum, making its production reliant on fossil fuels. Its recyclability is relatively limited compared to other polymers, and it can emit toxic fumes when burned. Despite these challenges, efforts are being made to improve ABS recycling processes and reduce its environmental footprint.

PLA (Polylactic Acid), on the other hand, is a biodegradable thermoplastic derived from renewable resources like corn starch or sugarcane. It is commonly used in packaging, disposable cutlery, and 3D printing. PLA's primary advantage is its biodegradability and origin from renewable resources, resulting in a lower carbon footprint compared to petroleum-based plastics. However, its biodegradation requires specific conditions, such as industrial composting facilities, and its mechanical properties can be inferior to those of ABS.

Process optimization using Response Surface Methodology (RSM) can lead to more efficient material usage and energy consumption. By identifying optimal conditions for printing, such as infill density and printing pressure, waste can be minimized, and the overall environmental impact of the production process can be reduced. Implementing vacuum-assisted extrusion can enhance print quality and reduce the need for post-processing, further decreasing material and energy usage.

Minimizing energy consumption is another critical aspect of sustainable design. The energy required for 3D printing processes should be minimized through strategies such as optimizing heating and cooling cycles, reducing idle times, and employing energy-efficient equipment. Efficient use of energy directly contributes to sustainability.

Effective waste management practices are essential for reducing the environmental impact of both PLA and ABS during the printing process. Recycling failed prints and reusing materials where possible can significantly reduce waste. For PLA, composting facilities can be utilized to handle waste, whereas for ABS, improving collection and recycling systems is crucial.

Incorporating sustainable design and development principles in this project involves a holistic approach that considers process optimization, energy consumption, and waste management. By focusing on these aspects, the project can contribute to reducing the environmental footprint of thermoplastic polymer usage in vacuum-assisted material extrusion systems. The optimization of process parameters such as infill density and printing pressure using RSM plays a crucial role in enhancing the sustainability of the project.

5.4 Complexity Element

This project encompasses several complexity elements. The use of a Coordinate Measuring Machine (CMM) for high-precision measurement necessitates meticulous calibration and accurate data handling, while the vacuum chamber requires maintaining constant pressure to ensure dimensional accuracy, adding further intricacy with its need for consistent environmental control. Optimizing process parameters like infill density and printing pressure is complex due to their interdependence and the varying behaviors of ABS and PLA under different conditions. Employing Response Surface Methodology (RSM) adds statistical complexity, requiring comprehensive experimental design and advanced data analysis. Additionally, the need for continuous monitoring and real-time adjustments to maintain process integrity further complicates the project. These elements combine to create a challenging project that advances sustainable and precise material extrusion processes.

REFERENCES

3D Print Stuck to Bed: What to do? (n.d.). Retrieved January 3, 2024, from https://www.wevolver.com/article/3d-print-stuck-to-bed-what-to-do

3D Printing Market Size, Growth, Share | Global Report [2030]. (n.d.). Retrieved October 28, 2023, from https://www.fortunebusinessinsights.com/industry-reports/3d-printing-market-101902

7 Amazing Real-World Examples Of 3D Printing | Bernard Marr. (n.d.). Retrieved January 3, 2024, from https://bernardmarr.com/7-amazing-real-world-examples-of-3d-printing/

Abdellatief, M., Elemam, W. E., Alanazi, H., & Tahwia, A. M. (2023). Production and optimization of sustainable cement brick incorporating clay brick wastes using response surface method. *Ceramics International*, *49*(6), 9395–9411. https://doi.org/10.1016/j.ceramint.2022.11.144

Abdullah, T., Qurban, R. O., Abdel-wahab, M. Sh., Salah, N., Melaibari, A. A., Zamzami, M. A., & Memić, A. (2022). Development of Nanocoated Filaments for 3D Fused Deposition Modeling of Antibacterial and Antioxidant Materials. *Polymers*. https://doi.org/10.3390/polym14132645

Adamu, M., Haruna, S. I., Ibrahim, Y. E., & Alanazi, H. (2022). Investigating the properties of roller-compacted rubberized concrete modified with nanosilica using response surface methodology. *Innovative Infrastructure Solutions*, *7*(1). https://doi.org/10.1007/s41062-021-00717-4

Adegoke, O., Andersson, J., Brodin, H., & Pederson, R. (2020). Review of Laser Powder Bed Fusion of Gamma-Prime-Strengthened Nickel-Based Superalloys. *Metals 2020, Vol. 10, Page 996*, *10*(8), 996. https://doi.org/10.3390/MET10080996

Adil, S., & Lazoglu, I. (2023a). A review on additive manufacturing of carbon fiber-reinforced polymers: Current methods, materials, mechanical properties, applications and challenges. *Journal of Applied Polymer Science*, *140*(7), e53476. https://doi.org/10.1002/APP.53476

Adil, S., & Lazoglu, I. (2023b). A review on additive manufacturing of carbon fiber-reinforced polymers: Current methods, materials, mechanical properties, applications and challenges. *Journal of Applied Polymer Science*, *140*(7), e53476. https://doi.org/10.1002/APP.53476

Akbaş, O. E., Hıra, O., Hervan, S. Z., Samankan, S., & Altınkaynak, A. (2019). Dimensional Accuracy of FDM-printed Polymer Parts. *Rapid Prototyping Journal*. https://doi.org/10.1108/rpj-04-2019-0115

Alkentar, R., & Mankovits, T. (2022). A Study on the Shape and Dimensional Accuracy of Additively Manufactured Titanium Lattice Structures for Orthopedic Purposes. *Periodica Polytechnica Mechanical Engineering*, *66*(4), 336–343. https://doi.org/10.3311/PPME.20382

Arivalagan, S., Rajakumar, S., Čep, R., & Kumar, M. S. (2023). Optimization and Experimental Investigation of 3D Printed Micro Wind Turbine Blade Made of PLA Material. *Materials*. https://doi.org/10.3390/ma16062508

Armani, A. M., Hurt, D. E., Hwang, D., McCarthy, M. C., & Scholtz, A. (2020). Low-tech solutions for the COVID-19 supply chain crisis. In *Nature Reviews Materials* (Vol. 5, Issue 6, pp. 403–406). Nature Research. https://doi.org/10.1038/s41578-020-0205-1

Aslani, K. E., Kitsakis, K., Kechagias, J. D., Vaxevanidis, N. M., & Manolakos, D. E. (2020). On the application of grey Taguchi method for benchmarking the dimensional accuracy of the PLA fused filament fabrication process. *SN Applied Sciences*, *2*(6), 1–11. https://doi.org/10.1007/S42452-020-2823-Z/TABLES/10

Bahnini, I., Rivette, M., Rechia, A., Siadat, A., & Elmesbahi, A. (2018). Additive manufacturing technology: the status, applications, and prospects. *International Journal of Advanced Manufacturing Technology*, *97*(1–4), 147–161. https://doi.org/10.1007/S00170-018-1932-Y/METRICS

Baig, M. A. (2023). *Implementation of 3D Printing in Various Healthcare Settings: A Scoping Review*. https://doi.org/10.3233/shti230518

Baran, E. H., & Yildirim Erbil, H. (2019). Surface modification of 3d printed pla objects by fused deposition modeling: A review. In *Colloids and Interfaces* (Vol. 3, Issue 2). MDPI AG. https://doi.org/10.3390/colloids3020043

Barrios, J. M., & Romero, P. E. (2019). Improvement of surface roughness and hydrophobicity in PETG parts manufactured via fused deposition modeling (FDM): An application in 3D printed self-cleaning parts. *Materials*, *12*(15). https://doi.org/10.3390/ma12152499

Bastin, A., & Huang, X. (2022). Progress of Additive Manufacturing Technology and Its Medical Applications. *Asme Open Journal of Engineering*. https://doi.org/10.1115/1.4054947

Beniak, J., Holdy, M., Križan, P., & Matúš, M. (2019). Research on parameters optimization for the Additive Manufacturing process. *Transportation Research Procedia*, *40*, 144–149. https://doi.org/10.1016/j.trpro.2019.07.024

Bikas, H., Lianos, A. K., & Stavropoulos, P. (2019). A design framework for additive manufacturing. *International Journal of Advanced Manufacturing Technology*, *103*(9–12), 3769–3783. https://doi.org/10.1007/S00170-019-03627-Z/METRICS

Bishop, E. G., & Leigh, S. J. (2020). Using large-scale additive manufacturing (LSAM) as a bridge manufacturing process in response to shortages in PPE during the COVID-19 outbreak. *International Journal of Bioprinting*, *6*(4). https://doi.org/10.18063/ijb.v6i4.281

Blakey-Milner, B., Gradl, P., Snedden, G., Brooks, M., Pitot, J., Lopez, E., Leary, M., Berto, F., & du Plessis, A. (2021). Metal additive manufacturing in aerospace: A review. *Materials and Design*, *209*. https://doi.org/10.1016/j.matdes.2021.110008

Boeing turns to 3D-printed parts to save millions on 787 Dreamliner - TechCentral.ie. (n.d.). Retrieved October 29, 2023, from https://www.techcentral.ie/boeing-turns-3d-printed-parts-save-millions-787-dreamliner/

Boschetto, A., & Bottini, L. (2015). Roughness prediction in coupled operations of fused deposition modeling and barrel finishing. *Journal of Materials Processing Technology*, *219*, 181–192. https://doi.org/10.1016/j.jmatprotec.2014.12.021

Callahan, C. J., Lee, R., Zulauf, K. E., Tamburello, L., Smith, K. P., Previtera, J., Cheng, A., Green, A., Azim, A. A., Yano, A., Doraiswami, N., Kirby, J. E., & Arnaout, R. A. (2020). Open development and clinical validation of multiple 3d-printed nasopharyngeal collection swabs: rapid resolution of a critical covid-19 testing bottleneck. *Journal of Clinical Microbiology*, *58*(8). https://doi.org/10.1128/JCM.00876-20

Caminero, M. Á., Chacón, J. M., García-Plaza, E., Núñez, P. J., Reverte, J. M., & Becar, J. P. (2019). Additive Manufacturing of PLA-Based Composites Using Fused Filament Fabrication: Effect of Graphene Nanoplatelet Reinforcement on Mechanical Properties, Dimensional Accuracy and Texture. *Polymers 2019, Vol. 11, Page 799*, *11*(5), 799. https://doi.org/10.3390/POLYM11050799

Carneiro, V. H., Puga, H., Peixinho, N., & Meireles, J. (2019). Thin-Rib and High Aspect Ratio Non-Stochastic Scaffolds by Vacuum Assisted Investment Casting. *Journal of Manufacturing and Materials Processing*. https://doi.org/10.3390/jmmp3020034

Chand, R., Sharma, V. S., Trehan, R., & Gupta, M. K. (2023). Numerical Investigations on Mechanical Properties of Bio-Inspired 3D Printed Geometries Using Multi-Jet Fusion Process. *Rapid Prototyping Journal*. https://doi.org/10.1108/rpj-10-2022-0350

Chen, J. M., Lee, D., Yang, J. W., Lin, S. H., Lin, Y. T., & Liu, S. J. (2020). Solution Extrusion Additive Manufacturing of Biodegradable Polycaprolactone. *Applied Sciences 2020, Vol. 10, Page 3189*, *10*(9), 3189. https://doi.org/10.3390/APP10093189

Choong, Y. Y. C., Tan, H. W., Patel, D. C., Choong, W. T. N., Chen, C. H., Low, H. Y., Tan, M. J., Patel, C. D., & Chua, C. K. (2020). The global rise of 3D printing during the COVID-19 pandemic. In *Nature Reviews Materials* (Vol. 5, Issue 9, pp. 637–639). Nature Research. https://doi.org/10.1038/s41578-020-00234-3

Christou, C. D., & Tsoulfas, G. (2022). Role of Three-Dimensional Printing and Artificial Intelligence in the Management of Hepatocellular Carcinoma: Challenges and Opportunities. *World Journal of Gastrointestinal Oncology*. https://doi.org/10.4251/wjgo.v14.i4.765

Colligon, J. S. (2022). A history of vacuum technology from 5th Century BC and a personal view of progress in the field, including medical applications, from 1959 to 2021. In *Vacuum* (Vol. 198). Elsevier Ltd. https://doi.org/10.1016/j.vacuum.2021.110821

Demiralp, E., Dogru, G., & Yilmaz, H. (2021). Additive Manufacturing (3D PRINTING) Methods and Applications in Dentistry. *Clinical and Experimental Health Sciences*, *11*(1), 182–190. https://doi.org/10.33808/CLINEXPHEALTHSCI.786018

Deng, Y., Mao, Z., Yang, N., Niu, X., & Lu, X. (2020). Collaborative Optimization of Density and Surface Roughness of 316L Stainless Steel in Selective Laser Melting.

Materials 2020, Vol. 13, Page 1601, *13*(7), 1601. https://doi.org/10.3390/MA13071601

Dey, A., & Yodo, N. (2019). A systematic survey of FDM process parameter optimization and their influence on part characteristics. In *Journal of Manufacturing and Materials Processing* (Vol. 3, Issue 3). MDPI Multidisciplinary Digital Publishing Institute. https://doi.org/10.3390/jmmp3030064

Dolev, O., Osovski, S., & Shirizly, A. (2021). Ti-6Al-4V hybrid structure mechanical properties—Wrought and additive manufactured powder-bed material. *Additive Manufacturing*, *37*, 101657. https://doi.org/10.1016/J.ADDMA.2020.101657

Elena Verdejo de Toro, Juana Coello Sobrino, Alberto Matinez Martinez, & Valentin Miguel Eguia. (2020). *Analysis of the influence of the variables of the Fused Deposition Modeling (FDM) process on the mechanical properties of a carbon fiber-reinforced polyamide*. https://doi.org/https://doi.org/10.1016/j.promfg.2019.09.064

El-Sayegh, S., Romdhane, L., & Manjikian, S. (2020). A critical review of 3D printing in construction: benefits, challenges, and risks. In *Archives of Civil and Mechanical Engineering* (Vol. 20, Issue 2). Springer. https://doi.org/10.1007/s43452-020-00038-w

Explosiv3Design | Discover Los Alamos National Laboratory}. (n.d.). Retrieved October 29, 2023, from https://discover.lanl.gov/publications/1663/2016-march/explosiv3-design/

Frunzaverde, D. (2023). The Influence of the Layer Height and the Filament Color on the Dimensional Accuracy and the Tensile Strength of FDM-Printed PLA Specimens. *Polymers*. https://doi.org/10.3390/polym15102377

Gaillard, R., Lustig, S., Peltier, A., Villa, V., Servien, E., & Neyret, P. (2016). Total knee implant posterior stabilised by a third condyle: Design evolution and post-operative complications. *Orthopaedics and Traumatology: Surgery and Research*, *102*(8), 1061–1068. https://doi.org/10.1016/j.otsr.2016.08.015

Gal-Or, E., Gershoni, Y., Scotti, G., Nilsson, S. M. E., Saarinen, J., Jokinen, V., Strachan, C. J., Boije Af Gennäs, G., Yli-Kauhaluoma, J., & Kotiaho, T. (2019). Chemical analysis using 3D printed glass microfluidics. *Analytical Methods*, *11*(13), 1802–1810. https://doi.org/10.1039/C8AY01934G

Ganeshkumar, S., Kumar, S. D., Magarajan, U., Rajkumar, S., Arulmurugan, B., Sharma, S., Li, C., Ilyas, R. A., & Badran, M. (2022). Investigation of Tensile Properties of Different Infill Pattern Structures of 3d-Printed PLA Polymers: Analysis and Validation Using Finite Element Analysis in ANSYS. *Materials*. https://doi.org/10.3390/ma15155142

Gao, X., Zhang, D., Qi, S., Wen, X., & Su, Y. (2019). Mechanical Properties of 3D Parts Fabricated by Fused Deposition Modeling: Effect of Various Fillers in Polylactide. *Journal of Applied Polymer Science*. https://doi.org/10.1002/app.47824

Garg, N., Rastogi, V., & Kumar, P. (2022). Process parameter optimization on the dimensional accuracy of additive manufacture Thermoplastic Polyurethane (TPU) using RSM. *Materials Today: Proceedings*, *62*, 94–99. https://doi.org/10.1016/J.MATPR.2022.02.309

Gibson, I., Rosen, D. W., & Stucker, B. (2010). Introduction and Basic Principles. *Additive Manufacturing Technologies*, 20–35. https://doi.org/10.1007/978-1-4419-1120-9_1

Giubilini, A., Bondioli, F., Messori, M., Nyström, G., & Siqueira, G. (2021). Advantages of Additive Manufacturing for Biomedical Applications of Polyhydroxyalkanoates. *Bioengineering 2021, Vol. 8, Page 29*, *8*(2), 29. https://doi.org/10.3390/BIOENGINEERING8020029

Godec, D., Pilipoviˊc, A. P., Breški, T., Ureña, J., Jordá, O., Martínez, M., Gonzalez-Gutierrez, J., Schuschnigg, S., Blasco, J. R., & Portolés, L. (2022). *Introduction to Additive Manufacturing*. 1–44. https://doi.org/10.1007/978-3-031-05863-9_1

Goh, O., Goh, W. J., Lim, S. H., Hoo, G. S., Liew, R., & Ng, T. M. (2022). Preferences of Healthcare Professionals on 3D-Printed Tablets: A Pilot Study. *Pharmaceutics 2022, Vol. 14, Page 1521*, *14*(7), 1521. https://doi.org/10.3390/PHARMACEUTICS14071521

Guimarães, A. S., Delgado, J. M. P. Q., & Lucas, S. S. (2021). Advanced Manufacturing in Civil Engineering. *Energies 2021, Vol. 14, Page 4474*, *14*(15), 4474. https://doi.org/10.3390/EN14154474

Hanon, M. M., Kovacs, M. S., & Zsidai, L. (2019). Tribology Behaviour Investigation of 3D Printed Polymers. *International Review of Applied Sciences and Engineering*. https://doi.org/10.1556/1848.2019.0021

He, H., Gao, M., Illés, B., & Molnar, K. (2020). 3D Printed and electrospun, transparent, hierarchical polylactic acid mask nanoporous filter. *International Journal of Bioprinting*, *6*(4). https://doi.org/10.18063/ijb.v6i4.278

Heidari-Rarani, M., Ezati, N., Sadeghi, P., & Badrossamay. (2020). Optimization of FDM Process Parameters for Tensile Properties of Polylactic Acid Specimens Using Taguchi Design of Experiment Method. *Journal of Thermoplastic Composite Materials*. https://doi.org/10.1177/0892705720964560

Herzberger, J., Sirrine, J. M., Williams, C. B., & Long, T. E. (2019). Polymer Design for 3D Printing Elastomers: Recent Advances in Structure, Properties, and Printing. In *Progress in Polymer Science* (Vol. 97). Elsevier Ltd. https://doi.org/10.1016/j.progpolymsci.2019.101144

Herzog, T., Schnell, G., Tille, C., & Seitz, H. (2022). Investigation of Suitable Material and Adhesion Promoter Combinations for Fused Filament Fabrication on Flexible Silicone Build Plates. *Rapid Prototyping Journal*. https://doi.org/10.1108/rpj-06-2021-0154

Hexcel launches conductive new HexPEKK polymer for 3D printing "flight ready" aerospace parts - 3D Printing Industry. (n.d.). Retrieved November 15, 2023, from

https://3dprintingindustry.com/news/hexcel-launches-conductive-new-hexpekk-polymer-for-3d-printing-flight-ready-aerospace-parts-176436/

Hitzler, L., Merkel, M., Hall, W., & Öchsner, A. (2018). A Review of Metal Fabricated with Laser- and Powder-Bed Based Additive Manufacturing Techniques: Process, Nomenclature, Materials, Achievable Properties, and its Utilization in the Medical Sector. In *Advanced Engineering Materials* (Vol. 20, Issue 5). Wiley-VCH Verlag. https://doi.org/10.1002/adem.201700658

Hodžić, D., & Pandžić, A. (2019). *Influence of Carbon Fibers on Mechanical Properties of Materials in FDM Technology*. https://doi.org/10.2507/30th.daaam.proceedings.044

Hong, C. J., Giannopoulos, A. A., Hong, B. Y., Witterick, I. J., Irish, J. C., Lee, J., Vescan, A., Mitsouras, D., Dang, W., Campisi, P., de Almeida, J. R., & Monteiro, E. (2019). Clinical Applications of Three-dimensional Printing in Otolaryngology–head and Neck Surgery: A Systematic Review. *The Laryngoscope*. https://doi.org/10.1002/lary.27831

Hou, H., Yue, Y., Liu, J., Xi, D., & Liu, S. (2023). *Numerical Simulation and Experimental Study of the Stress Formation Mechanism of FDM with Different Printing Paths*. https://doi.org/10.32604/jrm.2022.021167

Huanbutta, K., Burapapadh, K., Sriamornsak, P., & Sangnim, T. (2023). Practical Application of 3D Printing for Pharmaceuticals in Hospitals and Pharmacies. *Pharmaceutics*. https://doi.org/10.3390/pharmaceutics15071877

Impey, S., Saxena, P., & Salonitis, K. (2021). Selective Laser Sintering Induced Residual Stresses: Precision Measurement and Prediction. *Journal of Manufacturing and Materials Processing 2021, Vol. 5, Page 101*, *5*(3), 101. https://doi.org/10.3390/JMMP5030101

Iyengar, K., Bahl, S., Raju Vaishya, & Vaish, A. (2020). Challenges and solutions in meeting up the urgent requirement of ventilators for COVID-19 patients. *Diabetes and Metabolic Syndrome: Clinical Research and Reviews*, *14*(4), 499–501. https://doi.org/10.1016/j.dsx.2020.04.048

Jasiuk, I., Abueidda, D. W., Kozuch, C., Pang, S., Su, F. Y., & McKittrick, J. (2018). An Overview on Additive Manufacturing of Polymers. *JOM*, *70*(3), 275–283. https://doi.org/10.1007/S11837-017-2730-Y/METRICS

Javaid, M., & Haleem, A. (2019). Current status and applications of additive manufacturing in dentistry: A literature-based review. *Journal of Oral Biology and Craniofacial Research*, *9*(3), 179–185. https://doi.org/10.1016/J.JOBCR.2019.04.004

Javaid, M., Haleem, A., Singh, R. P., & Suman, R. (2022). 3D printing applications for healthcare research and development. In *Global Health Journal* (Vol. 6, Issue 4, pp. 217–226). KeAi Communications Co. https://doi.org/10.1016/j.glohj.2022.11.001

Jung, I. (2023). Study on CNT/TPU Cube Under the 3D Printing Conditions of Infill Patterns and Density. *Scientific Reports*. https://doi.org/10.1038/s41598-023-44951-5

Kalender, M., Kilic, S. E., Ersoy, S., Bozkurt, Y., & Salman, S. (2019). Additive manufacturing and 3D printer technology in aerospace industry. *Proceedings of 9th International Conference on Recent Advances in Space Technologies, RAST 2019*, 689–695. https://doi.org/10.1109/RAST.2019.8767881

Kam, M., İpekçi, A., & Şengül, Ö. (2023). Investigation of the effect of FDM process parameters on mechanical properties of 3D printed PA12 samples using Taguchi method. *Journal of Thermoplastic Composite Materials*, *36*(1), 307–325. https://doi.org/10.1177/08927057211006459

Kareem, S. A. (2022). Additive manufacturing of concrete in construction: potentials and challenges of 3D concrete printing. *International Journal of Civil Engineering and Construction*, *1*(1), 13–16. https://doi.org/10.22271/27078329.2022.V1.I1A.4

Kholil, A., Asyaefudin, E., Pinto, N., & Syaripuddin, S. (2022). Compression Strength Characteristics of ABS and PLA Materials Affected by Layer Thickness on FDM. *Journal of Physics: Conference Series*, *2377*(1). https://doi.org/10.1088/1742-6596/2377/1/012008

Kholil, A., Syaefuddin, E. A., Supardi, F., & Wulandari, D. A. (2022). The Effect of Layer Thickness on Impact Strength Characteristics of ABS and PLA Materials. *Journal of Physics: Conference Series*, *2377*(1). https://doi.org/10.1088/1742-6596/2377/1/012001

Kim, S., Korolovych, V. F., Muhlbauer, R. L., & Tsukruk, V. V. (2020). <scp>3D-printed</Scp> Polymer Packing Structures: Uniformity of Morphology and Mechanical Properties via Microprocessing Conditions. *Journal of Applied Polymer Science*. https://doi.org/10.1002/app.49381

Kleer, R., & Piller, F. T. (2019). Local manufacturing and structural shifts in competition: Market dynamics of additive manufacturing. *International Journal of Production Economics*, *216*, 23–34. https://doi.org/10.1016/j.ijpe.2019.04.019

Kursat Celik, H., Kose, O., Ulmeanu, M. E., Rennie, A. E. W., Abram, T. N., & Akinci, I. (2020). Design and additive manufacturing of medical face shield for healthcare workers battling coronavirus (COVID-19). *International Journal of Bioprinting*, *6*(4), 1–21. https://doi.org/10.18063/IJB.V6I4.286

Latiff, Z. A. (2024). Optimization of Topology and Mechanical Properties of 3D Printed Hollow and Thin-Walled Structures via Integration of Taguchi Method and Grey Relational Analysis. *Journal of Advanced Research in Applied Mechanics*. https://doi.org/10.37934/aram.115.1.1835

Lee, J. Y., An, J., & Chua, C. K. (2017). Fundamentals and applications of 3D printing for novel materials. In *Applied Materials Today* (Vol. 7, pp. 120–133). Elsevier Ltd. https://doi.org/10.1016/j.apmt.2017.02.004

Leirmo, T. S., & Martinsen, K. (2019). Evolutionary algorithms in additive manufacturing systems: Discussion of future prospects. *Procedia CIRP*, *81*, 671–676. https://doi.org/10.1016/J.PROCIR.2019.03.174

Lemeš, S., Zaimović-Uzunović, N., Bešlagić, E., & Varda, K. (2022). *Dimensional accuracy and tolerances in additive manufacturing*. 118–127. https://doi.org/10.5644/pi2022.202.25

Li, Y., Feng, Z., Hao, L., Huang, L., Xin, C., Wang, Y., Bilotti, E., Essa, K., Zhang, H., Li, Z., Yan, F., & Peijs, T. (2020). A Review on Functionally Graded Materials and Structures via Additive Manufacturing: From Multi-Scale Design to Versatile Functional Properties. *Advanced Materials Technologies*, *5*(6), 1900981. https://doi.org/10.1002/ADMT.201900981

Liu, X., Lv, C., Liu, B., Li, X., & Jia, X. (2023). Machining error analysis of large-size ceramic additive manufacturing based on scanning exposure technology. *Https://Doi.Org/10.1117/12.2688717*, *12744*, 44–49. https://doi.org/10.1117/12.2688717

Maidin, S., Fadani, I., Nor Hayati, N. M., & Albaluooshi, H. (2022). APPLICATION OF TAGUCHI METHOD TO OPTIMIZE FUSED DEPOSITION MODELING PROCESS PARAMETERS FOR SURFACE ROUGHNESS. *Jurnal Teknologi*, *84*(6), 29–37. https://doi.org/10.11113/jurnalteknologi.v84.18430

Maidin, S., Md, N., Hayati, N., & Muhammad, A. H. (2022). *Comparative analysis of Acrylonitrile Butadiene Styrene and Polylactic Acid Samples' Mechanical Properties Printed in Vacuum*. https://ssrn.com/abstract=4232356

Maidin, S., Mohamed, A. S., Akmal, S., Mohamed, S. B., & Wong, J. H. U. (2018). *FEASIBILITY STUDY OF VACUUM TECHNOLOGY INTEGRATED FUSED DEPOSITION MODELING TO REDUCE STAIRCASE EFFECT*. https://doi.org/10.4314/jfas.v10i1s.45

Maidin, S., Wong, J. H. U., Mohamed, A. S., Mohamed, S. B., Rashid, R. A., & Rizman, Z. I. (2018). Vacuum fused deposition modelling system to improve tensile strength of 3D printed parts. *Journal of Fundamental and Applied Sciences*, *9*(6S), 839. https://doi.org/10.4314/jfas.v9i6s.63

Manstan, T., & McSweeney, M. B. (2020). Consumers' attitudes towards and acceptance of 3D printed foods in comparison with conventional food products. *International Journal of Food Science & Technology*, *55*(1), 323–331. https://doi.org/10.1111/IJFS.14292

Maurya, N. K., Rastogi, V., & Singh, P. (2019). Investigation of dimensional accuracy and international tolerance grades of 3D printed polycarbonate parts. *Materials Today: Proceedings*, *25*, 537–543. https://doi.org/10.1016/j.matpr.2019.06.007

Mayandi, K. (2024). Effects of Infill Density on Mechanical Properties of Additively Manufactured Chopped Carbon Fiber Reinforced PLA Composites. *Materials Science-Poland*. https://doi.org/10.2478/msp-2024-0003

Mishra, D., & Das, A. K. (2021). Linear Model Analysis of Fused Deposition Modeling Process Parameters for Obtaining the Maximum Tensile Strength in Acrylonitrile Butadiene Styrene (ABS) and Carbon Fiber Polylactic Acid (PLA) Materials.

Multidiscipline Modeling in Materials and Structures. https://doi.org/10.1108/mmms-09-2020-0239

Mohamed, O. A., Masood, S. H., & Bhowmik, J. L. (2016). Mathematical modeling and FDM process parameters optimization using response surface methodology based on Q-optimal design. *Applied Mathematical Modelling*, *40*(23–24), 10052–10073. https://doi.org/10.1016/j.apm.2016.06.055

Mohammed, B. S., & Adamu, M. (2018). Mechanical performance of roller compacted concrete pavement containing crumb rubber and nano silica. *Construction and Building Materials*, *159*, 234–251. https://doi.org/10.1016/j.conbuildmat.2017.10.098

Mohanavel, V., Ashraff Ali, K. S., Ranganathan, K., Allen Jeffrey, J., Ravikumar, M. M., & Rajkumar, S. (2021). The roles and applications of additive manufacturing in the aerospace and automobile sector. *Materials Today: Proceedings*, *47*, 405–409. https://doi.org/10.1016/j.matpr.2021.04.596

Momenzadeh, N., Miyanaji, H., Porter, D. A., & Berfield, T. A. (2020). Polyvinylidene fluoride (PVDF) as a feedstock for material extrusion additive manufacturing. *Rapid Prototyping Journal*, *26*(1), 156–163. https://doi.org/10.1108/RPJ-08-2018-0203/FULL/PDF

Moradi, M., Beygi, R., Mohd. Yusof, N., Amiri, A., da Silva, L. F. M., & Sharif, S. (2023). 3D Printing of Acrylonitrile Butadiene Styrene by Fused Deposition Modeling: Artificial Neural Network and Response Surface Method Analyses. *Journal of Materials Engineering and Performance*, *32*(4), 2016–2028. https://doi.org/10.1007/S11665-022-07250-0/TABLES/9

Moradi, M., Karamimoghadam, M., Meiabadi, S., Casalino, G., Ghaleeh, M., Baby, B., Ganapathi, H., Jose, J., Abdulla, M. S., Tallon, P., Shamsborhan, M., Rezayat, M., Paul, S., & Khodadad, D. (2023). Mathematical Modelling of Fused Deposition Modeling (FDM) 3D Printing of Poly Vinyl Alcohol Parts through Statistical Design of Experiments Approach. *Mathematics*, *11*(13). https://doi.org/10.3390/math11133022

Mourya, V. (2023). Multiobjective Optimization of Tribological Characteristics of 3D Printed Texture Surfaces for ABS and PLA Polymers. *Journal of Thermoplastic Composite Materials*. https://doi.org/10.1177/08927057231185710

Myers, R. H., Montgomery, D. C., Geoffrey Vining, G., Borror, C. M., & Kowalski, S. M. (2004). Response Surface Methodology: A Retrospective and Literature Survey. In *Journal of Quality Technology* (Vol. 36, Issue 1, pp. 53–78). American Society for Quality. https://doi.org/10.1080/00224065.2004.11980252

NASA 3D prints aluminum RAMFIRE rocket engine nozzles to enable deep space exploration - 3D Printing Industry. (n.d.). Retrieved November 15, 2023, from https://3dprintingindustry.com/news/nasa-3d-prints-aluminum-ramfire-rocket-engine-nozzles-to-enable-deep-space-exploration-225432/

Naveed, N. (2024). Optimising <scp>3D</Scp> Printing Parameters Through Experimental Techniques and <scp>ANOVA-Based</Scp> Statistical Analysis. *Spe Polymers*. https://doi.org/10.1002/pls2.10122

Novakova-Marcincinova, L., & Novak-Marcincin, J. (2013). Experimental testing of materials used in fused deposition modeling rapid prototyping technology. *Advanced Materials Research*, *740*, 597–602. https://doi.org/10.4028/WWW.SCIENTIFIC.NET/AMR.740.597

Olatunji, G. (2023). Exploring the Transformative Role of 3D Printing in Advancing Medical Education in Africa: A Review. *Annals of Medicine and Surgery*. https://doi.org/10.1097/ms9.0000000000001195

Ouezgan, A., Mallil, E. H., & Echaabi, J. (2022). Manufacturing Routes of Vacuum Assisted Resin Infusion: Numerical Investigation. *Journal of Composite Materials*. https://doi.org/10.1177/00219983221111492

Öztürk, O. (2024). The Influence of Fused Filament Fabrication Parameters on the Fracture Behavior of Pla Specimens Considering Energy Consumption. *Konya Journal of Engineering Sciences*. https://doi.org/10.36306/konjes.1402235

Pandžić, A., Hodžić, D., & Milovanović, A. (2019). *Effect of Infill Type and Density on Tensile Properties of PLA Material for FDM Process*. https://doi.org/10.2507/30th.daaam.proceedings.074

Panwar, V., Kumar Sharma, D., Pradeep Kumar, K. V., Jain, A., & Thakar, C. (2020). Experimental investigations and optimization of surface roughness in turning of en 36 alloy steel using response surface methodology and genetic algorithm. *Materials Today: Proceedings*, *46*, 6474–6481. https://doi.org/10.1016/j.matpr.2021.03.642

Parvazian, E., Abdollah-zadeh, A., Dehghani, M., & Taghavinia, N. (2019). Photovoltaic Performance Improvement in Vacuum-Assisted Meniscus Printed Triple-Cation Mixed-Halide Perovskite Films by Surfactant Engineering. *Acs Applied Energy Materials*. https://doi.org/10.1021/acsaem.9b00707

Pragana, J. P. M., Bragança, I. M. F., Reis, L., Silva, C. M. A., & Martins, P. A. F. (2021). Formability of wire-arc deposited AISI 316L sheets for hybrid additive manufacturing applications. *Https://Doi.Org/10.1177/14644207211037033*, *235*(12), 2839–2850. https://doi.org/10.1177/14644207211037033

Pratama, J., & Adib, A. Z. (2022). Pengaruh Parameter Cetak Pada Nilai Kekerasan Serta Akurasi Dimensi Material Thermoplastic Elastomer (TPE) Hasil 3D Printing. *Jurnal Ilmiah Giga*. https://doi.org/10.47313/jig.v25i1.1712

Praveena, B. A., Lokesh, N., Buradi, A., Santhosh, N., Praveena, B. L., & Vignesh, R. (2022). A comprehensive review of emerging additive manufacturing (3D printing technology): Methods, materials, applications, challenges, trends and future potential. *Materials Today: Proceedings*, *52*, 1309–1313. https://doi.org/10.1016/j.matpr.2021.11.059

Pugalendhi, A., Arumugam, S., Ranganathan, R., & Ganesan, S. (2021). 3D Printed Patient-Specific Bone Models for Anatomy Education From Medical Imaging. *Journal of Engineering Research*. https://doi.org/10.36909/jer.icippsd.15521

Ramadan, M. A., Sabour, Hassan. A., & El-Shenawy, E. (2023). Tribological Properties of 3D Printed Polymers: PCL, ABS, PLA and Co Polyester. *Tribology in Industry*. https://doi.org/10.24874/ti.1410.11.22.02

Rana, K. I., Sajid, Z., Tao, J., & Khan, L. A. (2021). Effect of Vacuum Manipulation on Inter Laminar Shear Strength and Flexural Strength in Double Bag Vacuum Infusion Moulding. *Polymers and Polymer Composites*. https://doi.org/10.1177/09673911211004206

Rasheed, A. (2023). Experimental Investigation and Taguchi Optimization of FDM Process Parameters for the Enhancement of Tensile Properties of Bi-Layered Printed PLA-ABS. *Materials Research Express*. https://doi.org/10.1088/2053-1591/acf1e7

Rath, U., & Pandey, P. M. (2020). Experimental Investigations Into Extrusion-Based 3D Printing of PCL/CIP Composites for Microwave Shielding Applications. *Journal of Thermoplastic Composite Materials*. https://doi.org/10.1177/0892705720925131

Rayegani, F., & Onwubolu, G. C. (2014). Fused deposition modelling (fdm) process parameter prediction and optimization using group method for data handling (gmdh) and differential evolution (de). *International Journal of Advanced Manufacturing Technology*, *73*(1–4), 509–519. https://doi.org/10.1007/s00170-014-5835-2

Rittinghaus, S.-K., Schmelzer, J., Wilms, M. B., & Kruger, M. (2021). *Laser Additive Manufacturing of Intermetallic Alloys for High-Temperature Applications*. https://doi.org/10.20944/PREPRINTS202102.0056.V1

Seshadri, B., Hischier, I., Masania, K., & Schlueter, A. (2023). 3D Printed Liquid Crystal Polymer Thermosiphon for Heat Transfer Under Vacuum. *Advanced Materials Technologies*. https://doi.org/10.1002/admt.202300403

Shahrum, M. A. (2024). Dimensional Accuracy of Acrylonitrile Butadiene Styrene and Polylactic Acid Samples Printed in Vacuum-Assisted Material Extrusion System. *Engineering Research Express*. https://doi.org/10.1088/2631-8695/ad4306

Singh, A. (2024). Investigation on FDM Process Parameters for the Dimensional Accuracy With ABS Polymer Part. *Engineering Research Express*. https://doi.org/10.1088/2631-8695/ad52ee

Şirin, Ş., Aslan, E., & Akıncıoğlu, G. (2022). Effects of 3d-Printed PLA Material With Different Filling Densities on Coefficient of Friction Performance. *Rapid Prototyping Journal*. https://doi.org/10.1108/rpj-03-2022-0081

Soffel, F., Eisenbarth, D., & Wegener, K. (2021). Effect of clad height, substrate thickness and scanning pattern on cantilever distortion in direct metal deposition. *International Journal of Advanced Manufacturing Technology*, *117*(7–8), 2083–2091. https://doi.org/10.1007/S00170-021-06925-7/FIGURES/8

Solomon, I. J., Sevvel, P., & Gunasekaran, J. (2020). A review on the various processing parameters in FDM. *Materials Today: Proceedings*, *37*(Part 2), 509–514. https://doi.org/10.1016/j.matpr.2020.05.484

Sun, Z. (2020). Clinical Applications of Patient-Specific 3D Printed Models in Cardiovascular Disease: Current Status and Future Directions. *Biomolecules*. https://doi.org/10.3390/biom10111577

Syaefudin, E. A. (2023). The Effect of Orientation on Tensile Strength 3D Printing With ABS and PLA Materials. *Journal of Physics Conference Series*. https://doi.org/10.1088/1742-6596/2596/1/012002

Syaefudin, E. A., Kholil, A., Hakim, M., Wulandari, D. A., Riyadi, & Murtinugraha, E. (2023). The effect of orientation on tensile strength 3D printing with ABS and PLA materials. *Journal of Physics: Conference Series*, *2596*(1). https://doi.org/10.1088/1742-6596/2596/1/012002

Syrlybayev, D., Zharylkassyn, B., Seisekulova, A., Akhmetov, M., Perveen, A., & Talamona, D. (2021). Optimisation of Strength Properties of FDM Printed Parts—A Critical Review. *Polymers*. https://doi.org/10.3390/polym13101587

Tesikova, K., Jurkova, L., Dordevic, S., Buchtova, H., Tremlova, B., & Dordevic, D. (2022). Acceptability Analysis of 3D-Printed Food in the Area of the Czech Republic Based on Survey. *Foods*, *11*(20), 3154. https://doi.org/10.3390/FOODS11203154/S1

Thumsorn, S., Prasong, W., Kurose, T., Ishigami, A., Kobayashi, Y., & Ito, H. (2022). Rheological Behavior and Dynamic Mechanical Properties for Interpretation of Layer Adhesion in FDM 3D Printing. *Polymers*. https://doi.org/10.3390/polym14132721

Tofail, S. A. M., Koumoulos, E. P., Bandyopadhyay, A., Bose, S., O'Donoghue, L., & Charitidis, C. (2018). Additive manufacturing: scientific and technological challenges, market uptake and opportunities. *Materials Today*, *21*(1), 22–37. https://doi.org/10.1016/J.MATTOD.2017.07.001

Tsuchiya, S., & Takahashi, K. (2021). Improving Fatigue Limit and Rendering Defects Harmless through Laser Peening in Additive-Manufactured Maraging Steel. *Metals 2022, Vol. 12, Page 49*, *12*(1), 49. https://doi.org/10.3390/MET12010049

Tura, A. D., & Mamo, H. B. (2022). Characterization and parametric optimization of additive manufacturing process for enhancing mechanical properties. *Heliyon*, *8*(7). https://doi.org/10.1016/j.heliyon.2022.e09832

Ujfalusi, Z., Pentek, A., Told, R., Schiffer, A., Nyitrai, M., & Maróti, P. (2020). Detailed Thermal Characterization of Acrylonitrile Butadiene Styrene and Polylactic Acid Based Carbon Composites Used in Additive Manufacturing. *Polymers*. https://doi.org/10.3390/polym12122960

Unger, L., Scheideler, M., Meyer, P., Harland, J., Gorzen, A., Wortmann, M., Dreyer, A., & Ehrmann, A. (2018). Increasing Adhesion of 3D Printing on Textile Fabrics by Polymer Coating. *Tekstilec*. https://doi.org/10.14502/tekstilec2018.61.265-271

Vafadar, A., Guzzomi, F., Rassau, A., & Hayward, K. (2021). Advances in Metal Additive Manufacturing: A Review of Common Processes, Industrial Applications, and Current Challenges. *Applied Sciences 2021, Vol. 11, Page 1213*, *11*(3), 1213. https://doi.org/10.3390/APP11031213

Vardhan, H., Kumar, R., & Chohan, J. S. (2019). Investigation of tensile properties of sprayed aluminium based PLA composites fabricated by FDM technology. *Materials Today: Proceedings*, *33*, 1599–1604. https://doi.org/10.1016/j.matpr.2020.05.335

Velu, R., Calais, T., Jayakumar, A., & Raspall, F. (2019). A Comprehensive Review on Bio-Nanomaterials for Medical Implants and Feasibility Studies on Fabrication of Such Implants by Additive Manufacturing Technique. *Materials 2020, Vol. 13, Page 92*, *13*(1), 92. https://doi.org/10.3390/MA13010092

Vilanova, M., Escribano-garcía, R., Guraya, T., & Sebastian, M. S. (2020). Optimizing Laser Powder Bed Fusion Parameters for IN-738LC by Response Surface Method. *Materials 2020, Vol. 13, Page 4879*, *13*(21), 4879. https://doi.org/10.3390/MA13214879

Vranić, A., Bogojević, N., Ćirić-Kostić, S., Croccolo, D., & Olmi, G. (2017). Advantages and drawbacks of additive manufacturing. *IMK-14 - Istrazivanje i Razvoj*, *23*(3), 57–62. https://doi.org/10.5937/imk1702057v

What is CMM | Coordinate Measuring Machine Types. (n.d.). Retrieved December 11, 2023, from https://www.creaform3d.com/blog/what-is-cmm-and-their-types/

What's the ideal filament for FDM 3D printing? 3D printing materials compared | Hubs. (n.d.). Retrieved October 29, 2023, from https://www.hubs.com/knowledge-base/fdm-3d-printing-materials-compared/

Wu, W., Geng, P., Li, G., Zhao, D., Zhang, H., & Zhao, J. (2015). Influence of layer thickness and raster angle on the mechanical properties of 3D-printed PEEK and a comparative mechanical study between PEEK and ABS. *Materials*, *8*(9), 5834–5846. https://doi.org/10.3390/ma8095271

Yang, C.-J., Huang, W.-K., & Lin, K.-P. (2023). Three-Dimensional Printing Quality Inspection Based on Transfer Learning With Convolutional Neural Networks. *Sensors*. https://doi.org/10.3390/s23010491

Yang, Y., Zhang, C., Wang, D., Nie, L., Wellmann, D., & Tian, Y. (2020). Additive manufacturing of WC-Co hardmetals: a review. *The International Journal of Advanced Manufacturing Technology 2020 108:5*, *108*(5), 1653–1673. https://doi.org/10.1007/S00170-020-05389-5

Yap, Y. L., Toh, W., Koneru, R., Lin, R., Chan, K. I., Guang, H., Chan, W. Y. B., Teong, S. S., Zheng, G., & Ng, T. Y. (2020). Evaluation of structural epoxy and cyanoacrylate adhesives on jointed 3D printed polymeric materials. *International Journal of Adhesion and Adhesives*, *100*. https://doi.org/10.1016/j.ijadhadh.2020.102602

Yi, B., & Saitou, K. (2021). Multicomponent topology optimization of functionally graded lattice structures with bulk solid interfaces. *International Journal for Numerical Methods in Engineering*, *122*(16), 4219–4249. https://doi.org/10.1002/NME.6700

Zakharov, O. V., Pugin, K. G., & Ivanova, T. N. (2022). Modeling and Analysis of Delta Kinematics FDM Printer. *Journal of Physics: Conference Series*, *2182*(1), 012069. https://doi.org/10.1088/1742-6596/2182/1/012069

Zhang, X., Xiao, J., Kim, J., & Cao, L. (2022). A Comparative Analysis of Chemical, Plasma and in Situ Modification of Graphene Nanoplateletes for Improved Performance of Fused Filament Fabricated Thermoplastic Polyurethane Composites Parts. *Polymers*. https://doi.org/10.3390/polym14235182

Gantt Chart for PSM 1

No.	Task	Week															
		1	2	3	4	5	6	7	8	9	10	11	12	13	14	15	16
1	Title Registration	█															
2	Project Title Briefing	█															
3	Searching for related journal		█	█	█	█	█	█		█	█	█	█	█	█	█	█
4	Introduction		█	█	█												
5	Literature review					█	█	█		█	█	█	█	█			
6	Methodology											█	█	█	█	█	
7	Abstract														█	█	
8	Table of content														█	█	
9	refenrence														█	█	
10	Logbook submission														█		
11	Presentation															█	
12	PSM 1 report Submission																█

MID SEMESTER BREAK (Week 8)

Gantt Chart for PSM 2

No.	Task	Week															
		1	2	3	4	5	6	7	8	9	10	11	12	13	14	15	16
1	PSM 2 briefing	■															
2	Discussion with supervisor	■	■	■	■	■	■	■		■	■	■	■	■	■	■	■
3	Design planning	■															
4	Experimental setup		■	■													
5	Samples Printing				■	■	■	■									
6	Measurement testing					■	■		M	■							
7	Result Analysis								I	■	■	■	■				
8	Log Book Submission								D					■			
9	PSM 2 mock presentation													■			
10	PSM 2 presentation								S						■		
11	PSM 2 Report submission								E							■	■

(Week 8 column: MID SEMESTER BREAK)